



Norwegian University of
Science and Technology

Heave Control System For A Surface Effect Ship

Disturbance Damping of Wave Induced Motion at Zero Vessel Speed

Øyvind Fidje Auestad

Master of Science in Engineering Cybernetics

Submission date: February 2012

Supervisor: Jan Tommy Gravdahl, ITK

Co-supervisor: Asgeir Sørensen, Marintek

Minkang Wu, Marintek

Trygve Halvorsen, Umoe, Mandal



MSc thesis assignment

Name of the candidate: Øyvind Fidje Auestad

Subject: Engineering Cybernetics

Title: Heave Control System for a Surface Effect Ship: Disturbance Damping of Wave Induced Motion at Zero Vessel Speed

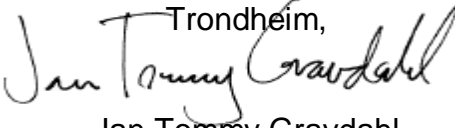
Background

The topic of the assignment is design of a heave control system for active damping of heave motions for a Surface Effect Ship (SES) at zero velocity.

Assignments:

- 1) Present the SES concept in general and the Wave Craft vessel in particular. Also, investigate previous work on control of such vessels.
- 2) Describe the software tools to be used for simulations as well as the model for the SES
- 3) Design and simulate a control system for active damping of heave motions that are a result of wave induced forces.

To be handed in by: 7/2-2012

Trondheim,

Jan Tommy Gravdahl
Professor, supervisor

Abstract

This master thesis will cover vertical motion damping of a Surface Effect Ship (SES) at zero vessel speed where the motion are induced due to wave propagations. The vital SES principle is the air cushion that partly lifts the vessel together with the hydrodynamic buoyancy. The air cushion is enclosed by two catamaran twin hulls and two rubber seals at the ends.

The motion damping takes place on the vessel bow. This is necessary and important while the wind turbine maintenance workers boards the turbine.

A heave control system (HCS) is created for performing this task. This notation is chosen since the control systems only task is to keep the control point closest possible to a constant heave (vertical) reference position.

The HCS actively controls the air flow actuators to the air cushion. The air flow actuators are the lift fan (blowing air into the air cushion) and adjustable louvers (letting air out of the cushion). By closing the louver pins and gaining maximum effect from the lift fan, the vessel will increase its vertical position (upwards). The opposite effect will appear by opening the louver and "choking" the lift fan, which results in a downwards motion.

The control system is discussed, implemented and tested in simulation. A Kalman filter using a mathematical model has been implemented to reject heave measurement noise and to estimate non-measurable states.

The HCS will be added to an already existing SES simulation model that does not support any active control of the air flow.

Task Description

Actuating the air flow in the air cushion is the main task of this thesis. The actuation needs to be in such a way that the system tries to obtain a steady heave reference position. This point is noted as the control point.

By varying the pressure inside the air cushion one can vary and control the vertical position of the vessel at the control point. Louver(s) and lift fan(s) are used to actuate the pressure. The louver works as a valve that emits air out of the air cushion by varying the louver pins position. The fan gathers air outside the cushion and blows it into the air cushion.

While a wave approaching the vessel, the system needs to actuate in accordance with the induced vertical motion in order to maintain around the reference position. A large error between reference and current vertical position will demand a large change in actuator position. This control idea is known as proportional control. The control system is noted as a Heave Control System (HCS).

The HCS will damp wave effects with active control of the cushion's air inflow and outflow. This air regulation is obtained by varying the louver leakage area and the air inlet area for the fan. The fan outflow is proportional to the inlet area.

A suitable HCS will be introduced both in theory and simulation. The simulation tool is VeSim [1] created by D. Fahti and Marintek which simulate behavior of ships in various sea states such as wave effects and current. Wind can also be added. VeSim is a plugin in Marinteks hydrodynamic workbench "ShipX". Vessel Response (VeRes) is another ShipX plugin used to calculate ship motions and loads. These calculations are performed pre-simulation. This allows the simulation to run quickly (real time or faster). VERES uses hull geometry, mass and other aspects defining the vessel and calculates supplementary results used in the simulation [2]. The third plugin is Simulation Visualization (SimVis) and is used to visualize the vessels behavior in the specified sea state.

In 2008, Trygve H. Espeland created a SES model for VeSim [3]. This model calculates enclosed cushion volume, cushion air leakage, airflow from fans, uniform cushion pressure and several other aspects in order to calculate the forces acting on the cushion. These forces are sent to the existing VeSim model which calculates all hydrodynamic forces and corresponding vessel motion. This master thesis will develop this SES model.

Two cases will be simulated and discussed, a simplified squared SES and the actual planned offshore wind turbine vessel that this thesis deals with.

Acknowledgement

I would like to express my appreciation to my advisors: Jan Tommy Gravdahl for always taking the time to discuss problems, the comprehensive knowledge on control systems, the weekly meetings and helping solving problems along the way. Asgeir J. Sørensen for his unique expertise on Ride Control Systems on a SES. The discussions of practical solutions resulted in a major boost for the work motivation. The advises that were given led the system and what it is today. A special thanks to Trygve H. Espeland for a the theoretical and practical teaching of the SES principle, for always being positive, supportive and only a phone call away.

I would also like to thank MingKang Wu for the weekly team-efforts that took place when figuring out problems, understanding code and developing the SES-model (on seperate aspects).

Gratitude is sent to Dariusz Fahti at Marintek for (several) system setup and helping with problems concerning the software.

A sincerely thanks and appreciation goes out to Umoe, Mandal and Nere Skomedal, Anders Nybø, Trygve H. Espeland and the rest, for giving me the opportunity I am given. Thank you!

I also want to thank to my grandfather Jarl Egil Fidje for being a great friend and showing huge interest for the work covered in this thesis.

Contents

Abstract	iii
Task Description	v
Acknowledgement	vii
1 Introduction	1
1.1 Background and motivation	1
1.2 Organization of thesis	2
1.3 Main contributions	3
2 Properties of a Surface Effect Ship	5
2.1 Advantages of a SES	9
3 The Wave Craft (SES - Offshore Service Vessel)	13
3.1 Introduction	13
4 Control Literature Review	17
4.1 Cobblestone Effects	18
4.2 Kaplan & Davis - System Analysis Techniques For Designing RCS of SES craft in waves	20
4.2.1 Mathematical model	20
4.2.2 State space model	20
4.2.3 Louver Area Leakage Control Design	21
4.2.4 Fan Blade Angle Control Design	21
4.2.5 Fan Area Control Design	23
4.3 Sørensen & Egeland - Design of RCS for a SES using Dissipative Control	24
4.3.1 Mathematical model	25
4.3.2 State space model:	26
4.3.3 Control system design:	27

4.4	Air Cushion Adaptive Disturbance Cancellation of Reduction of Wave Induced Motion of Ramp-Connected Ships	28
5	Software Tools	31
5.1	VeSim	32
5.2	SimVis	33
5.3	System setup	34
6	The Existing Model at Project Takeover	37
6.1	Introduction	38
6.2	Cushion Volume	38
6.3	Cushion inflow - Fan	39
6.4	Cushion outflow - Passive leakage under demi-hull, seals and between demi-hull and seals	40
6.4.1	Leakage under hull	40
6.4.2	Forces acting on the seal and seal leakage	41
6.5	Air Cushion equations	41
6.6	Essential manner of operation	43
6.7	Input/Output Diagram for the Java classes	44
7	Solution - Heave Control System	45
7.1	Heave control system diagrams	45
7.2	The Louver System	47
7.2.1	Louver Federate Interface	50
7.2.2	Contraction of air flow out from the air cushion	52
7.3	The Lift Fan System	53
7.3.1	Fan Federate Interface	56
7.4	Heave Control	57
7.4.1	Heave Control Federate Interface	59
7.4.2	Mathematical model	61
7.4.3	State space model	61
7.4.4	Controller Design	63
7.4.4.1	Alternative fan control:	65
7.4.5	Stability properties	67
7.5	Actuator saturation and limitations	68
7.5.1	Actuator saturation	68
7.5.2	Actuator lag - restriction of cushion air flow rate	70
8	Results	73
8.1	Process estimating - Kalmanfiltering	75
8.2	Large actuator lag leads to instability	76

<i>CONTENTS</i>	xi
8.3 Change of control point	79
8.4 Satisfactory behavior of the controlled fan and louver system	80
8.5 Alternative set point for fan control	80
8.6 Heave Control	83
8.6.1 Simplified SES Hull (Case1_1)	83
8.6.2 The Wave Craft	89
8.6.2.1 Control point changes from Center Of Gravity to Vessel Bow	94
9 Conclusion	97
9.1 Further work	98
10 Summary	101
Bibliography	105
Appendix A Contents on enclosed DVD	107
Appendix B The Kalman Filter	109
Appendix C VERES hydrostatics for the Square-SES (Case 1_1) Model	111
Appendix D Derivation Of Transfer Function H(s) for stability anal- ysis	113

Chapter 1

Introduction

A control system that damps vertical motions of a Surface Effect Ship (SES) is presented. A SES can be described as a hybrid between a catamaran and a hovercraft (Air Cushion Vehicle). The concept of this vessel is to partly lift the hull using an overpressure inside an air cushion. The air cushion is enclosed within two side/demi hulls, a rubber bow and stern seal.

A SES offers high speed, excellent seakeeping, high comfort & ride quality for crew in various sea states compared to like sized catamarans.

1.1 Background and motivation

Wind-turbines or wind power plants are becoming increasingly common worldwide as governments seek to meet their obligation to provide more renewable energy.

The particular Surface Effect Ship covered in this project is an offshore service vessel (The Wave Craft) that is under development. The Wave Craft allows the crew to operate wind farms more often than today's wind farm service vessel. These vessels are usually equal-sized catamarans.

The catamarans experience problems facing wave elevation that approximately exceeds 1.5 m significant wave height [4]. Wind turbine service personnel (crew) can not take the risk of jumping from a highly restless vessel bow and over to a (stationary) wind turbine platform. A result of this is that the crew can not reach the turbines.

Thus, wind turbines in need of service will remain unused. According to the British organization Carbon Trust (promotes carbon-friendly initiatives) this re-

sults in large economical problems. A necessary solution for the Wave Craft is to be able to handle noticeable larger wave elevations than 1.5 m (significant wave height). As a result of this; the Wave Craft should decrease wind turbine maintenance costs and increase operational time. This implies wind power to be distributed at a lower cost.

The idea of damping wave induced vertical motions on a ship could also be used in other situations. For instance, extreme weather and sea conditions force ferries and other ships to remain docked at harbor. These ships would benefit from the SES idea where the 80% of the ship is carried by air pressure only. A suitable, robust control system could revolutionize transportation in extreme sea condition.

1.2 Organization of thesis

Chapter 2 Properties of a Surface Effect Ship:

Explanation of the SES concept. Properties and advantages will be presented along with the most important aspects of the vessel.

Chapter 3 The Wave Craft (SES - Offshore Service Vessel):

In this section the Wave Craft will be presented. The Wave Craft is a SES - offshore service vessel that this thesis deals with.

Chapter 4 Control Literature Review:

Will present what existing control system that has been published today. Three cases will be presented: Kaplan & Davies (1978), Sørensen & Egeland (1995) and Basturk, Doblack & Krstic (2011).

Chapter 5 Software Tools:

Is introducing the software used in this thesis. It also explains how to set up the system.

Chapter 6 The Existing Model at Project Takeover:

This chapter presents the starting point of the work. The work has been done by Trygve Espeland (2008). It was his project and master thesis at NTNU.

Chapter 7 Solution - Heave Control System:

This chapter includes the work that has been done by the writer of this thesis. Implementation and explanation of actuator and control system is given.

Chapter 8 Results:

Results and simulation outcome from this project. Two major tests has been done, the first test using two lift fans the other one.

1.3 Main contributions

1. Trygve H. Espeland's help and his already existing SES model
2. Control theory from "Reguleringsteknikk" and Model And Simulation, respectively (Balchen, Andresen, Foss) and (Gravdahl, Egeland)
3. Technical Support from Asgeir Sørensen and software setup from Dariusz Fahti

Chapter 2

Properties of a Surface Effect Ship

The figure below describes the air cushion that is enclosed within two side hulls, a rubber bow and a stern seal:

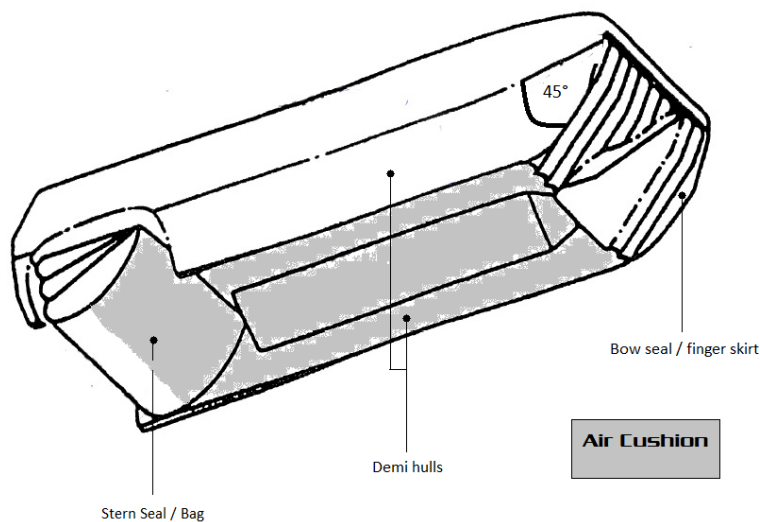


Figure 2.1: The SES Concept [5]

Note that there are several different approaches on the design of an air cushion for a SES, however the properties described below is a typical and robust SES implementation based on Faltinsen [6].

The air cushion described above supports the buoyancy of the vessel. As rule of thumb during transit, can assume that the cushion carries 80 percent of the

weight of the vessel, leaving the buoyancy with the remaining 20 percent. The bow and stern seal possess flexibility, allowing some air leakage to occur.

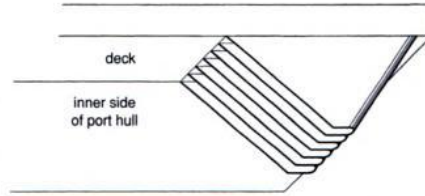


Figure 2.2: Bow seal [7]

Figure 2.2 a bow seal. The bow seal is often referred to as the skirt. The seal is a row of several (approximate 10) vertical loops or rubber fingers. When the vessel is on cushion, the rubber fingers will be blown open, closing all air gaps between each other. Similar, in zero wave propagation the finger tip should touch the water level denying air leakage between finger skirt and water surface.

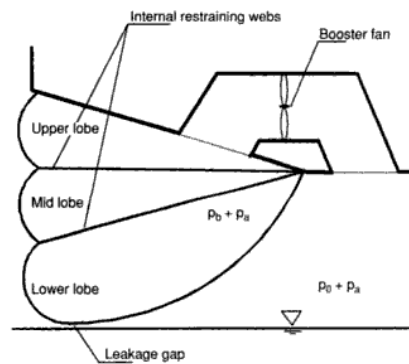


Figure 2.3: Stern seal [7]

The stern seal is referred to as bag or aft lobe stern. For this report the former notation will be used.

A typical three loop bag can be observed in figure 2.3 above. From the figure one can observe the two internal restraining webs, "gluing" the three bags together. These webs possess small holes in order to equalize the pressure between the loops. For vessel stabilization and sea-keeping properties it is desired that the pressure inside the bag is 10-20 percent higher than inside the air cushion ([8]).

The seal is open toward the side hulls allowing some leakage to occur between the bag and hull. Unlike the skirt, the bag will experience some area gap between

the bottom of the bag and the water surface (in zero wave propagation). This gap is approximately 3 cm ([8]).

Lift fan(s) supplies the cushion with air inflow creating the overpressure that lifts the SES up. This excess pressure (p_0) causes the water level inside the cushion to be h units lower than outside. See figure 2.4 below.

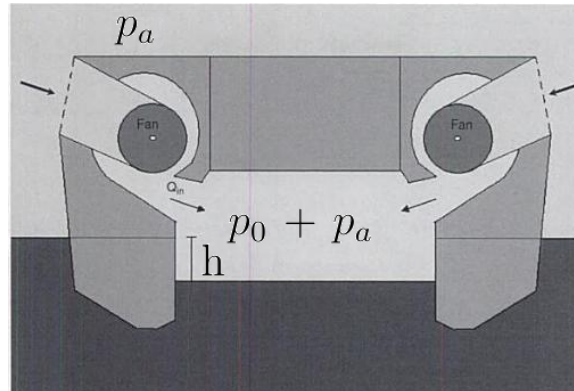


Figure 2.4: SES cross section [7]

- Air cushion pressure:

$$p_c = p_a + p_0(1 + \mu) \quad (2.0.1)$$

Where p_a , p_0 , $p_0\mu$ and p_c is respectively atmospheric, excess, dynamic and total air cushion pressure.

- Static water level height difference due to air cushion pressure (see fig: 2.4):

$$h = \frac{p_0}{\rho g} \quad (2.0.2)$$

Where ρ denotes the sea water density and g is the gravity.

This lift provides less water resistance than an equal sized catamaran. The 80 percent lift lowers the draft, allowing the vessel to partially ignore various wave influence.

The lift fan(s) has a varying effect based on cushion pressure and lift fan motor rotation speed (rpm). Figure 2.5 below shows this coherence which has a natural damping effect on the vertical motion of a SES.

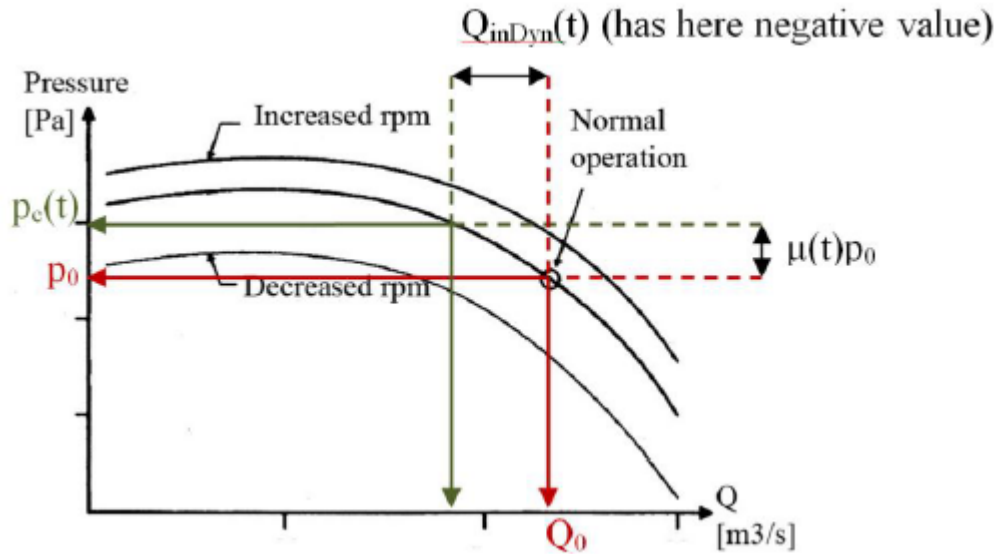


Figure 2.5: Fan Characteristic [9] (b)

The louvers allows the air cushion to contain an active leakage contribution. Adjusting the louver pins will vary the amount of air flowing out from the cushion via the louvers. Note that the leakage described above this section is referred to as passive leakage. Thus:

Definition 1. *All the cushion leakage that leaks through the lower system is defined as **louver leakage**, all other leakages from the air cushion is defined as **passive leakage**.*

Varying and controlling the louvers in order to obtain a favorable leakage is known as a Ride Control System (RCS), where one can control pitch and heave motion. This thesis only covers the latter one, therefore it was decided to use the term Heave Control System(HCS) instead.

HCS or RCS is the main topic of this thesis. Figure 2.6 below shows the louver system for the minesweeper class Alta [10]. The louvers from the figure are positioned side by side near the front of the air cushion.

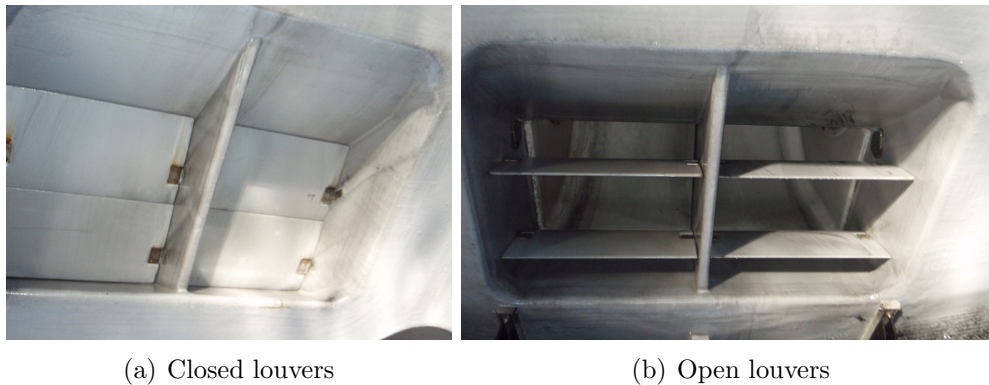


Figure 2.6: Louver System [11]

2.1 Advantages of a SES

Compared to a catamarans of the same size, the main benefit of a SES is low hydrodynamic resistance. This includes minor impact from viscous forces and wave propagation since a relative small part of the hull is below water level. Thus the affected resistance area is set to a minimum and the SES can profit from fuel consumption at medium/high speed. However, in small sea states at small velocity, one will witness a relative high fuel consumption in order to operate the lift fans. A solution is to go off-cushion, forcing the vessel to act like a catamaran.

Umoe Mandal has delivered several Surface Effect Ships to the Royal Norwegian Navy. Among these are the classes Oksøy and Alta, respectively mine hunters and mine sweepers. Because of the lift, a SES has low sensitivity for underwater explosions.



Figure 2.7: Minesweeper Otra of the Alta class [10]

As mentioned, the SES has a natural passive damping of vertical motion, increasing the ride comfort:

1. A wave approaching a SES head sea. The wave will lift the water in the fore part of the cushion. This will decrease bow seal leakage.
2. The wave continues to propagate through the cushion taking up more and more space. This will decrease the air cushion volume. Decreased volume and leakage will increase the cushion pressure.
3. The vessel will experience a heave force that act upward.
4. As the pressure keeps increasing, the cushion input flow from the fan will decrease, see fan characteristic from figure (2.5 and 7.5). This will damp the upward motion.
5. As the wave passes the vessel, the cushion volume and bow seal leakage will increase while pressure will decrease.
6. The vessel will gain a heave force acting downwards.
7. As before, only opposite; the pressure decrease will result in an increase of the air flow from the fan. This along with a growing leakage area will damp the downward motion significantly.

The dynamics can be modeled as a spring-damper system, see [12]. Implementing a RCS/HCS will increase the ride comfort significantly.

Another aspect that favors a SES compared to other similar vessels is performance and stability considering the benefits listed above. With less resistance one can exploit the engine power to obtain high vessel velocity. “KNM Skjold” is another SES class created by Umoe Mandal for the Royal Norwegian Navy.. These Motor Torpedo Boats (MTB) are probably the fastest military vessels that has ever existed. These vessels can achieve velocities above 60 knots [10].



Figure 2.8: KNM Storm -MTB Skjold class [10]

Chapter 3

The Wave Craft (SES - Offshore Service Vessel)

3.1 Introduction



Figure 3.1: The Wave Craft in a wind turbine park

This master thesis is written in co-operation with Umoe Mandal. The control system is intentionally designed for a new vessel project called the Wave Craft.

The Wave Craft, which is Umoe Mandals design of a SES - Offshore Service Vessel,

was one of the winner of the "Offshore Wind Accelerator Access Competition". The competition is held by the non-profit organization Carbon Trust [13]. Carbon Trust mission is to reduce carbon action. Umoe Mandal plans to commercialize the vessel in 2012 [14]. Figure 3.2 made by the Umoe Mandal illustrates a possible appearance if the Wave Craft. Along with Carbon Trust, Forskningsrådet is also a sponsor of the craft. A crucial aspect concerning the realization of the Wave



Figure 3.2: SES - Offshore Service Vessel

Craft is the air cushion that allows vertical motion damping. This concerns safety, comfort and the arrangement of a workable environment for the offshore crew.

While being transported from mainland to an offshore windmill, a crew member on duty wants to reach the destination as pleasant and as quickly as possible. The SES concept allows comfort and high speed in various sea states. In transportation mode (SES mode) the majority of the vessels mass is carried by the air cushion, allowing one to float above parts of the wave propagation. This exhibits a quick and hopefully seasick-less ride for the crew, where the majority aren't going to be "habit-formed" seafarers.

Boarding the wind turbine from the vessel -and visa versa- needs to be a safe experience.

Length (loa)	25 m
Width	8 m
Draught	0.7 m/2m (transit / docking)
Cargo	Max 10 ton
Transit Speed	35 knots +
Propulsion	Water Jets
Range	500 nm +
Passengers	12

Figure 3.3: Specifications - Wave Craft [15]

- The idea is to deliver effective operational solutions for maintenance of offshore wind power installations. Low costs for operation and maintenance has been selected as one of the main challenges in order to create such power installations. Anders Nybø CEO Umoe Mandal, [14]

Figure 3.4 shows the intended behaviour when switching between transit mode and offshore wind turbine docking mode.

The equilibrium cushion pressure will approximately be halved when going from transit to docking mode. This allows a larger lift ratio interval which results in a larger damping specter for the motion control. The lift ratio is the relation between vessel mass held by the air cushion alone and total mass. For instance, with the vessel bow at the top of a wave, a low lift ratio is desired. With vessel bow at the bottom of a wave, a high lift ratio is desired in order to try to reach the reference heave position.

The figure below explains transit and dockin mode of the Wave Craft:

16 CHAPTER 3. THE WAVE CRAFT (SES - OFFSHORE SERVICE VESSEL)



Offshore wind turbine docking mode

During offshore wind turbine docking operation the cushion pressure will vary to compensate for wave effects and will carry in average 30-50% of the weight of the ship.

A significant reduction of vertical ship motions will be achieved.



SES mode in transit

The air cushion carries approximately 80% of the weight, lifting the vessel up in the water. The flexible stern bag and bow finger skirts keep a tight seal between the hulls, providing a controlled air-pressure for maximum stability and motion control. This will result in a safe operation of the vessel with improved crew comfort and reduced seasickness.



Wave through

The air pressure is increased to compensate for less buoyancy of the side hulls.



Wave crest

The air pressure is decreased to compensate for increased buoyancy of the side hulls.

Figure 3.4: [15]

Chapter 4

Control Literature Review

Exclusive (active) damping of vessel bow heave position due to wave induced vertical forces, has previously not been documented. However, accurate studies concerning vertical dynamics on a SES and ride control systems (RCS) for active damping of heave and/or pitch motion in forward vessel speed has been documented. The former is covered by Kaplan & Davis in [16], Kaplan in [17] and Sørensen, Steen & Faltinsen in [18].

There exists two comprehensive full-scale works regarding ride control systems for a SES. The first one created in 1974 by Kaplan and Davis [19] and the second one in 1995 by Sørensen A.J and O. Egeland [12]. Both focusing on actively reducing vertical accelerations during relative high vessel velocity in low and moderate sea states. This is done by altering the pressure variations within the cushion. The vertical accelerations that arises at fixed frequencies are called cobblestone effect. A brief introduction to this phenomena will be given in 4.1.

During the writing of this thesis, Basturk, Doblack and M. Kristic [20] published interesting simulation results [20] regarding adaptive wave disturbance cancellations. In resemblance to this thesis, the vessel acts on zero velocity but has a ramp connected to a LMSR (large, medium-speed, roll-on/off) vessel.

All three cases will be discussed.

Concerning implemented simulation validation: all the discussed cases include some kind of a simulation / datatests. However, none implements passive leakage (leakage under seals, between bag and hull, under hull). In [17], Kaplan shows the importance of including these. Note that both Kaplan and Sørensen performed successfully full-scale experiments, so there is no doubt concerning system validation.

4.1 Cobblestone Effects

Cobblestone effects are high frequency resonance oscillations. These oscillations usually occur at relative high forward speed when water waves dynamically changes the air cushion volume in moderate and small sea states. These rapid vertical vibrations are the biggest comfort problems for passengers on a Surface Effect Ship. The effects can result in a non-workable environment [21].

The cobblestone effects are of great importance of the Wave Craft while being transported from mainland to wind turbine. However, the presented control design will not cover damping of these oscillations.

In 1998, T. Ulstein and Odd M. Faltinsen performed a comprehensive research regarding this topic [21]. (Although this phenomenon was nothing new, Asgeir J. Sørensen had three years earlier pointed out and damped these oscillations using dissipative control [12])

Ulstein and Faltinsen performed a full-scale experiment on a 35 m SES. A typical setting to provoke the cobblestone effects is facing 0.4 meter waves at 45 knots velocity. Using these settings they confirmed the two most important resonance frequencies that causes the highest vertical accelerations. These frequencies are named eigenmodes or modes.

The lowest eigenmode is constant in space, it affects mainly heave accelerations. The second eigenmode which corresponds to the lowest acoustic resonance frequency has a node at midship. This can be approximated by a sinusoidal function with modal wave length twice the ship length. Thus, the second eigenmode affects mainly the pitch accelerations [21].

Figure 4.1 shows the power spectrum for cobblestone effects. Note the two resonance frequencies and their respective amplitude. (Note that the two amplitude peak roughly around 2 Hz denotes the same eigen mode).

Figure 4.1 shows that the lowest (2Hz) and the highest resonance frequencies (5.5Hz). These values will experience some minor adjustments based vessel properties such as vessel mass, cushion length and breadth.

Therefore it is important to divide cobblestone effects into the two types.

1. Uniform pressure resonance – First eigenmode (Mode 0).
2. Spatial pressure (or acoustic wave effect) resonance – (Mode 1, Mode 2,...)

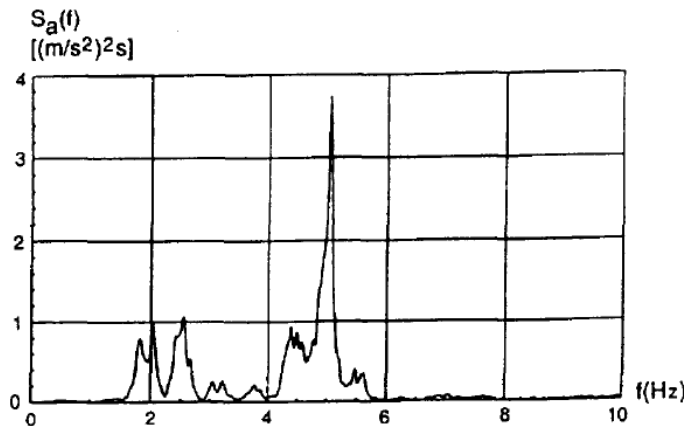


Figure 4.1: Full scale measured spectrum $S_a(f)$ of vertical acceleration at vessel bow for mode 0 (uniform pressure variations) and mode 1 (first acoustic mode). [21]

Spatial pressure resonance treats pressure variations in longitudinal direction. One can always assume that the pressure is constant in height and lateral direction. This results in a one dimensional pressure varying system. At midships one will observe that the spatial cushion pressure equals zero (a node positioned at $L_c/2$). As mentioned, the pressure displacement can be approximated by a sine function with modal wave length twice the vessel length, therefore the second eigenmode mainly affects the pitch motions.

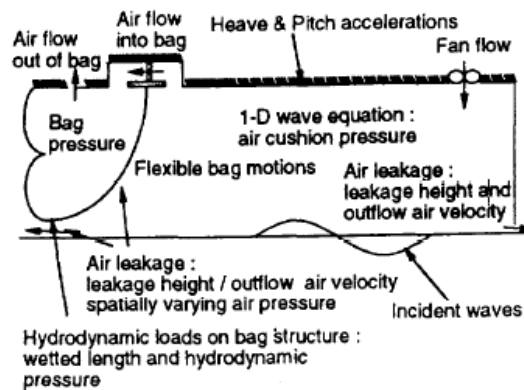


Figure 4.2: Physics inside the air cushion [[21]]

4.2 Kaplan & Davis - System Analysis Techniques For Designing RCS of SES craft in waves

Kaplan and Davies [19] presents a useful toolbox and procedures on design of a Ride Control System for reducing vertical plane accelerations on a Surface Effect Ship. A final design is presented on a 100 ton testcraft. Test results shows that Kaplan is able to damp out 60 - 80 % of vertical accelerations.

As mentioned, Kaplan is the first to present a control system for a SES. Feedback signals in terms of craft state variables are established. Actuator nonlinearity, saturation limit and lag is discussed. A louver system, axial fans with variable blade angles and varying the input area of the fan are discussed as air flow actuators. The former one is implemented in the full-scale test.

All figures are taken from [19].

4.2.1 Mathematical model

The presented equation of motion concerns heave acceleration only:

$$m\ddot{\eta}^3(t) + A_c p_0 \mu(t) = 0 \quad (4.2.1)$$

and uniform pressure equation:

$$K_1 \dot{\mu}(t) + K_3 \mu(t) - \rho_a A_c \dot{\eta}^3(t) = -K_2 \Delta A_L - \rho_a \dot{V}_{b,Waves}(t) \quad (4.2.2)$$

where η^3 is heave position (the power of three symbols that heave is the third degree of freedom), total uniform cushion pressure is defined: $p = p_0(1 + \mu)$, therefore μ describes dynamic uniform cushion variations around equilibrium pressure p_0 . m : total mass of craft, A_c : cushion area, ρ_a : density of air, ΔA_L : controlled louver leakage and $\dot{V}_{b,Waves}(t)$ is the time rate of cushion volume pumping due to waves. Also: $K_1 = \frac{\rho_a A_c h_b}{\gamma(1 + \frac{p_a}{p_0})}$ $K_2 = \rho_a c_n \sqrt{\frac{2p_0}{\rho_a}}$ $K_3 = \frac{\rho_a Q_0}{2} - \rho_a \left(\frac{\partial Q}{\partial p} \right) p_0$

Where h_b is height of cushion, γ is ratio of specific heats of air, p_a atmospheric pressure, c_n is orifice coefficient.

4.2.2 State space model

$$\dot{\bar{z}} = A\bar{z} + \bar{b}A_L + \bar{c}\dot{V}_{b,Waves} \quad (4.2.3)$$

where

$$\bar{z} = \begin{bmatrix} \dot{\eta}^3 \\ \mu \end{bmatrix} \quad \bar{b} = \begin{bmatrix} 0 \\ b \end{bmatrix} \quad \bar{c} = \begin{bmatrix} 0 \\ c \end{bmatrix} \quad A = \begin{bmatrix} 0 & -g \\ a_1 & a_2 \end{bmatrix} \quad (4.2.4)$$

and

$$a_1 = \frac{\rho_a A_c}{K_1} \quad a_2 = \frac{-K_3}{K_1} \quad b = \frac{-K_2}{K_1} \quad c = \frac{-\rho_a}{K_1} \quad (4.2.5)$$

Where K_i ($i=1,2,3$) is defined on the previous page.

4.2.3 Louver Area Leakage Control Design

Since (A, B) is controllable, Kaplan suggests the following commanded change in leakage:

$$\Delta A_{L,Controlled} = [\hat{k}_1 \quad \hat{k}_2] \bar{z} = \hat{k}_1 \dot{\eta}_3 + \hat{k}_2 \mu \quad (4.2.6)$$

where

$$\hat{k}_1 = \frac{k_1}{b} \quad \hat{k}_2 = \frac{k_2}{b} \quad (4.2.7)$$

where k_1 and k_2 are the control parameters which can be found by trial and error.

4.2.4 Fan Blade Angle Control Design

Another possibility for controlling heave motion is fan blade angle control. This approach controls the pitch angle of the fan blades while the fan runs at constant speed. Increasing blade pitch angle corresponds to an increase in air inflow to the cushion.

The following figure shows a typical pressure versus flow rate for various blade angles:

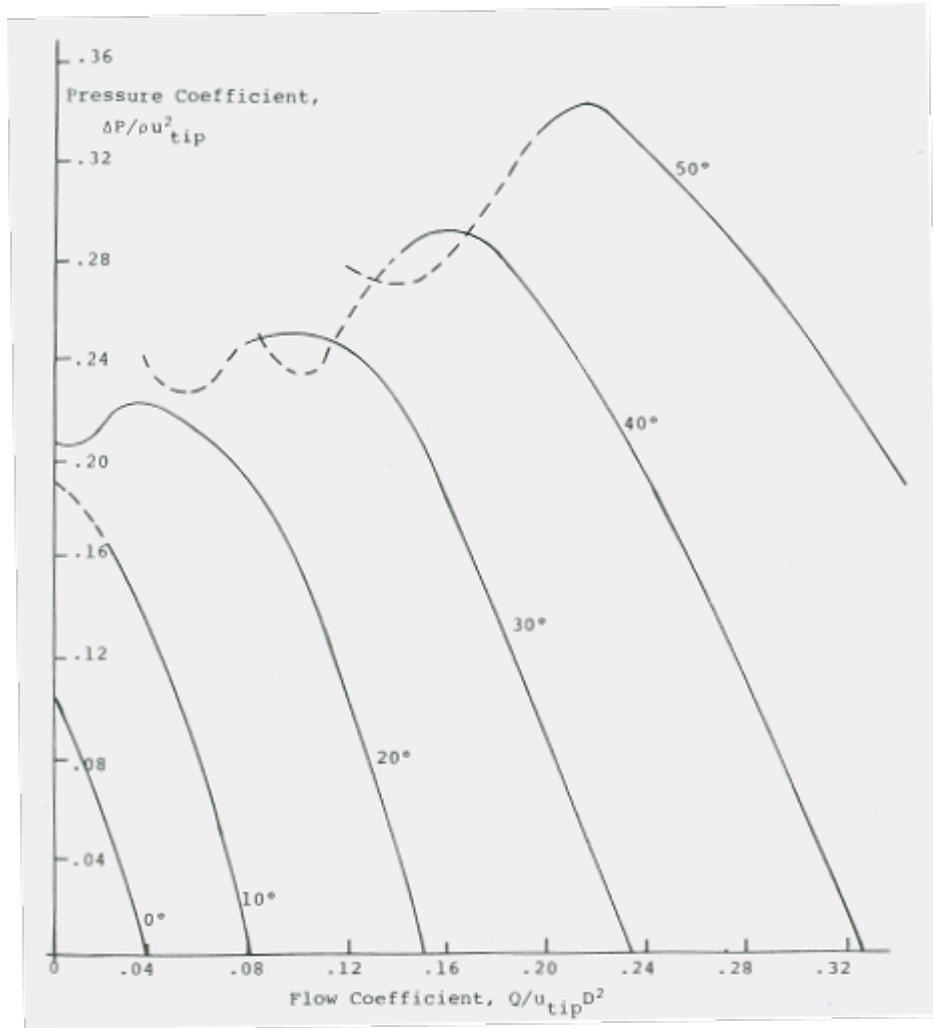


Figure 4.3: Air inflow (Q_{in}) vs. cushion pressure (p_c) for various blade angles [19]

For the purpose of the presented results in figure 4.3. As one can see, the curves has the same basic slope but different flow value for different blade angles. The coherence can be described as one equilibrium and one dynamic in flow rate:

$$Q_{in} = Q_0 + \left(\frac{\partial Q}{\partial p} \right) p_0 \mu \quad (4.2.8)$$

When using blade angle control for active damping of vertical acceleration, Kaplan claims that this only influence the equilibrium flow rate Q_0 . Thus, the representation of the fan flow into the cushion using fan blade control yields:

$$Q_{in} = Q_0 \left(1 + \frac{\Delta \alpha}{\alpha_{ref}} \right) + \left(\frac{\partial Q}{\partial p} \right)_0 p_0 \mu \quad (4.2.9)$$

4.2. KAPLAN & DAVIS - SYSTEM ANALYSIS TECHNIQUES FOR DESIGNING RCS OF SES CRA.

where α_{ref} is the reference blade angle about which angle the changes take place and $\Delta\alpha$ is the change in the fan blade angle. $\Delta\alpha$ equals zero at the equilibrium point.

According to [16] mass rate out of the cushion:

$$\dot{m}_{out} = \rho_a Q_{out} = \rho_a Q_0 + \frac{1}{2} K_2 A_{L_0} \mu + K_2 \Delta A_L \quad (4.2.10)$$

Where A_{L_0} and ΔA_L is respectively mean and dynamic leakage area and $\rho_a Q_0 = K_2 A_{L_0}$

Total mass rate:

$$\begin{aligned} \dot{m}_{cushion} &= \rho_a (Q_{in} - Q_{out}) \\ &= K_2 A_{L_0} \frac{\Delta\alpha}{\alpha_{ref}} - K_3 \mu - K_2 \Delta A_L \end{aligned} \quad (4.2.11)$$

Except for the scenario where there are no commanded leakage (i.e. $\Delta A_L = 0$) the quantity $A_{L_0} \frac{\Delta\alpha}{\alpha_{ref}}$ is essentially equivalent to the controlled leakage area change if the sign of the control gains is reversed.

In other words, any wanted louver control contribution will be equivalent to the present fan blade angle control except for the sign change of the control gains.

4.2.5 Fan Area Control Design

While Kaplan wrote his paper in 1974 a new way of altering the fan airflow was presented [22]. This technique is introduced by Kaplan and of great interest since the actual implementation of fan control in this master thesis is based on this technology. This type of fan control is still highly relevant today, along with a secondary option: controlling a valve on the outflow tube (a pipeline from fan to cushion) [4]

By varying the fan inlet area, the output air flow is therefore altered. Instead of controlling pitch blade angle ($\Delta\alpha$) one wish to alter the inlet area (ΔA).

The controlled command signal is given in a same manner as the fan blade approach:

$$\frac{\Delta A}{A_{ref}} = - \begin{bmatrix} \hat{k}_1 & \hat{k}_2 \end{bmatrix} \begin{bmatrix} \dot{\eta}_3 \\ \mu \end{bmatrix} \quad (4.2.12)$$

Using this approach one can specify desired air outflow by defining the input area as percentage of openness. The figure below shows a typical effect out flow effect based on %openness.

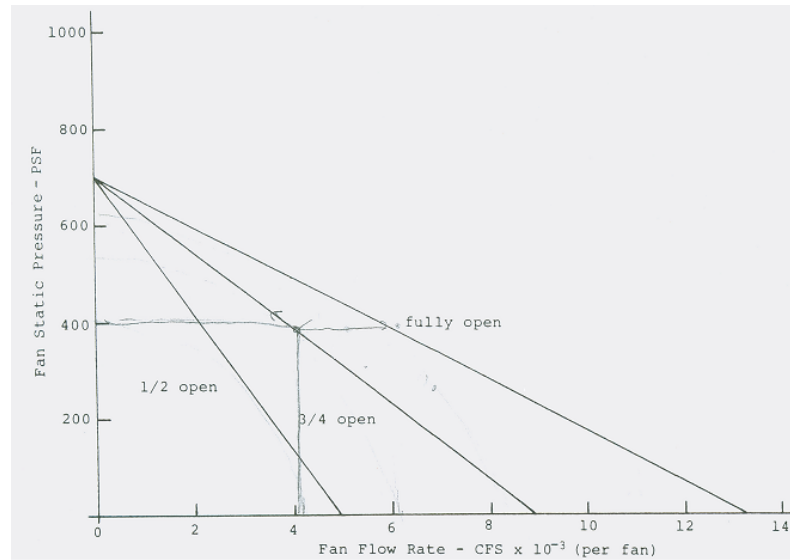


Figure 4.4: Air inflow (Q_{in}) vs. cushion pressure (p_c) for varying the fan inlet area

4.3 Sørensen & Egeland - Design of RCS for a SES using Dissipative Control

Asgeir J. Sørensen (with guidance from O. Egeland) presents a RCS for active damping of heave and pitch accelerations [12]. In this comprehensive full-scale experiment using a 35 meter, 150 ton SES, Sørensen and Egeland were able to neglect vertical motions using dissipative control. Special attention is given to actuator and sensor placement. The work shows how collocation has a major impact on stability and performance. Sørensen and Egeland shows the importance of including the acoustic nodes that occur due to the cushion spatial pressure variations. Note that the control system involves a vessel in moderate/high speed, unlike this thesis.

Figure 4.5 shows the results. Note that the figure also covers a third resonance frequency (acoustic mode 2), approximately 8Hz.

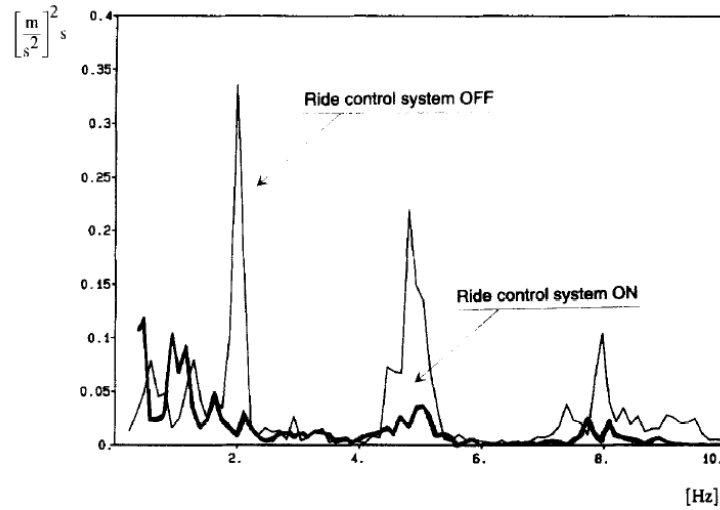


Figure 4.5: A. J Sørensen and O. Egeland's damping of vertical accelerations. Full scale power spectra [12]

The results had been highly innovative. Previous ride control systems derived by Kaplan and Davies [17] was based on the assumption that the dominating contribution to the cobblestone effects was induced by uniform cushion pressure alone. Thus, excluding pitch contribution to vertical accelerations.

(...) Their work was based on the assumption that the major part of the wave-induced loads from the sea was imparted to the craft as dynamic uniform air pressure acting on the wet-deck, while a minor part of the wave-induced loads from the sea was imparted to the craft as dynamic water pressure acting on the side-hulls.

- Asgeir J. Sørensen [12]

Kaplan and Davis [17] proved the importance of the first eigenmode (mode 0), while Steen, Sørensen and Faltinsen [23], [18] showed the importance of including the acoustic standing wave effects (mode 1,2..n), where the increasing number inhabits a smaller power spectrum.

4.3.1 Mathematical model

The dynamic heave motion system is given in eq. (18) - (21) in [19]. This process system include heave equation:

$$(m + A_{33})\ddot{\eta}_3(t) + b_{33}\dot{\eta}_3(t) + C_{33}\eta_3(t) - A_c p_0 \mu_u(t) = F_3^e(t) \quad (4.3.1)$$

And pitch equation:

$$(I + A_{55})\ddot{\eta}_5(t) + B_{55}\dot{\eta}_5(t) + C_{55}\eta_5 - 2p_0b \sum_{j=1,3,\dots} \left(\frac{L}{j\pi}\right)^2 \dot{p}_j(t) = F_5^e(t) \quad (4.3.2)$$

Where m is vessel mass, η_k is the k 'th DOF, A_c is cushion area. Uniform cushion pressure is defined: $P_c = P_0(1 + \mu)$, where μ describes dynamic cushion variations. A_{ii} and B_{ii} is respectively the hydrodynamic added-mass coefficient and water wave radiation damping coefficient. C_{ii} is the hydrostatic term found by integrating over the water-plane area of the side hulls.

F_k^e is hydrodynamic excitation force (or moment if $k > 3$) in the k 'th DOF. These are derived from hydrodynamic loads on the side hulls.

For pitch equation: I_{55} is the moment of inertia around the y -axis, L is ship length and $p_{j=1,3,\dots}(t)$ describes spatial pressure at odd modes.

4.3.2 State space model:

The dynamic system can be written in standard state space form:

$$\dot{\mathbf{x}}(\mathbf{t}) = \mathbf{A}\mathbf{x}(\mathbf{t}) + \mathbf{B}\mathbf{u}(\mathbf{t}) + \mathbf{E}\mathbf{v}(\mathbf{t}) \quad (4.3.3)$$

$$\mathbf{y}(\mathbf{t}) = \mathbf{C}\mathbf{x}(\mathbf{t}) \quad (4.3.4)$$

Where $\mathbf{x}(\mathbf{t})$ is the state space vector:

$$\mathbf{x}(\mathbf{t}) = [\eta_3 \ \eta_5 \ \dot{\eta}_3 \ \dot{\eta}_5 \ \mu_u \ p_1 \ p_2 \ \dots \ p_k \ \dot{p}_1 \ \dot{p}_1 \ \dots \ \dot{p}_k]^T \quad (4.3.5)$$

$\mathbf{u}(\mathbf{t})$ is the r -dimensional control input vector:

$$\mathbf{u}(\mathbf{t}) = [u_0(t) \ u_1(t) \ \dots \ u_r(t)]^T \quad (4.3.6)$$

where r denotes the number of louvers and:

$$u_i(t) = \Delta A_i^{RCS}(x_{si}, t) \quad (4.3.7)$$

is the current controlled area leakage from louver i , longitudinal positioned at x_{si} at time t .

$\mathbf{v}(\mathbf{t})$ is the process and wave disturbance vector:

$$\mathbf{v}(\mathbf{t}) = [F_3^e, F_5^e, \dot{V}_0, \dot{V}_1, \dots, \dot{V}_k]^T \quad (4.3.8)$$

Where $\dot{V}_i(t)$ for $i = 0, 1, 2, \dots, k$ is wave volume pumping and i is the i 'th mode. Thus, $i = 0$ is the uniform mode while the rest denotes the acoustic volume wave pumping. This is an effect that alters the volume with time because of the wave motion in the cushion area and the varying heave motion.

4.3.3 Control system design:

It is shown that the pair (A,B) is controllable and (A,C) is observable, thus the dynamical system can be presented as:

$$\mathbf{y}(\mathbf{s}) = \mathbf{H}_p(\mathbf{s})\mathbf{u}(\mathbf{s}) + \mathbf{H}_d\mathbf{v}(\mathbf{s}) = \mathbf{y}_u(\mathbf{s}) + \mathbf{y}_v(\mathbf{s}) \quad (4.3.9)$$

$$\mathbf{H}_p(\mathbf{s}) = \mathbf{C}(s\mathbf{I}_n - \mathbf{A})^{-1}\mathbf{B} \quad (4.3.10)$$

$$\mathbf{H}_d(\mathbf{s}) = \mathbf{C}(s\mathbf{I}_n - \mathbf{A})^{-1}\mathbf{E} \quad (4.3.11)$$

where

I_n is the $n \times n$ identity matrix.

Lemma 1 in [12] and corresponding proof shows that \mathbf{A} have negative real parts. *Lemma 2* and corresponding proof shows that the process operator \mathbf{H}_p is passive. Therefore the controller is defined as a linear time-invariant operator \mathbf{H}_c between the input y and output \mathbf{u}_c , thus:

$$\mathbf{u}_c(\mathbf{s}) = \mathbf{H}_c(\mathbf{s})\mathbf{y}(\mathbf{s}) \quad (4.3.12)$$

$$\mathbf{H}_c(\mathbf{s}) = \mathbf{G}_p \quad (4.3.13)$$

where

$\mathbf{G}_p = \text{diag}[g_{pi}] > 0$ is a constant diagonal feedback gain matrix.

Also note that the controller is not a tracking problem. The control system tries to achieve p_0 which the dynamics are linearized about. Also zero spatial pressure is the desired reference for the acoustic modes.

Sørensen & Egeland presents following feedback system (Theorem 1 [12]):

$$\mathbf{y} = \mathbf{y}_u + \mathbf{y}_v \quad (4.3.14)$$

$$\mathbf{u} = -\mathbf{u}_c = -\mathbf{H}_c\mathbf{y} \quad (4.3.15)$$

The system proves to be L_2^m stable and since \mathbf{H}_d , \mathbf{H}_p and \mathbf{H}_c is linear, L_2^m stability is equivalent to L_∞^m (BIBO) stability.

4.4 Air Cushion Adaptive Disturbance Cancellation of Reduction of Wave Induced Motion of Ramp-Connected Ships

The studies made by Basturk, Doblack and Krstic considers relative large cargo transfer (such as motor vehicles etc..) in high sea states over a ramp from the T-Craft to a LMSR vessel. The work is based modeling, simulation and computational tools such as Matlab, Aegir and Rhino.

The T-Craft is also developed by Umoe, Mandal and has characteristic of both a SES and an Air Cushion Vehicle (ACV). The work made by Krstic *et al* has strong similarities to this thesis but differs from the ramp connection and pitch control which this thesis does not cover.

The control system is divided between two cases; the ships are oriented side by side and in a bow to stern vessel configuration. This review will cover the former one since it only deals with heave motion and that the required two separate pressure chambers has shown high tendency to be torn off during high vessel velocity [4].

An adaptive back-stepping method has been implemented to regulate the pressure in the air cushion. The heave dynamics are based on Sørensen and Egeland work in [12]:

$$(m + A_{33})\ddot{\eta}_{33}(t) + B_{33}\dot{\eta}_{33}(t) + C_{33}\eta_{33} - A_c p_c = F_3^e(t) \quad (4.4.1)$$

Where η_{33} is the ships heave position. The remaining terms are explained in section 4.2.1.

Along with this thesis, the control difficulties arises due to the unmeasured wave disturbance. Using [24] the scaled unknown wave is represented as:

$$v = \frac{F_3^e}{(m + A_{33})} = \theta^T z \quad (4.4.2)$$

Using the states (similar to this project):

$$x = \begin{bmatrix} \eta^3 \\ \dot{\eta}^3 \end{bmatrix} \quad (4.4.3)$$

Where η^3 denote heave position. The following state space modeled is used:

$$\dot{x} = Ax + BP_c + b_0 v \quad (4.4.4)$$

4.4. AIR CUSHION ADAPTIVE DISTURBANCE CANCELLATION OF REDUCTION OF WAVE IN

Basturk, Doblack and Krstic presents the adaptive proportional/derivative (PD) air cushion controller:

$$P_c = \frac{(m + A_{33})}{A_c} (Kx - \hat{\theta}^T \hat{z}) \quad (4.4.5)$$

Where $\hat{\theta}^T$, \hat{z} is the estimate of θ^T and z . K is controller gain $\mathbb{R}^{2 \times 2}$.

Using Lyapunov stability, the following update law is chosen:

$$\dot{\hat{\theta}} = \gamma z b_0^T P X \quad (4.4.6)$$

The positive definite matrix $P \in \mathbb{R}^{2 \times 2}$ is a solution of the matrix equation

$$(A + BK)^T P + P(A + BK) = -2I \quad (4.4.7)$$

The system shows excellent results but suffer from the lack of actuator implementation / saturation. Documentation of Basturk and Doblack implementation and simulation runs can be found in [20].

Chapter 5

Software Tools

The programs that has been used during this (and previous) master thesis is Vessel Simulator (VeSim) [1] and Simulator Visualization (SimVis) [25].

VeSim and SimVis are both plug-ins for the integrated ship design tool named "ShipX". ShipX [26] along with the plug-ins are developed at Marintek, NTNU [27].

"The basic idea behind ShipX is to make a platform that integrates all kinds of hydrodynamic analysis into an integrated design tool. ShipX is built upon a STEP-compatible product model implemented in an easily extendable database. The database stores ship geometries with related results, which can be generated by calculations or by model testing. By removing the need for file format conversions and re-entering of input for each new program, systematic design studies using highly advanced hydrodynamic analysis tools is fully possible."

A summary from the ShipX information page [26]

A requirement for running VeSim is pre-simulation calculations. This ensures that the simulation can be run in real time or faster. These calculations are done by another ShipX plugin called VERES (Vessel Responses) [2]. VERES calculates ship motions and loads for a mono or multi-hull at varying vessel speed. The motion includes displacements, velocities and accelerations.

By specifying relevant vessel properties (hull, weight, cg etc..) one can achieve accurate vessel behavior for different sea states. VERES only need to run once before simulation.

Advanced wave, current and wind models are implemented (in VeSim) provoking any desired sea state.

5.1 VeSim

Running the ShipX plugin VeSim looks something like this:

The screenshot shows the VeSim browser window. The browser address bar displays 'localhost:81/#'. The page title is 'Case1_1.HeaveControlFederate - SES-Offshore_Service_V'. The interface is divided into a sidebar on the left and a main content area on the right.

Parameters Table:

Name:	Description:	Current value:	New value:
K_p_fan	Proportional gain, tuning parameter for fan-controller	27.000	<input type="text"/> set»
K_p_louwer	Proportional gain, tuning parameter for louver-controller	0.580	<input type="text"/> set»
Q_diag	Diagonal value of Q. Tracking error weights.	10.00	<input type="text"/> set»
R_diag	Diagonal value of R. Input weights.	0.01	<input type="text"/> set»
cg_and_bow_height_diff	Height difference [m] between CG and bow deck.	2.00	<input type="text"/> set»
fan_control_active	Set fan controller active or non-active	true	<input type="button" value="set false»"/>
louwer_control_active	Set louver controller active or non-active	true	<input type="button" value="set false»"/>
point_of_control	Decide what to control: 0 = cg, 1 = vessel bow	1	<input type="text"/> set»
pos_heave_REF	Reference heave position for heave controller (autotuned at startup)	-3.872	<input type="text"/> set»
ref_point_calibrated	Set false to re-calibrate reference point for the controller	true	<input type="button" value="set false»"/>
stdv_x	Standard process deviation. (Process noise)	0.060000	<input type="text"/> set»
stdv_z	Standard measurement deviation. (Measurement noise)	0.010000	<input type="text"/> set»

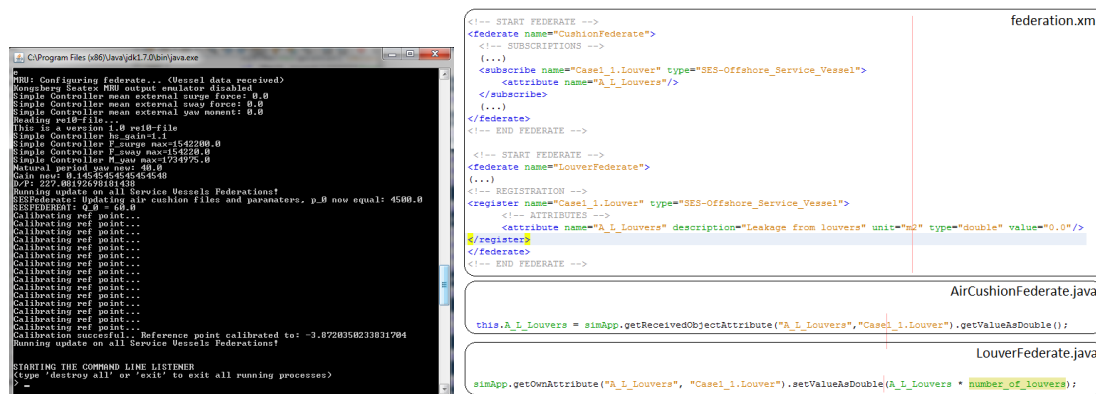
Attributes Table:

Name:	Description:	Current value:	Open graph:
_logicaltime	Federate logical time	359.85 s	<input type="button" value="new window"/> <input type="button" value="trend»"/>
_lookahead	lookahead (time step)	0.05 s	<input type="button" value="new window"/> <input type="button" value="trend»"/>
_stepcycle	step cycle (time used internally by federate)	0.25 ms	<input type="button" value="new window"/> <input type="button" value="trend»"/>
controlled_fan_pos	Wanted fan position from controller (0-100)	49	<input type="button" value="new window"/> <input type="button" value="trend»"/>
controlled_louwer_pos	Wanted louver position from controller (0-100)	50	<input type="button" value="new window"/> <input type="button" value="trend»"/>
noisyPosMeasurement	CG down (Glob. coord.) MRU noisy sensor readings (input to Kalman filter)	-3.87 m	<input type="button" value="new window"/> <input type="button" value="trend»"/>
u	Input from controller	0.86 m/s ²	<input type="button" value="new window"/> <input type="button" value="trend»"/>
u1	Input from controller	5970.04 m/s ²	<input type="button" value="new window"/> <input type="button" value="trend»"/>
u2	Input from controller	4.84 m/s ²	<input type="button" value="new window"/> <input type="button" value="trend»"/>
x_est_pos	Estimated position from Kalmanfilter	-3.74 m	<input type="button" value="new window"/> <input type="button" value="trend»"/>

The sidebar on the left contains several sections: 'Object View' with a 'Change Object View' link; 'Controller' with a tree view including 'Case1_1.SimpleController', 'Environment', 'Logger', 'ScenarioManager', 'Sensor', 'Time', 'Vessel', and 'VesselMotionSolver'; 'CSI Loggers' with 'New CSI Logger', 'New CSI Playback', and 'Available log files'; 'Views' with 'Metric view'; and 'System messages' showing a log of simulation events.

Figure 5.1: VeSim browser window

The blue column to the left is the list of all active federates. The browser enables simulator monitoring and modifying. Note that the figure does not represent the final design.



- (a) Command window for printout (b) Sending an attribute (current area leakage from louvers) from the LouverFederate to AirCushionFederate via the CSI bus

Figure 5.2:

Another tool for verification is printout to the command window displayed in figure 5.2(a). The printout is ordered from the java files.

Figure 5.2(b) shows how the federates communicate with each other through a federate file (federation.xml). This is an example of how the attribute *A_L_Louvers* is sent from the LouverFederate to the CushionFederate. CushionFederate subscribe to LouverFederate. LouverFederate registers its own parameter making it reachable for all other federates. The attribute is sent via the CSI bus. At the bottom of the figure one can observe the corresponding java calls.

5.2 SimVis

SimVis is ShipX simulation visualization:

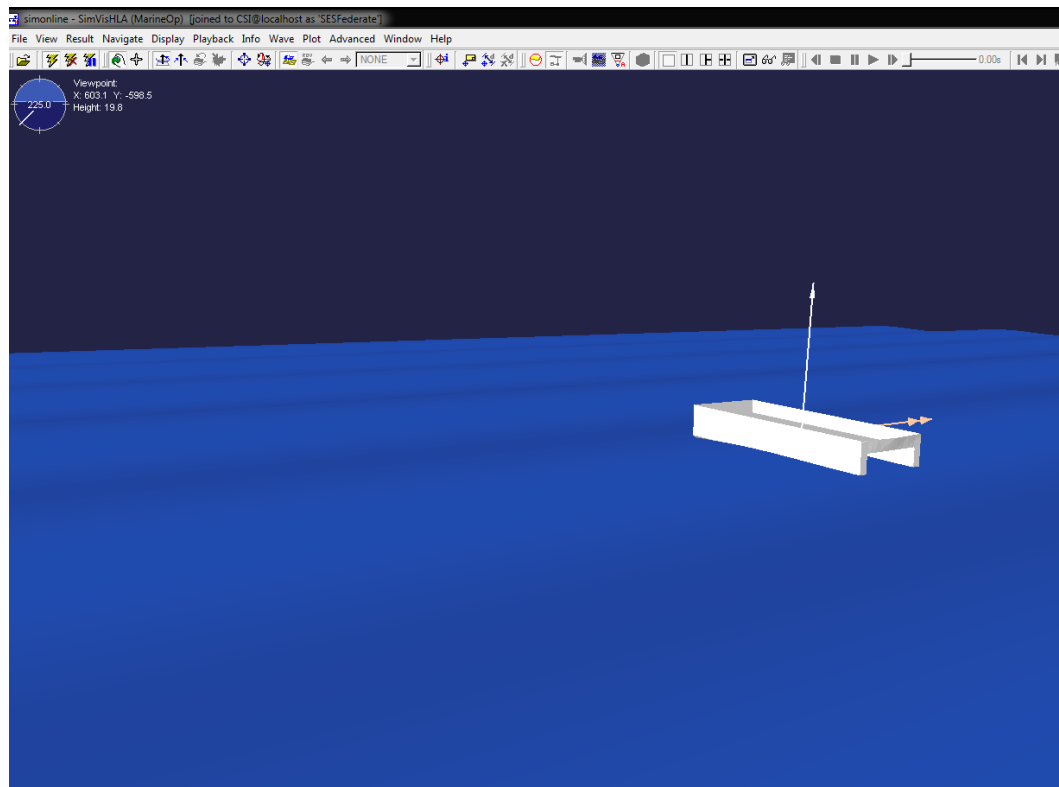


Figure 5.3: SimVis with the simple hull from Case1_1. The arrows are dynamic and shows which forces that are acting on the vessel's center of gravity.

5.3 System setup

- 1) Install ShipX to program files. On the first ShipX run, VeSim and SimVis will be downloaded as plugins. Put these two folders in C:\marintek. Also install NetBeans and java jdk 1.7 or newer (or 1.6 is also good enough) 32 bit, not 64 bit!
- 2) On the thesis enclosure CD-ROM find and copy the folder: SESFederate
- 3) Create and put this folder in C:\
- 4) Open NetBeans, File → open project → locate C:\SESFederate → ok
- 5) When asked for Reference Problems do this: Resolve Problem → Resolve → locate C:\marintek \VeSim\lib and add all the needed jar files.
- 6) Make a shortcut to:

C:\SESFederate\ShipX\root\Fle71D3F37A\XShip4D3E66D0\LoaCE7F6599\runs
\RunCB9EC2B6\input

7) From this folder (the shortcut) you will find the files "VeSim - start_simulation" and "SimVis - start_visualization". This folder will also contain the federation xml file. Inside the subfolder Case1_1 one will find hull geometry, fan characteristic and other files that specifying Case1_1. Inside another subfolder "ShipX" one will find the pre-simulation calculations made by VERES.

8) All the java files are located in C:\SESFederate\src folder is available for editing. The library (standard VeSim) files are not.

9) If questions or problems, feel free to contact me on oeyvind.auestad@gmail.com

Chapter 6

The Existing Model at Project Takeover

This section will describe what was handed over by Trygve H. Espeland. It is a summary made in order to describe the most important aspects concerning the SES model in VeSim. The creation of the SES-model is Espelands project and master thesis at NTNU [3].

The ultimate goal for the SES model is to send the induced air cushion forces and moment to the marintek developed Vessel federation, where it will be added along with the hydrodynamic forces acting on the vessel:

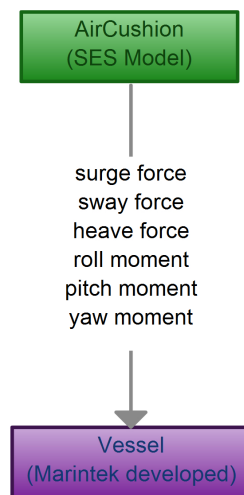


Figure 6.1:

6.1 Introduction

This section will describe the linear theory implemented by Espeland when creating the SES-model. The implementation is based on Faltinsen (see [6]) equations for cushion dynamics. (Eq. (6.5.1) - (6.5.5))

The results presented by Espeland has shown very good resemblance to a real SES [3].

Note that Espelands main java class (which is his only federate class) called SES-Federate has changed name to AirCushion. And the old AirCushion java class has changed name to AirCushionGeometry.

The overpressure in the air cushion is given by:

$$p_c(t) = p_u(t) + p_{sp}(t) \quad (6.1.1)$$

Where $p_u(t)$ is uniform overpressure and $p_{sp}(t)$ is spatial overpressure. Espelands SES-model is simplified by neglecting the spatial pressure variations. According to Wines et. al. [28] this assumption shows very good agreement for heave motions but degenerating results for the pitch motion during high vessel speed. However, this thesis deals with a system at zero speed. In this situation, all longitudinal pressure differations are extremely small [4]. **Therefore, at all practical considerations, a uniform pressure modell is considered very accurate.**

Spatial pressure variations will therefore not be implemented in this SES model, but are discussed in 4.1 - Cobblestone Effects page 18.

Finding the uniform pressure $p_c(t) = p_u(t)$ is the ultimate goal in order to calculate the forces acting on the vessel. Once this is calculated, the 6 DOF forces (surge, sway, heave, roll, pitch and yaw) are found by integrating the dry area of the air cushion multiplied with this $p_c(t)$.

6.2 Cushion Volume

The enclosed air cushion volume Ω is numerically calculated for each time step (0.05s). The SES federate (Case1_1.AirCushion) gets vessel motion and wave elevation as input from other VeSim federations. Respectively Case1_1.Vessel and Case1_1.Wave:

$$\Omega(t) = \iint_{A_c} h_c(x, y) + \eta_3(t) + y\eta_4(t) - x\eta_5(t) - \zeta(x, y, t) dA \quad (6.2.1)$$

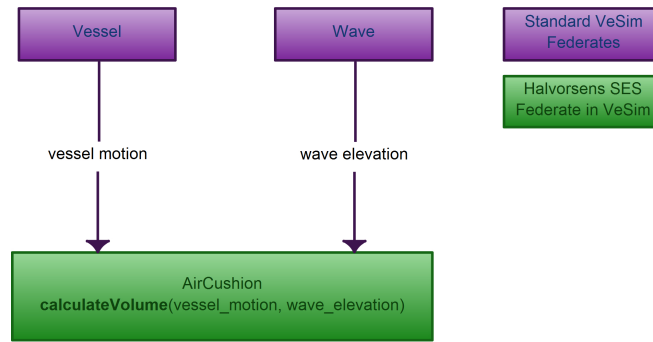


Figure 6.2: The federate class `AirCushion` gets motion and wave elevation as input from the CSI bus and calculates cushion volume

Where η_i correspond to the i -th DOF which is sent from the Vessel federate to the federate java class called `AirCushion` via the CSI bus.

T and ζ are respectively draught and wave elevation fetched likewise from the Wave federate. See figure 6.3.

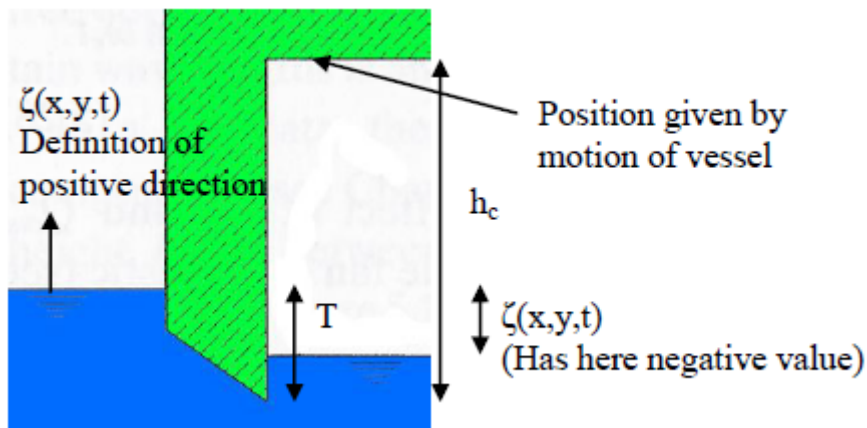


Figure 6.3: Definition for $\text{volume}(\Omega)$ calculations, [9](a)

6.3 Cushion inflow - Fan

As mentioned in section 2 page 5, the air inflow into the air cushion (Q_{in}) is due to fan(s).

$$Q_{in}(t) = Q_0 + Q_{inDyn}(t) \quad (6.3.1)$$

Where Q_0 is the mean air flow static rate, and Q_{inDyn} is the dynamic contribution.

6.4 Cushion outflow - Passive leakage under demi-hull, seals and between demi-hull and seals

The air outflow ($Q_{out}(t)$ through total passive leakage area $A_L(t)$ which is shortened down for $Area_{Leakage}$) is estimated by the formula:

$$Q_{out}(t) = c_n A_L(t) \sqrt{\frac{2p_c}{\rho_a}} = c_n A_L(t) \sqrt{\frac{2p_0(1 + \mu_u(t))}{\rho_a}} \quad (6.4.1)$$

Where $c_n \in [0, 1]$ is a correction term for orifice, p_c is cushion pressure and $\mu_u \in [0, 1]$ is dynamic uniform varying overpressure coefficient. Remember that spatial pressure differences (μ_{sp}) are neglected. The calculation of μ_u is the calculation of the cushion behavior, since:

$$P_c = P_0(1 + \mu_u) \quad (6.4.2)$$

Where p_0 is known. Section 6.5 will describe this calculation.

The sub-sections below describes how the leakage area (A_L) is found.

6.4.1 Leakage under hull

In large sea states one can experience leakage under the demi-hull (the two side hulls). However, in smaller and medium sea states this will not happen.

The lowest point on the hull is checked for leakage (see figure 6.4. If several coordinates are equally low, the one closest to the center line is used, this node is defined as `cushion.localyCoord[secNr][0]`, see the figure. This position responds to the border between the air cushion and the hull.

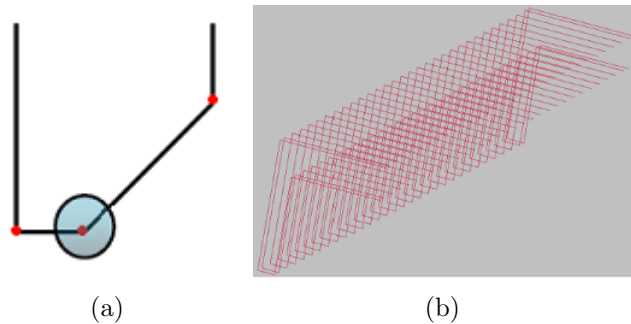


Figure 6.4: Hull section

The algorithm iterates through each section. If the described node is above water line the submergence will be calculated. That is the vertical gap between water

line and the described hull node. $Submergence = cushion.localyCoord[secNr][0] - draught + \text{water level height difference}$ (see fig 2.4).

If this leakage exist the sections static leak area:

$$A = Submergence \cdot dx \quad (6.4.3)$$

Where dx is the width of the section in longitudinal direction. The static leakage is only called initially, assume zero wave propagation and cover leakages that occur if you lift the entire vessel above draft (useful for testing).

Instantously leakage occur if a wave propagation lifts the demi-hull allowing leakage to occur out of the cushion. If a hull node (like described in the section above) is found to be above the water, this sections instant leakage will be:

$$Leakage+ = leakDistance \cdot dL \quad (6.4.4)$$

Where $leakDistance = \min(submergence, cushion.localyCoord[secNr][0])$, and dL is the sections length. (There are a total of 30 sections in longitudinal direction (x-direction) that describes the hull.)

6.4.2 Forces acting on the seal and seal leakage

During the writing of this thesis, Umoe Mandal hired MingKang Wu from MARIN-TEK to improve the dynamics of the stern (bag) and front seal. This modification was done in order to include seal leakage and forces acting on the vessel. The former is created for realistic leakages at zero velocity and the latter did not pre-exist. However, the leakage that (can) occur under the hull remained unchanged. For documentation of this work see [29].

6.5 Air Cusion equations

Three equations must be satisfied in order to calculate the cushion pressure. The rate of air mass which is $\dot{m} = \dot{m}_{in} - \dot{m}_{out}$ and the adiabatic relation $PV^\gamma = \text{constant}$, where the air is treated as ideal gas. The last equation is air out flow (Q_{out}) eq. 6.4.1. Q_{in} is fetched directly from and according to the fan characteristic file.

1. Continuity equation for the air mass inside cushion using the chain rule:

$$\dot{m} = \frac{d}{dt}(\rho_c \Omega) = \dot{\rho}_c \Omega + \rho_c \dot{\Omega} = \rho_a (Q_{in} - Q_{out}) \quad (6.5.1)$$

Where ρ_a and ρ_c is respectively atmospheric density of air and air cushion, Q is cushion air flow rate and Ω is enclosed air cushion volume.

2. Adiabatic equation relating pressure and mass density:

$$\frac{p(t)}{p_0 + p_a} = \left(\frac{\rho_c}{\rho_a} \right)^\gamma \quad (6.5.2)$$

Where p_a, p_0 and $p(t)$ is respectively atmospheric, mean overpressure and total instantaneous air cushion pressure. Using eq (6.5.3) & (6.1.1) and neglecting spatial pressure we get:

$$p(t) = p_a + p_c = p_a + p_0(1 + \mu_u) \quad (6.5.3)$$

The air pressure flow rate in and out is described and is calculated for every iteration. As far as it concerns, these cushion equations that Espelands implemented are the same except for the additional louver leakage area ($A_{L_Louvers}$). Rewriting eq. (6.4.1) yields:

$$Q_{out}(t) = A^* \sqrt{\frac{2p_c(t)}{\rho_a}} = A^* \sqrt{\frac{2p_0(1 + \mu_u(t))}{\rho_a}} \quad (6.5.4)$$

where

$$A^* = c_n(A_{L_Passive} + A_{L_Louvers}) \quad (6.5.5)$$

Using Taylor Expansion on $Q_{out}(t)$ with respect to $\mu_u(t)$ around eq. point zero yields:

$$Q_{out}(t) \approx A^* \sqrt{\frac{2p_0}{\rho_a}} + \frac{1}{2} A^* \sqrt{\frac{2p_0}{\rho_a}} \mu_u(t) \quad (6.5.6)$$

By dividing total leakage into a static and a dynamic term we get:

$$\begin{aligned} A^* &= A_{Stat}^* + A_{Dyn}^*(t) \\ &= A_{L_PassiveStat} + A_{L_PassiveDyn}(t) + A_{L_LouversStat} + A_{L_LouversDyn}(t) \end{aligned} \quad (6.5.7)$$

In static equilibrium condition (steady state) we have that $Q_{in} = Q_{out}$ and $\mu_u = 0$. Using this on eq. (6.5.4) yields:

$$Q_0 = A_{Stat}^* \sqrt{\frac{2p_0}{\rho_a}} \Rightarrow A_{Stat}^* = Q_0 \sqrt{\frac{\rho_a}{2p_0}} \quad (6.5.8)$$

Using eq. (6.5.8) in eq. (6.5.6) yields:

$$\begin{aligned} Q_{out}(t) &\approx \left(Q_0 \sqrt{\frac{\rho_a}{2p_0}} + A_{Dyn}^* \right) \sqrt{\frac{2p_0}{\rho_a}} + \frac{1}{2} (A_{Stat}^* + A_{Dyn}^*) \sqrt{\frac{2p_0}{\rho_a}} \mu_u(t) \\ &= Q_0 + A_{Dyn}^* \sqrt{\frac{2p_0}{\rho_a}} + \frac{1}{2} A^* \sqrt{\frac{2p_0}{\rho_a}} \mu_u(t) \end{aligned} \quad (6.5.9)$$

Inserting this into the continuity equation 6.5.1 for air mass and using that $Q_{Dym} = Q_{in} - Q_0$ yields:

$$\rho_a \left(Q_{inDym}(t) - A_{Dym}^* \sqrt{\frac{2p_0}{\rho_a}} - \frac{1}{2} A^* \sqrt{\frac{2p_0}{\rho_a}} \right) = \frac{dp_c}{dt} \Omega + \rho_c \frac{d\Omega}{dt} \quad (6.5.10)$$

$\frac{dp_c}{dt}$ is fetched from the adiabatic eq. 6.5.2. Re writing this yields:

$$\rho_c = \rho_a \left(1 + \frac{\mu_u(t)p_0}{p_0 + p_a} \right)^{\frac{1}{\mu}} \quad (6.5.11)$$

Taylor expanding and differentiating with respect to time:

$$\frac{d\rho_c}{dt} = \frac{\rho_a p_0}{\rho_a(p_0 + p_a)} \frac{d\mu_u}{dt} \quad (6.5.12)$$

Combining (6.5.12) and (6.5.10) (where ρ_a can be crossed out, Espeland made a calculation error here) yields :

$$Q_{inDym}(t) - A_{Dym}^* \sqrt{\frac{2p_0}{\rho_a}} - \frac{1}{2} A^* \sqrt{\frac{2p_0}{\rho_a}} = \frac{p_0}{\gamma(p_0 + p_a)} \dot{\mu}_u + \left(1 + \frac{\mu_u(t)p_0}{\gamma(p_0 + p_a)} \right) \dot{\Omega} \quad (6.5.13)$$

Can be re-written as:

$$\dot{\mu}_u + A\mu_u(t) = B \quad (6.5.14)$$

Where $\dot{\Omega} = \frac{\Omega_k - \Omega_{k-1}}{dt}$, dt is sampling time (0.05s) and the only unknown is $\mu_u(t)$. Espelands solves this equation in his report p. 28.

6.6 Essential manner of operation

This is the essential parts that take place every time step, post initialization.

While (running):

- 1) Calculate the enclosed cushion volume
- 2) Calculate total cushion leakage
- 3) Look up airflow from fan
- 4) Use results from 1) to 4) to solve air cushion pressure: $p_c = p_0(1 + my)$
- 5) Calculate the forces (6 DOF) acting on the cushion, by integrate dry cushion area multiplied with p_c .
- 6) Calculate and add viscous forces (if enabled) to the calculated cushion forces.
- 7) Send the 6 DOF forces (plus the point of attack coordinate) to the Vessel federation

End

For further details see [3].

6.7 Input/Output Diagram for the Java classes

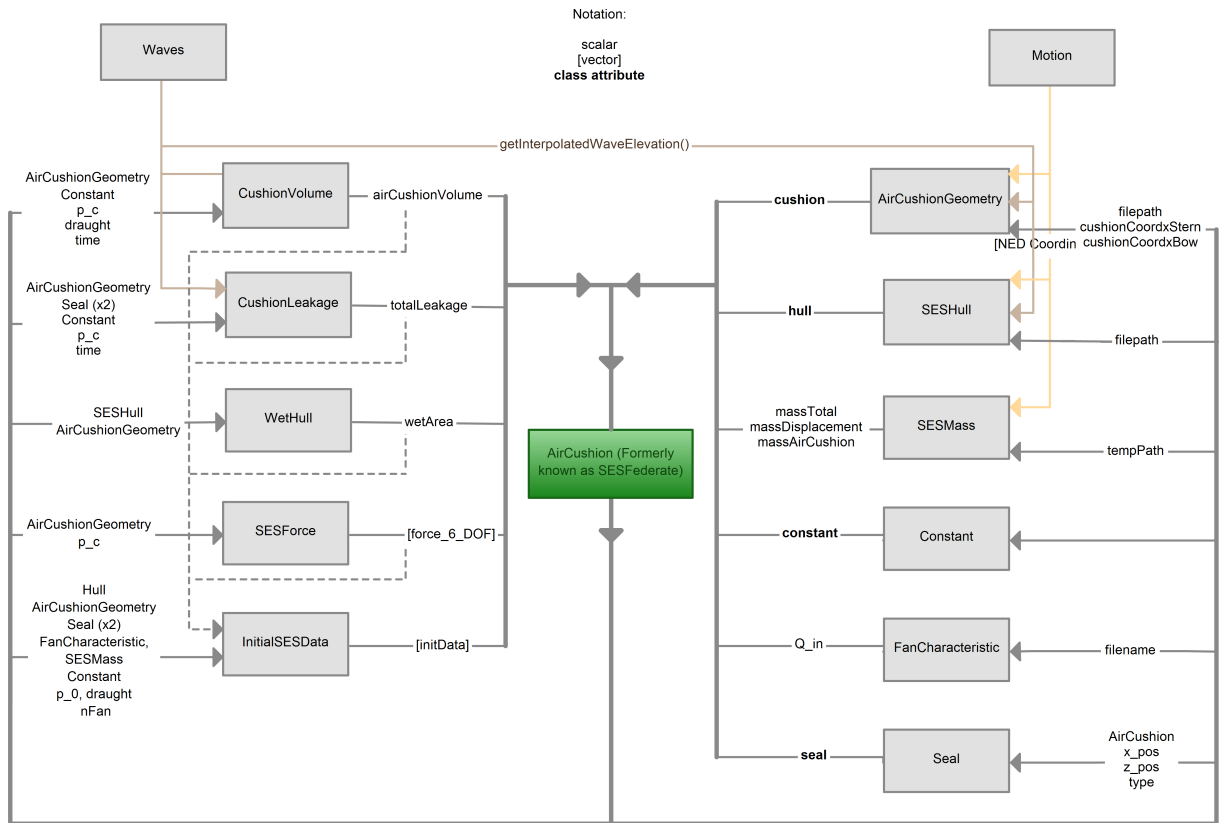


Figure 6.5: Input/Output Diagram for the Java classes at project takeover

Chapter 7

Solution - Heave Control System

A louver and a fan system with saturation limits have been designed and implemented in order to supply the air cushion with realistic air flows. The actuators receive desired actuator position (*controller_louwer/fan_pos*) from the heave controller.

The diagrams below will illustrate the larger picture of the system:

7.1 Heave control system diagrams

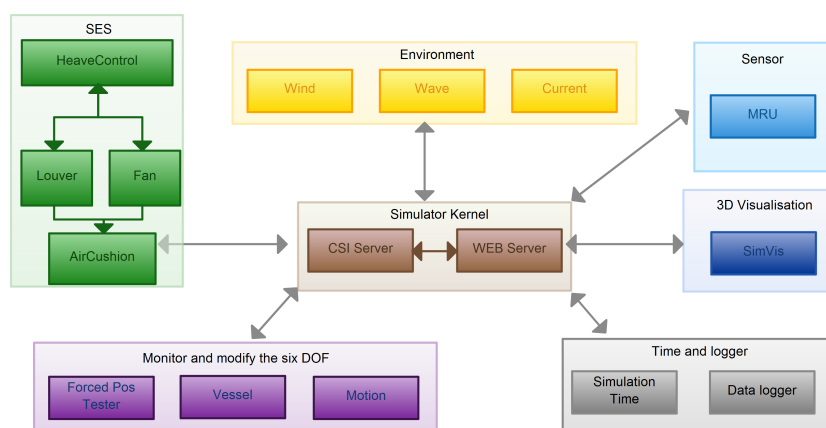


Figure 7.1: VeSim Architecture

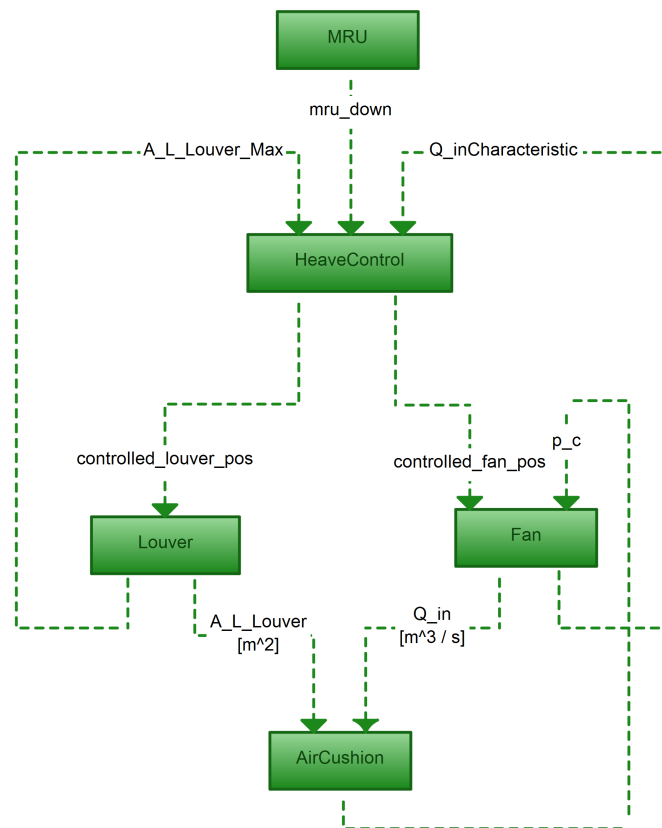


Figure 7.2: Heave Control System

Figure 7.2 describes the implemented system. The MRU is a default federate included in VeSim.

The federate java class AirCusion (name changed from SESFederate) made by Espeland has been highly modified. This include simplification of the code, strongly shortened down main loop, dividing code into separate functions and classes. The code is now more readable.

The remaining federate-boxes have been made by the author of this thesis.

7.2 The Louver System

The louver system is one of the two cushion air flow actuators. The louver actively emit air flow out of the air cushion (Q_{out} [$\frac{m^3}{s}$]). The louver is implemented in Louver.java (see the enclosure) which is a federate class (allowing it to send and receive attributes to other federate classes).

As mentioned; previously there were no louvers implemented in the model. The only cushion air leakages that occurred at project-takeover, was leakages under stern seal, bow seal, hull and between stern seal and hull. The louver system work procedure:

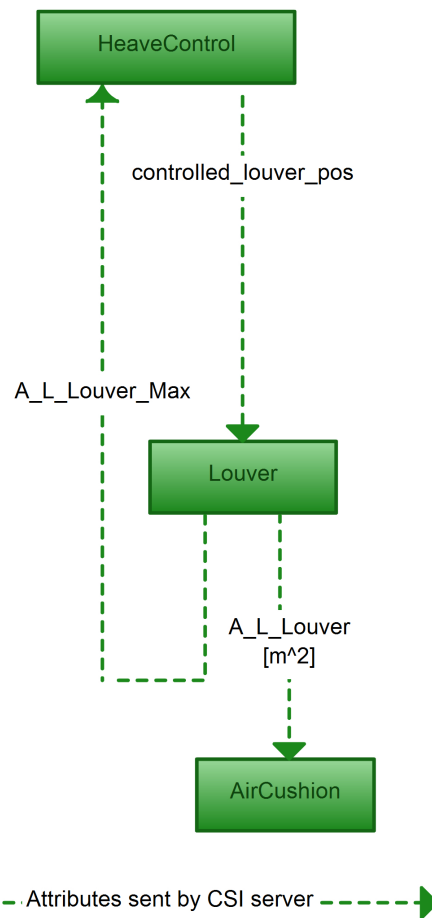


Figure 7.3: Input / Output for louver federate

Initially or on system update:

- I Valve sends a numerical value describing the maximum leakage area possible (A_L_Louver_Max). This value is sent to the Heave Controller

For each iteration:

- II The Louver system receives what position the louver should be set to (controlled_louver_pos). This position is requested by the heave controller.
- III Places the louver pins (or blades) to the demanded position but with a lag (or delay) depending on current pin position. (Saturation of air flow).
- IV When the louver blades are in position, the current leakage area is calculated

and sent to the cushion dynamic equations which is inside the federate class `AirCushion.java`.

The VeSim browser window (see section 5 - Software Tools page 31 or section 7.2.1) visualizes the maximum area leak value ($A_L_Louver_Max$). This value corresponds to the physical maximal leakage area that can occur. Therefore one can experiment with different louver sizes while observing the corresponding effect on the vessel online.

Definition 2. *$louver_pos = 0$ corresponds to a fully closed louver system. Lower blades pointing downwards, blocking all air leakage.*

$louver_pos = 100$ corresponds to a fully open louver system. Lower blades pointing outwards of air cushion, allowing maximum air leakage.

The effect of altering $A_L_Louver_Max$ is visible through heave control. Starting with the control point at the top of a wave: The larger maximum louver area available, the sooner the cushion can empty itself for air until one has reached the bottom of the wave. Thus, allowing a larger Q_{out} [$\frac{m^3}{s}$] corresponds to a larger damping of vertical motion. How much can air can you let out while the wave is decreasing? And visa versa starting the control point at the bottom of a wave.

If it's not already clear, this brings us to the fundamental job for the louver system at wind-mill docking position. When the control point (center of gravity or wet-deck at the bow) is in equilibrium position, the louvers (along with the fan) is at mean value position which corresponds to $louver_pos = 50$. This will always be true since the equilibrium point or control reference point is found by actuating the fan and louvers to the mean position. At this position the louver air leakage equals:

$$A_L_Louvers = \frac{A_L_Louver_Max}{2} \quad (7.2.1)$$

The same principle yields for the fan system, only here $Q_{in} = \frac{Q_{inCharacteristic}}{2}$ which will be explained later.

When the control point reaches the top of an any given wave, it is desired that the louvers are at a maximum gap giving a maximum air leakage ($louver_pos = 100$) working against the increased heave position caused by the wave propagation. An adaptive control system is therefore required. This will be discussed later.

Contrary, at the bottom of the wave one wants to increase the control points heave position, leaving the louvers at zero gap ($louver_pos = 0$). A closed louver along with a running fan results in an increased cushion volume and increased heave position.

7.2.1 Louver Federate Interface

The louver system was created in order to perform motion control, but also to make the air flow (into the cushion equation, see eq. 6.5.13) as realistic as possible. The situation at project take-over involved leakage that did not possess a proper source. All leakage are now calculated either from the louver, under & between seals and hull.

When designing the Wave Craft, it is desired to try out different solution for louver design. This concern varying the physical size and the number of louvers and see the results in the simulation. At docking mode (as well as in transfer mode), one must possess enough leakage area capacity in order to perform satisfactory heave damping.

Since this SES-model only concern cushion uniform pressure variations, the louvers doesn't possess any longitudinal (or latitudinal) position in the cushion. The model only considers the total leakage area out of the cushion.

Case1_1.Louver - SES-Offshore_Service_Ve

Parameters

Name:	Description:	Current value:	New value:
A_L_Louver_Max	Area gap for one louver (Max leakage area per louver)	1.00m2	<input type="text"/>
number_of_louvers	The number of louvers	4	<input type="text"/>
open_close_actuator_delay	Define the delay, going from a closed to an open louver	0.500s	<input type="text"/>

Attributes

Name:	Description:	Current value:	Open graph:
A_L_Louver_Max	Max leakage area per louver	1.000m2	new window ▼
A_L_Louvers	Total leakage from all louvers	1.960m2	new window ▼
A_L_Mean_Louvers	Mean leakage for all louvers: fully_open_louver_area / 2	2.000m2	new window ▼
_logicaltime	Federate logical time	1486.86s	new window ▼
_lookahead	lookahead (time step)	0.02s	new window ▼
_stepcycle	step cycle (time used internally by federate)	0.18ms	new window ▼
louver_pos	Actual louver position (0 - 100)	49	new window ▼

Figure 7.4: The Louver Federate interface in VeSim

The figure above shows the louver federate interface. The two first parameters are self-explanatory. The third is defining the actuator delay described in section 7.5.1 - Actuator saturation, page 68. The three first attributes are also self-explanatory but note that *A_L_Louvers* denotes current total leakage area from all valves, while the other two describes properties of each single louver.

The next three are default time attributes and doesn't concern the louver federate itself.

The last two attributes respectively describes what position (from 0 - 100) the

louver **should be** in (in order to damp heave motion) and the **actual** louver position at current time step. The difference between these two correspond to the parameter "open_close_actuator_delay" described in section 7.5.1.

7.2.2 Contraction of air flow out from the air cushion

The contraction of air flow (c_n) is a function of leakage area and shape. It involves all leakage which mainly is the louver leakage. The passive leakage is a lot smaller than louver leakage. The value is assumed constant for all leakages, but changes whenever one change the physics of the actuator and design pressure (P_0). The software will automaticly calculate the contraction value.

The contraction value is vital in order to keep the cushion equation valid. Remember that the total air flow out is:

$$Q_{out} = c_n(A_{L_Louvers} + A_{L_Passive})\sqrt{\frac{2p_c(t)}{\rho_a}} \quad (7.2.2)$$

Where $\rho_a = 1.23$ (mass density of air), c_n is the contraction of air flow.

At equilibrium (static) air flow there will be approximately zero passive leakage:

$$Q_{in} = Q_{out} \quad (7.2.3)$$

$$Q_0 = c_n \left[\frac{\text{Number_of_Louvers} \cdot A_{L_Louvers_Max}}{2} \right] \sqrt{\frac{2p_0}{\rho_a}} \quad (7.2.4)$$

$$Q_0 = c_n \cdot A_{L_Louvers_MEAN} \sqrt{\frac{2p_0}{\rho_a}} \quad (7.2.5)$$

Re-arranging this results in:

$$c_n = \frac{Q_0}{A_{L_Louvers_MEAN} \sqrt{\frac{2p_0}{\rho_a}}} \quad (7.2.6)$$

Note that the total number of fans will vary Q_0 since Q_0 is the sum of each fan at design pressure p_0 [Pascal].

The function that calculats c_n is named calculateContraction() was implemented and put into Calculations.java. The code attributes are named likewise as the equations above.

7.3 The Lift Fan System

The lift fan is the second air flow actuator. As opposed to the louver, the lift fan provide air cushion in flow, $Q_{in} [\frac{m^3}{s}]$. The fan is implemented in Fan.java which is a federate class.

In contrast to simulation done by Kaplan and Sørensen & Egeland; the lift fan and the air inflow contribution to the cushion is implemented by a nonlinear fan characteristic table. This characteristic table shows the relation between air flow into the cushion v.s. current cushion pressure given a constant fan motor speed (constant rpm). The cushion pressure is calculated every iteration and the corresponding accessible air in-flow from the fan can be directly fetched from the fan file describing this characteristic. This file can be found in the enclosure at: SESFederate/Case1.1/Case1_1.fan and the relation is showed in figure 7.5.

The lift fan is typical made by the the lift-fan manufacture.

Figure 7.5 shows that a new (more powerful) lift fan was designed in order to meet.

Explanation of the term "fan position":

Umoe Mandal has successfully experienced with varying the fan inflow area in order to vary the output air flow. This is explained in section 4.2.5, Fan Area Control Design - page 23. The variation of the inlet area is physically done by varying the position of a cone-object in and out towards the fan inlet. For instance, fan_pos = 0 corresponds to the scenario when the cone-object is fully pressed towards the fan inlet area, covering the entire inlet area. Thus the induction zero. The fan does not receive any air and will not produce any either (the vacuum principle). At fan_pos = 100 the cone-object is completely pulled out and does not affect the inlet area. The relationship between fan inlet area and and fan position is linearized.

One can easily add multiple fans. This benefits the project since Umoe is interesting in trying different design approaches on the Wave Craft.

Fan control has been implemented by varying the fan air-inlet area in order to obtain heave control. This allows the lift fan to produce airflow between 0 percent openness and the characteristic airflow ($Q_{inCharacteristic}$ which is 100 percent openness) which is fetched every iteration. This "percent openness" is in the code noted as *fan_pos*. The lift fan is running on constant motor speed.

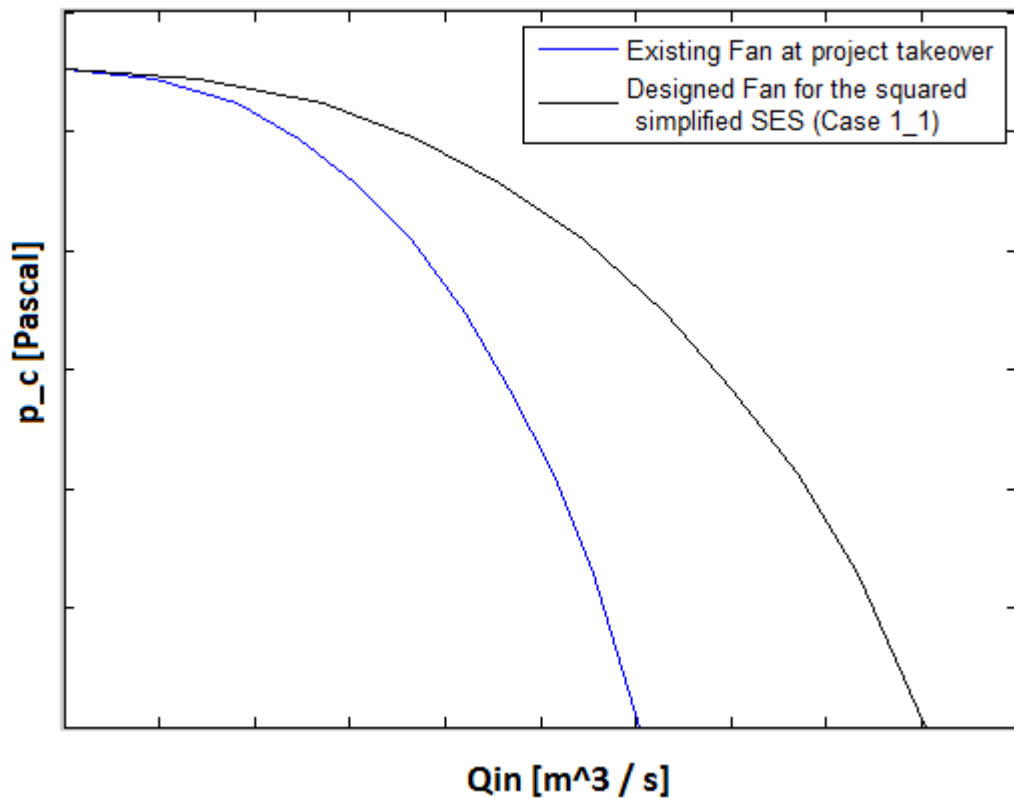


Figure 7.5: Fan characteristic

Positioning the "fan choker" has time limitations. An actuator delay and air flow rate restriction is implemented, see section 7.5.1.

The fan has been divided into a separate federation, and no longer as a java class. This has been done in order to try to separate the actuator from the software package that is being developed, making the system as realistic as possible. Figure 7.6 below illustrates this separation principle.

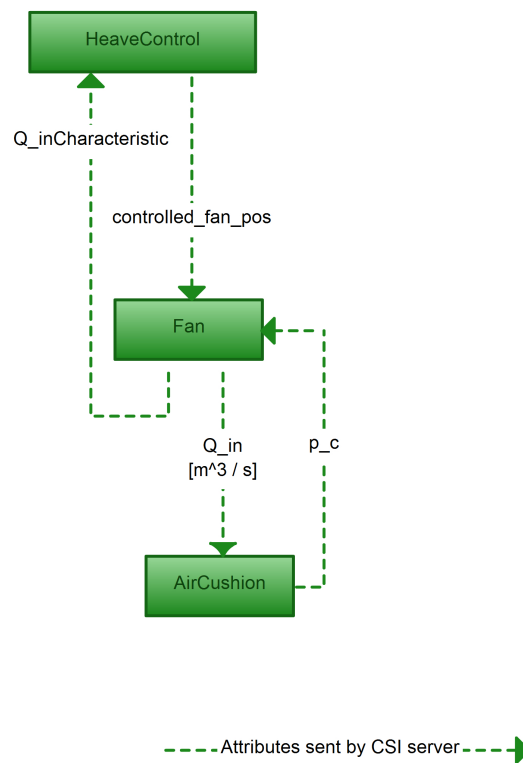


Figure 7.6: Input / Output diagram for the Fan federate

The lift fan systems essential algorithm visualized in figure 7.6:

- I The fan system reads current cushion pressure (p_c)
- II The fan system looks up the air inflow (Q_{in}) that corresponds to the given cushion pressure. This value is noted $Q_{in_Characteristic}$ and sent to the controller (HeaveControl).
- III The controller can now calculate a desired air in-flow rate. This air flow value can vary between 0 (controlled_fan_pos = 0 which correspond to $Q_{in} = 0$) and maximum available fan contribution (controller_fan_pos = 100 which corresponds to $Q_{in} = Q_{in_Characteristic}$). Remember that $Q_{in_Characteristic}$ will vary each time step based on current cushion pressure. The controller sends the attribute controlled_fan_pos to the fan system.
- IV The fan system receives this desired position to be in. A lag occur while transferring the fan from current(fan_pos) to the desired position. This lag is described in section - 7.5.1 - Actuator saturation.

V The air flow (Q_{in}) sent from the Fan to AirCushion is based on the current position of the fan, and not the desired fan position (from the controller)

7.3.1 Fan Federate Interface

Similar to the louver system, the fan does not possess any spatial position of the fan. The cushion pressure is uniform (as well as a real full-scale SES lying at zero speed) implying that such a thing would be pointless.

Case1_1.Fan - SES-Offshore_Service_Ves

Parameters

Name:	Description:	Current value:	New value:
number_of_fans	Select number of fans	1	<input type="text"/>
open_close_actuator_delay	Actuator lag while going from closed to open louvers	0.500s	<input type="text"/>

Attributes

Name:	Description:	Current value:	Open graph:
Q_0	Equilibrium air flow. Air flow actuators at 50% effect	126.073m3/s	<input type="button" value="new window"/> ▼
Q_in	Current air flow into cushion from the fan(s)	126.114m3/s	<input type="button" value="new window"/> ▼
Q_in_characteristic	Max air flow into cushion available (as a function of p_c) for EACH fan	125.847m3/s	<input type="button" value="new window"/> ▼
_logicaltime	Federate logical time	841.06s	<input type="button" value="new window"/> ▼
_lookahead	lookahead (time step)	0.02s	<input type="button" value="new window"/> ▼
_stepcycle	step cycle (time used internally by federate)	0.24ms	<input type="button" value="new window"/> ▼
fan_pos	Actual fan position from controller (0-100)	100.000	<input type="button" value="new window"/> ▼

Figure 7.7: The Lift Fan interface in Vesim

The first parameters of figure 7.7 is self-explanatory and the latter one is ex-

plained in section 7.5.1 - Actuator saturation, p. 68.

Attributes: Remember that $Q_{in_characteristic}$ is the air flow value obtained by looking up in the fan characteristic table showed in figure 7.5. This is the maximum possible airflow from **every single** fan, while Q_0 and Q_{in} is total airflow from all fans. However, the example given in the figure above possesses only one fan.

fan_pos denotes the percent of full air flow effect and this is chosen by the heave controller.

7.4 Heave Control

An important aspect that separate this control system from the one discussed in section 4 - Control Literature Review, is that the presented thesis controls in order to obtain a specific heave position (η_{REF}^3), and not a specific cushion pressure ($p_{c,REF}$).



Figure 7.8: The Wave Craft at zero speed in control mode next to a wind turbine. The vessel bow is the control point. A video simulating the motion damping can be found in the DVD enclosure. See "Wave Craft at turbine.wmv"

This section covers what happens in the HeaveControl federate (HeaveControl.java) and the state estimation filter (Kalmanfilter.java). Process, control design and stability will be discussed.

The diagram below completely describes the input/output attributes for the heave controller and how the control system works:

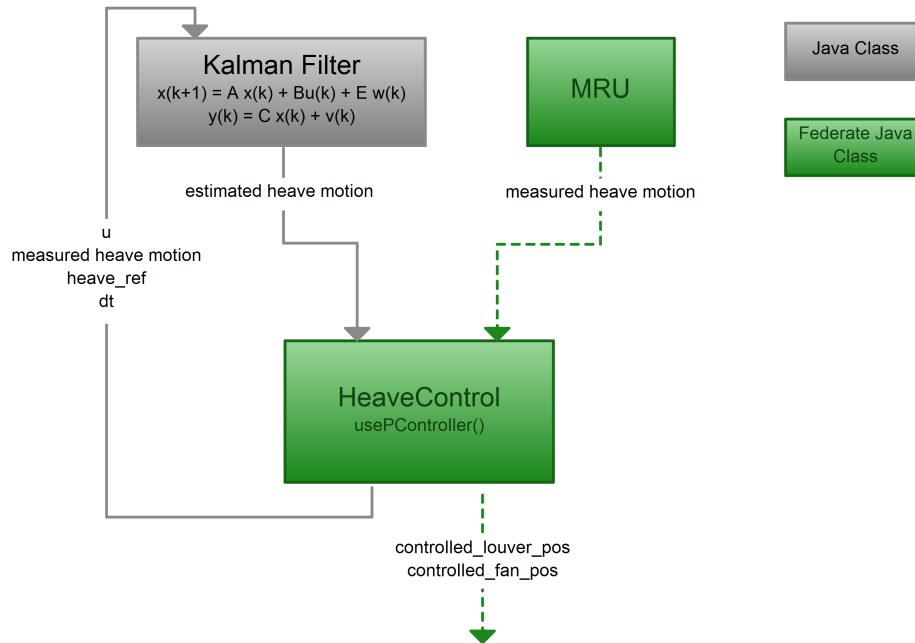
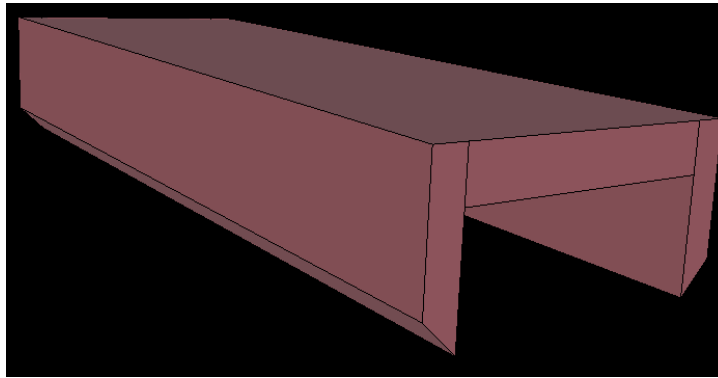


Figure 7.9: Heave Control and Kalman filter

The implementation consists of:

1. Hull design described in figure 7.10 with corresponding sea-keeping and resistance calculations performed in VERES.
2. Process plant for the Kalman filter, a double integrator (the equation of motion).
3. The heave control is performed by a proportional controller.
4. The applied lift fan can be found in figure 7.5.

In his master thesis [3], Espeland presents a simple straight sided shape hull with corresponding VERES calculations called Case1_1. Separate VERES calculations were done for the Wave Craft simulation using the specific Umoe Mandal developed Wave Craft hull.



(a) Hull model used for VERES calculations and simulation for the simplified square SES

Main details	Symbol	Value	Unit
Length over all	L_{oa}	30	m
Length between perpendiculars	L_{pp}	30	m
Height to wet deck relative base line	h_c	3.5	m
Moulded depth	D_r	5	m
Breadth	B	10	m
Breadth demi hull	B_d	1	m
Draught	T	1.20	m
Wetted surface (zero speed)	S_D	144.98	m^2
Static air cushion volume	Q_0	647	m^3
Cushion length	L_c	30	m
Mean cushion breadth	B_c	8	m
Static overpressure in air cushion	p_0	4000	Pa
Ride control parameter	k	0	[-]
Displacement	-	42	ton
Air cushion support	-	70	%
Air cushion lifted	-	98	ton
Total mass	M	140	ton
Vertical center of gravity, relative base line	V_{CG}	3	m
Longitudinal center of gravity, relative stern	L_{CG}	15	m
Distance between sections in *.mgf file	-	1	m

(b) Main dimensions and data

Figure 7.10: Case1.1 is Espelands hull and sea-keeping calculations [3]

The second simulation case is the Wave Craft. and corresponding hull and VERES calculations. Details considering these aspects will not be given.

7.4.1 Heave Control Federate Interface

The VeSim browser window for the heave controller:

Case1_1.HeaveControl - SES-Offshore_Ser

Parameters

Name:	Description:	Current value:	New value:
K_d	Derivative gain, tuning parameter for controller	0.200	<input type="text"/>
K_p	Proportional gain, tuning parameter for controller	1.000	<input type="text"/>
cg_and_bow_height_diff	Height difference [m] between CG and bow deck	2.00	<input type="text"/>
fan_control_active	Set fan controller active or non-active	true	<input type="text"/>
louver_control_active	Set louver controller active or non-active	true	<input type="text"/>
point_of_control	Decide what to control: 0 = cg, 1 = vessel bow	1	<input type="text"/>
pos_heave_REF	Reference heave position for heave controller (autotuned at startup)	-3.799	<input type="text"/>
ref_point_calibrated	Set false to re-calibrate reference point for the controller	true	<input type="text"/>
stdv_x	Standard process deviation. (Process noise)	0.060000	<input type="text"/>
stdv_z	Standard measurement deviation. (Measurement noise)	0.010000	<input type="text"/>

Attributes

Name:	Description:	Current value:	Open graph:
_logicaltime	Federate logical time	152.32s	<input type="button" value="new window"/>
_lookahead	lookahead (time step)	0.02s	<input type="button" value="new window"/>
_stepcycle	step cycle (time used internally by federate)	0.31ms	<input type="button" value="new window"/>
controlled_fan_pos	Wanted fan position from controller (0-100)	98	<input type="button" value="new window"/>
controlled_louver_pos	Wanted louver position from controller (0-100)	51	<input type="button" value="new window"/>
noisyPosMeasurement	CG down (Glob. coord.) MRU noisy sensor readings (input to Kalman filter)	-3.70m	<input type="button" value="new window"/>
u	Output from controller, input to process equation and actuators	0.01m/s ²	<input type="button" value="new window"/>
x_est_pos	Estimated position from Kalmanfilter	-3.81m	<input type="button" value="new window"/>
x_est_vel	Estimated velocity from Kalmanfilter	-0.03m	<input type="button" value="new window"/>

Figure 7.11: Heave Control Federate Interface

The parameters and attributes are explained in the description field..

7.4.2 Mathematical model

The mathematical model is implemented in order to estimate non-measurable states ($\dot{\eta}^3, \ddot{\eta}^3$) and to reject the noise that lays upon a measurement. A Kalman filter has been implemented and the only measurement available is heave position. The result will be illustrated in 8 - Results, figure 8.2 and 8.3.

The equation of motion:

$$p_t = p_{t-1} + v_{t-1}t + \frac{1}{2}a_t t^2 \quad (7.4.1)$$

$$v_t = v_{t-1} + a_t t \quad (7.4.2)$$

where p_t , v_t and a_t respectively are position, velocity and acceleration at current time step t .

Re-writing this to heave, heave rate and heave acceleration, respectively η_t^3 , $\dot{\eta}_t^3$ and $\ddot{\eta}_t^3$ at the control point yields (note that the power to 3 indicates the third degree of freedom which is heave):

$$\eta_t^3 = \eta_{t-1}^3 + \dot{\eta}_{t-1}^3 t + \frac{1}{2}\ddot{\eta}_{t-1}^3 t^2 \quad (7.4.3)$$

$$\dot{\eta}_t^3 = \dot{\eta}_{t-1}^3 + \ddot{\eta}_{t-1}^3 t \quad (7.4.4)$$

Also note that the implemented system can change between two control points; either vessel center of gravity or vessel bow. This change corresponds to position placement of the MRU-sensor (which is set in the MRU-fedrate) and different initial heave position.

7.4.3 State space model

The mathematical model can be described on state space form:

$$\dot{\mathbf{x}} = \mathbf{A}\mathbf{x} + \mathbf{B}u \quad (7.4.5)$$

and measurement equation:

$$y = \mathbf{C}\mathbf{x} \quad (7.4.6)$$

$$\mathbf{x} = \begin{bmatrix} \eta_t^3 \\ \dot{\eta}_t^3 \end{bmatrix} \quad u = \ddot{\eta}_t^3 \quad \mathbf{A} = \begin{bmatrix} 1 & t \\ 0 & 1 \end{bmatrix} \quad \mathbf{B} = \begin{bmatrix} \frac{1}{2}t^2 \\ t \end{bmatrix} \quad \mathbf{C} = [1 \quad 0] \quad (7.4.7)$$

Thus, it is the heave acceleration $\ddot{\eta}_t$ that will be used as feedback to the system.

The corresponding discrete time model is simply:

$$\mathbf{x} = \begin{bmatrix} \eta^3[k] \\ \eta^3[k+1] \end{bmatrix} \quad u = \eta^3[k+2] \quad \mathbf{A} = \begin{bmatrix} 1 & dt \\ 0 & 1 \end{bmatrix} \quad \mathbf{B} = \begin{bmatrix} \frac{1}{2}dt^2 \\ dt \end{bmatrix} \quad (7.4.8)$$

The theoretical model in eq. (7.4.6) demands ideal sensors and actuators. This involves linearity and instantaneous with no noise. The process plant is a double integrator based on the equation of motion of the control point (either vessel bow or CG). Therefore, the process noise involves actuator inaccuracy and wave propagation disturbance, while a MRU measurement will possess some noise with a given magnitude.

Kalman filter:

Details considering derivation of the Kalman filter will be given in appendix B.

Given system noise, a Kalman filter produces values that tend to be closer to the truth than measurements and their associated calculated/predicted values. By weighting the relationship between predicted and measured states, a Kalman filter is an optimal state estimator.

The Kalman filter's process and measurement noise is assumed to be zero mean Gaussian white noise.

Consider the following state space model for state prediction:

$$\dot{\mathbf{x}} = \mathbf{A}\mathbf{x} + \mathbf{B}u + \mathbf{E}w \quad (7.4.9)$$

$$y = \mathbf{C}\mathbf{x} + v \quad (7.4.10)$$

Where $\mathbf{E}w$ and v respectively denote process and measurement error/noise terms or co-variance matrices. The rest of the terms correspond to the mathematical model from the former section.

The standard measurement deviation is defined as (σ_y) and since the system is a single input single output system:

$$v = \sigma_y^2 \quad (7.4.11)$$

The standard process deviation is defined as (σ_{ACC}^2) denoting the magnitude of the input process noise. Thus, the process noise is defined to appear through the process input u , therefore one wishes to see on the effect this has on the given states $(\eta^3, \dot{\eta}^3)$. Remember that a co-variance matrix (\mathbf{Q}) for a two state system, e.g. the states are position (p) and velocity (V):

$$\mathbf{Q} = \begin{bmatrix} \sigma_p \sigma_p & \sigma_p \sigma_v \\ \sigma_v \sigma_p & \sigma_v \sigma_v \end{bmatrix} \quad (7.4.12)$$

Therefore, given $\mathbf{B} = \begin{bmatrix} b_1 \\ b_2 \end{bmatrix}$:

$$\mathbf{E}\mathbf{w} = \begin{bmatrix} b_1 b_1 & b_1 b_2 \\ b_2 b_1 & b_2 b_2 \end{bmatrix} \sigma_{ACC}^2 = \begin{bmatrix} \frac{1}{4} dt^4 & \frac{1}{2} dt^3 \\ \frac{1}{4} dt^3 & dt^2 \end{bmatrix} \sigma_{ACC}^2 \quad (7.4.13)$$

Since the process noise also includes the wave propagation, the final design after trial and error gave a process deviation six times larger than the measurement deviation:

$$\sigma_{ACC}^2 = 0.06 \quad (7.4.14)$$

$$\sigma_y^2 = 0.01 \quad (7.4.15)$$

7.4.4 Controller Design

Last section showed that the Kalman filter's input is $u = \ddot{\eta}_3$.

This is successfully implemented by setting a direct but saturated connection between the heave acceleration and the actuators, where the connection-dynamics are held by the proportional gain K_p . For instance, opening a louver will excite a heave acceleration towards the center of the earth (positive z -direction in the global NED frame). While increasing the lift fan air flow will produce an acceleration upwards (negative z -direction in the global NED frame).

Thus, both actuator inputs are proportional to the heave acceleration, but with switched signs.

Finding the connection-dynamics between heave acceleration and actuator is done by tuning the proportional gain K_p using a trial and error approach. In addition one must saturate away any non-possible actuator positions. For instance, the current leakage area can not exceed maximum physical louver area and the fan air inflow must be non-negative. The input feedback signal u is saturated at both fan and louver actuator limits, therefore it is important to tune both gains so both the controlled actuator position is saturating in order to obtain maximum damping effect. If tuned to high, the vessel will not regain equilibrium position. Figure 8.8 in section 8 illustrates a satisfactory actuator behavior.

The proportional controller where the heave acceleration is proportional to the actuator position:

$$error = \eta_{REF}^3 - \eta_{est}^3 \quad (7.4.16)$$

$$u = error \quad (7.4.17)$$

Next step is to saturate u according to section 7.5.1 - Actuator saturation. u which is heave acceleration is fed back through the kalman filter.

The actuator input:

$$u_{LOUVER} = K_{p_LOUVER} * u; \quad (7.4.18)$$

$$u_{FAN} = -K_{p_FAN} * u; \quad (7.4.19)$$

Where u_{louver} and u_{fan} is respectively explained in section 7.2 and 7.3.

The result section 8.1 - Process estimating - Kalmanfiltering proves that the Kalman filter estimates the states with high precision compared to the true states. This means that one can easily add a derivative effect to the controller. Along with the already existing proportional effect, this forms a PD-Controller:

$$u = \dot{\eta}^3 = [(K_{p_LOUVERS} + K_{p_FAN}) \quad (K_{d_LOUVERS} + K_{d_FAN})] \begin{bmatrix} e \\ \dot{e} \end{bmatrix} \quad (7.4.20)$$

Where K_{p_X} and K_{d_X} is respectively proportional feedback and derivative gain and:

$$e = \eta^{3,REF} - \eta_{est}^3 \quad (7.4.21)$$

$$\dot{e} = \dot{\eta}^{3,REF} - \dot{\eta}_{est}^3 = 0 - \dot{\eta}_{est}^3 = -\dot{\eta}_{est}^3 \quad (7.4.22)$$

However, no significant improvement was observed. It was therefore decided to drop the derivative effect (although the PD-controller is implemented in the code, but derivative gains are set to zero).

7.4.4.1 Alternative fan control:

At the end of the writing of this thesis, an alternative approach for fan control was implemented in order to try to achieve better damping effect from the fan. This effect was achieved. The approach was implemented to decrease complexity and from observing that the major damping effect was performed by the louvers.

Briefly explained; instead of controlling around the set point $\frac{Q_{fanCharacteristic}}{2}(P_0)$ the controller uses $Q_{fanCharacteristic}(P_0)$ instead. Previously, the controller finds its equilibrium point by setting both actuators (louver and fan) to 50% effect. Now in order to find the equilibrium controller point the louver is set 50% open, while the fan is running at 100% effect. Thus, fan_pos = 100 and louver_pos = 50.

This indicate better performance. With the control point (cg or bow) at the top of a wave the uniform cushion pressure will be at a minimum. At the bottom of a wave the pressure will be maximized. Remember the fan characteristic figure (7.5): low cushion pressure corresponds to a high outflow air rate from the fan ($Q_{in}[\frac{m^3}{s}]$), while a high cushion pressure corresponds to a lower outflow air rate from the fan.

Therefore, the most important job performed by fan control is to choke the fan at a wave top, where the air-flow is maximized (on a wave top one wants to decrease the heave position).

With the control point is at the bottom of a wave, the pressure will be large, thus the fan outflow low. While one wants to increase its heave position, not much effect is gained from the fan. Therefore it is better to have the fan positioned at full effect (fan_pos = 100).

Another aspect was changed. Prior to this the change, the fan control is described as (for simplicity, not showing derivative effect):

$$Q_{in} = \frac{Q_{inCharacteristic}}{2} + u_{FAN} \quad (7.4.23)$$

(Remember that $Q_{inCharacteristic}$ changes every iteration) and:

$$u_{FAN} = K_{p.FAN}(\eta_{REF}^3 - \eta^3) \quad (7.4.24)$$

The controller is now changed to follow the exact complimentary value of the louver position. The fan actuator is at the complete oposite position as louver actuator.

For instance when the louver is at 63% openness, the fan gives 37% of maximal effect. Using this along with the new set point as specified above has showed great improvement. The new way of controlling the fan is to look up the louver position according to the following figure:

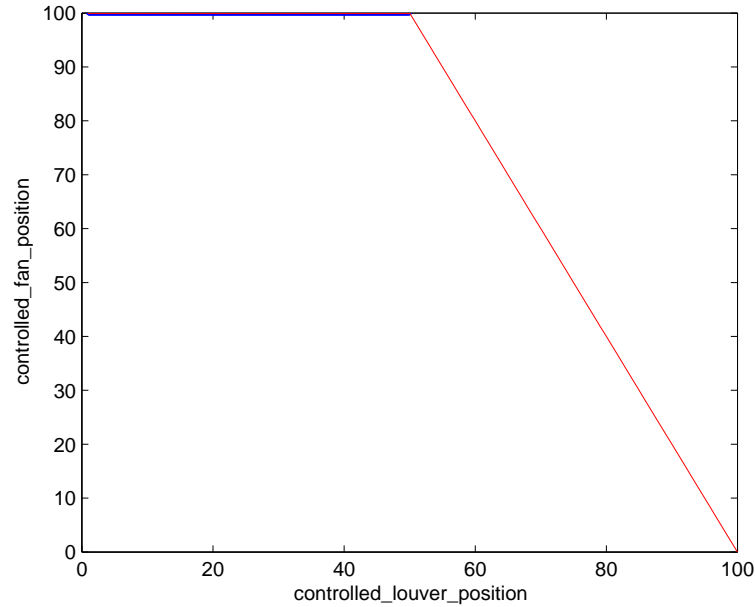


Figure 7.12: New fan controller which is applied in the latter result section 8.6 and discussed in section 8.5 - Alternative set point for fan control page 80.

To sum up the alternative control structure:

$$u = K \cdot error = K \cdot e \quad (7.4.25)$$

Where K is a scalar and the error as described above. Then one must saturate u according to section 7.5.1 - Actuator saturation. The louver position yields:

$$louver_pos = 100 \left(\frac{\frac{A_{L.Louver.MAX}}{2} + u}{A_{L.Louver.MAX}} \right) \quad (7.4.26)$$

fan_pos is calculated according to figure 7.12:

$$fan_pos = f(x) = 100 \cdot \mathcal{H}[50 - x] + (100 - 2 \cdot (x - 50)) \cdot \mathcal{H}[x - 50] \quad (7.4.27)$$

Where x is the louver position and $\mathcal{H}[x]$ is the heaviside step function:

$$\mathcal{H} = \begin{cases} 0 & x < 0 \\ \frac{1}{2} & x = 0 \\ 1 & x > 0 \end{cases} \quad (7.4.28)$$

A positive aspect with the alternative control structure versus the former is that it is easier to tune and decreases complexity. A negative aspect is that both the actuators can't be utilized at fully effect at the same time.

Thus, if the louver leakage area has reached its maximum value, and this corresponds to `louver_position = 100`, then `fan_position` will equal zero, even tough it could be favourable to obtain small but low air inflow. Earlier the two actuators where independant of each other. Now they are dependant. It is important to discuss and test both these setups due to these important pros and cons.

7.4.5 Stability properties

Based on a Kalman filter that follows the true state solution (heave position and heave velocity) see figure 8.2 and 8.3. This figure shows the accuracy based on only a noisy heave position measurement available. Since the filter shows such satisfying results the stability properties of the closed loop system will be discussed. Since the process input is proportional to the actuator input, the analyse is done using superposition on the fan and louver controller, simply using $u = K \cdot error$.

The frequency response for the closed loop system is:

$$\mathbf{y}(s) = \mathbf{H}(s)r = \mathbf{H}(s)x_1^{REF} \quad (7.4.29)$$

Where

$$x_1^{REF} = \eta_{REF}^3 \quad (7.4.30)$$

$$H(s) = \frac{\frac{1}{2}K dt^2}{s^2(1 - dt) + \frac{1}{2}K dt^2 - 1} \quad (7.4.31)$$

The derivation of this expression can be found in appendix D.

Plotting the Bode diagram for H and using Gardner 2005, chapter 4.6.2 that states that the closed loop system is stable when the gain-crossover frequency is less than 1 (0 dB). Gardner also states: ”..It is possible that the phase crossovers could occur at more than one frequency..”

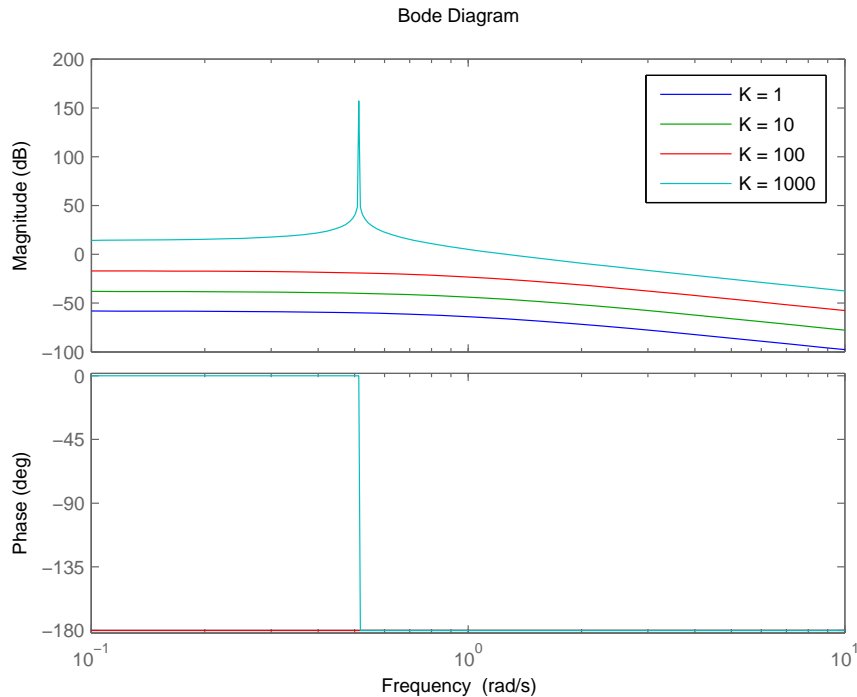


Figure 7.13: The figure shows stability for proportional gain (K) that is less than 1000. For $K < 1000$, the phase is constant at -180° and has a negative gain for all frequencies.

Thus, the system is stable for $K < 1000$.

7.5 Actuator saturation and limitations

In order to make the model as realistic as possible, actuator lag or delay has been implemented. The method is the same for both louver and fan.

7.5.1 Actuator saturation

In order to avoid either a leakage area that exceeds the specified maximum louver size, or a fan inflow that exceeds behavior according to the fan characteristic, actuator saturation is implemented. The saturation also provide a realistic control input to the Kalman filter (heave acceleration: $u = \ddot{\eta}^3$). Remember that the dynamics between this control input (u) and the change of actuator position, for instance the louver change area is held within the proportional gain ($K \cdot p$).

```

1      // Saturation
      double sat_louwer = A_L_Louwer_Max / (2*K_p_louwer);
3      double sat_fan = Q_in_characteristic / (K_p_fan);
      if (u > sat_louwer){
5          u = sat_louwer;
      }else if(u < -sat_louwer){
7          u = -sat_louwer;
      }else if(u > sat_fan){
9          u = sat_fan;
      }else if(u < - sat_fan){
11         u = - sat_fan;
      }

```

The saturation principle for the two saturation cases are identical. For instance, let's discuss the louver case.

Section 7.4.4 - Controller Design introduced the louver controller:

$$u_{Louver} = K_{p_Louver} \cdot u \quad (7.5.1)$$

Where u (see saturation code above) is the input to the process equation and Kalman filter. The air leakage out of the cushion is defined as:

$$A_{L_Louver} = \frac{A_{L_Louver_Max}}{2} + u_{Louver} \quad (7.5.2)$$

The leakage area saturation is:

$$0 \leq A_{L_Louver} \leq A_{L_Louver_Max} \quad (7.5.3)$$

Inserting eq. 7.5.1 and 7.5.2 into 7.5.3 yields:

$$-\frac{A_{L_Louver_Max}}{2 \cdot K_{p_Louver}} \leq u \leq \frac{A_{L_Louver_Max}}{2 \cdot K_{p_Louver}} \quad (7.5.4)$$

As the code above indicates. The leakage area will not concede actual louver size and the process input $u = \eta^3$ is restricted.

7.5.2 Actuator lag - restriction of cushion air flow rate

```

louver_position (from controller) = 0   louver_position (actual position) = 0
louver_position (from controller) = 1   louver_position (actual position) = 1
louver_position (from controller) = 2   louver_position (actual position) = 2
louver_position (from controller) = 4   louver_position (actual position) = 4
louver_position (from controller) = 5   louver_position (actual position) = 4
louver_position (from controller) = 6   louver_position (actual position) = 6
louver_position (from controller) = 7   louver_position (actual position) = 6
louver_position (from controller) = 9   louver_position (actual position) = 9
louver_position (from controller) = 10  louver_position (actual position) = 9
louver_position (from controller) = 11  louver_position (actual position) = 11
louver_position (from controller) = 13  louver_position (actual position) = 11
louver_position (from controller) = 14  louver_position (actual position) = 14
louver_position (from controller) = 16  louver_position (actual position) = 14
louver_position (from controller) = 17  louver_position (actual position) = 17
louver_position (from controller) = 19  louver_position (actual position) = 17
louver_position (from controller) = 21  louver_position (actual position) = 21
louver_position (from controller) = 22  louver_position (actual position) = 21
louver_position (from controller) = 24  louver_position (actual position) = 21
louver_position (from controller) = 26  louver_position (actual position) = 26
louver_position (from controller) = 28  louver_position (actual position) = 27
louver_position (from controller) = 29  louver_position (actual position) = 29
louver_position (from controller) = 33  louver_position (actual position) = 29
louver_position (from controller) = 34  louver_position (actual position) = 34
louver_position (from controller) = 37  louver_position (actual position) = 37

```

Figure 7.14: Actuator lag between requested actuator position (from controller) and actual actuator position. Each line is the same time step.

The delay itself is specified in a parameter that is found in both the actuator federations and is set independent of each other in `LouverFederate.java` and `FanFederate.java`. This parameter defines the actuators total "closed to open" time-period and vice versa. Thus, the time it takes to go from an open actuator to a closed one (closed louver to open louver, or a completely choked fan to a non-choked-fan..).

The implemented algorithm observes what position the actuator was in last iteration and figures out how long time it will take to put it to the wanted position. The coherence is a linear. For example, say the open-close actuator lag is 0.5 seconds then if the actuator is at zero position (closed louvers or fully choked fan(s)) and controller suddenly demanded actuator position 15, the lag would be:

$$\begin{aligned}
 d &= \frac{\text{open_close_actuator_delay} \cdot |\text{louver_pos} - \text{controlled_louver_pos}|}{100} \\
 &= \frac{0.5 \cdot |(0-15)|}{100} = 0.075s
 \end{aligned}
 \tag{7.5.5}$$

While the delay is in progress, that is the actual actuator position has not reached the position demanded by the controller, the previously achieved actuator position is the applicable position. This is a good assumption since the actuator position rate will change in coherence with the state error ($x - x^{reference}$). This results in a continuous process as figure 7.14 proves, which again results in a smooth, continuous and realistic airflow in or out of the air cushion. Thus, there will be no instant large actuator jumps. Testing has proved that in smooth first order wave forces, the biggest actuator alteration is 2-3% per iteration using a P-controller. The actuator properties such as the number of louvers and fans, the actual louver area size and fan characteristic graph (Pressure versus possible cushion air inflow) restricts the air flow magnitude. That is, a louver can't provide more leakage area

than its actual area size, and a fan can not contribute with more air inflow than its physical limitations.

The actuator delay is restricting the flow rate. The change of air flow through the actuators can not happen any quicker than determined by the `close_open_actuator_delay` (lets call this one "act_del") parameter.

The delay/lag function:

```
boolean actuatorInWantedPosition(double act_del, double t){
2   // Returns true if handle is in wanted controlled pos
   if(gap*(act_del/100) + ctrl_louver_pos_arrival_time<=t){
4     // In position
       ctrl_louver_pos_arrival_time = time;
6     gap = Math.abs(louver_pos - ctrl_louver_pos);
       return true;
8   }else{
       // Not in position!
10    return false;
   }
12 }
```


Chapter 8

Results

If not stated otherwise, the actuator setup for the results are 1 lift fan with fan characteristic stated in figure 7.5 section 7.3. Four louvers each on 1 m^2 . The design pressure is $P_0 = 3500 \text{ Pa}$.

Section 8.6.2 shows simulation results using the currently planned Wave Craft hull with confidential actuator properties. The rest are taken from a simplified squared SES hull (*Case1_1*) with fan characteristic according to figure 7.5.

Note that the noise inducted in the MRU heave position measurement is white Gaussian noise. A short explanation of some of the figure text fields:

Case1_1.AirCushion cg_down [x] remove from graph	True/exact/actual down position of cg in the global coord. syst (NED frame)
Case1_1.AirCushion bow_down [x] remove from graph	Same as the above only positioned the bow. (Non measurable)
Case1_1.HeaveControl x_est_pos [x] remove from graph	Estimated control position which can be either cg or vessel bow. (Varied by the parameter point_of_control)
Case1_1.HeaveControl noisyPosMeasurement [x] remove from graph	Heave position (down) measurement from the MRU. Includes noise.

Figure 8.1:

8.1 Process estimating - Kalmanfiltering

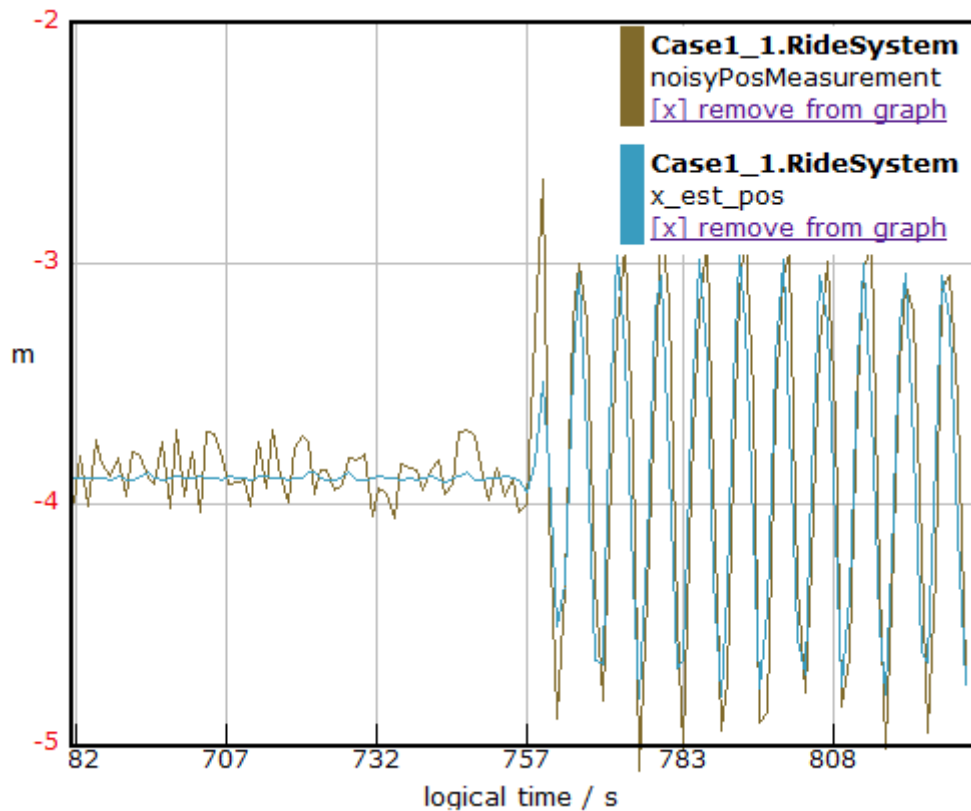


Figure 8.2: The Kalman filter estimates the heave position at the bow receiving an extremely noisy heave position from the MRU. Prior to $t = 757$: zero wave propagations, the vessel vertical position is truly constant. Afterwards $t = 757$ the vessel faces a regular wave with elevation 2 m

Important: The figure above shows a heave measurements that has a very high standard deviation (0.1 m). This is to prove the robustness of the filter. For remaining result the the standard deviation will halved (0.05 m) and the measurement will weighted stronger, therefore a quicker response that the illustration in figure 8.2:

Figure 8.3 below shows that the estimated position and velocity shows good resemblance to the actual/true position and velocity. The true position and velocity is off course not available in real life.

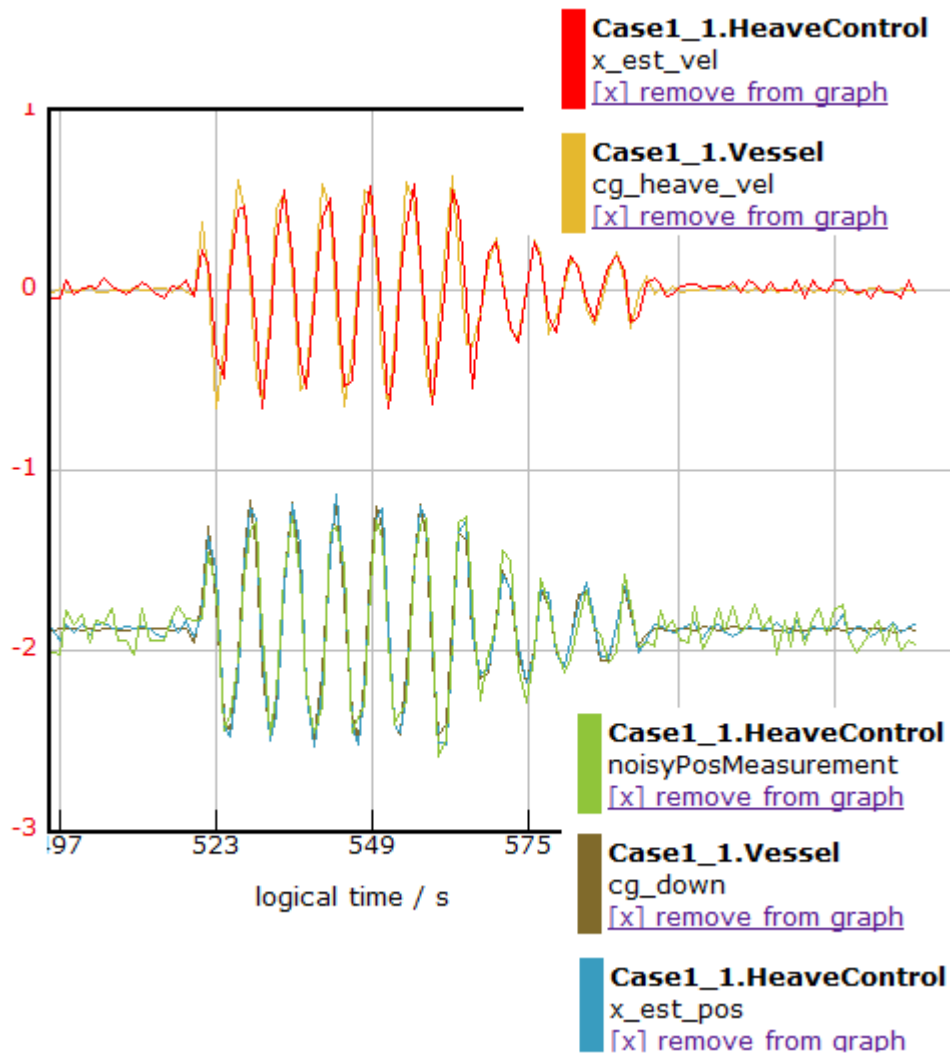


Figure 8.3: Estimated position and velocity (based on process equation and noisy MRU measurement) are close to the true state. Between $t \in \{522, 560\}$ a wave propagation with 2 meters elevation is added.

8.2 Large actuator lag leads to instability

The section 7.5.2 - Actuator lag - restriction of cushion air flow rate describes how the air flow is restricted due to actuator lag. The actuator can only move in a certain speed. The speed is determined by the parameter *open_close_actuator_delay*. This parameter is found in both the louver and fan federate VeSim window. If this parameter exceeds half the wave period than the controller will only worsen the

situation. With a constant wave elevation of 2 meters, figure 8.4 proves this.

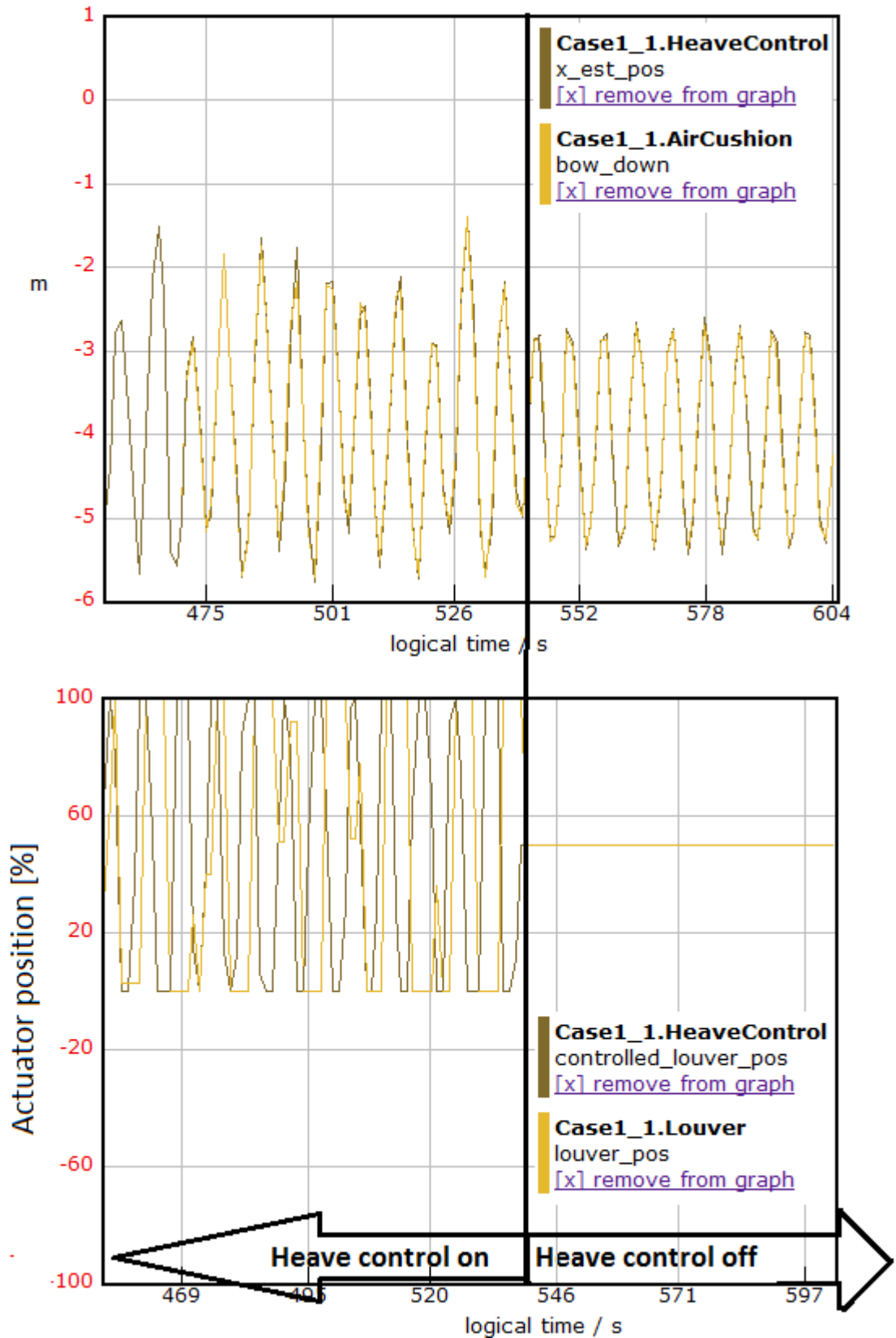


Figure 8.4: Heave control. Upper figure: bow heave position. Bottom figure: Shows actuator position where 0 is a closed louver and 100 is fully open. There exist a lag between controlled/requested and actual actuator position. The actuator lag is too large forcing the controller to perform worse than no control at all. Showing $\text{open_close_actuator_delay} = 5$ sec while wave period = 7 sec. The fan actuator is not shown, although the principle is exactly same only in anti-phase.

Definition 3. *The controller shows instability for:*

$$\text{open_close_actuator_delay} \geq \frac{\text{wave_period}}{2}$$

8.3 Change of control point

The figure below shows how the control point is changed from the center of gravity to vessel bow at $t \approx 880$. Wave elevation is 2 meters.

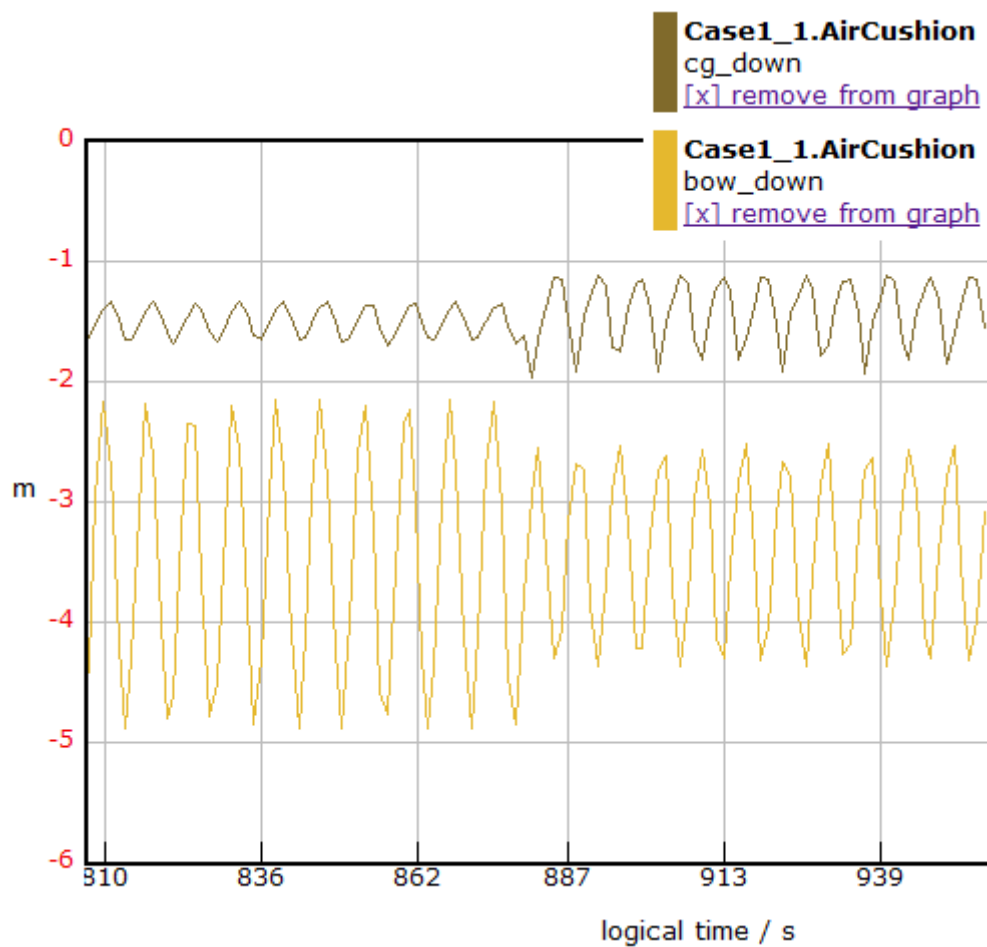


Figure 8.5:

$t \in \{0, 880\}$: control point is cg, proportional gain: $K_{p-FAN} = 190$, $K_{p-LOUVER} = 5.5$

$t \in \{880, \infty\}$: control point is vessel bow, $K_{p-FAN} = 50$, $K_{p-LOUVER} = 1.5$

8.4 Satisfactory behavior of the controlled fan and louver system

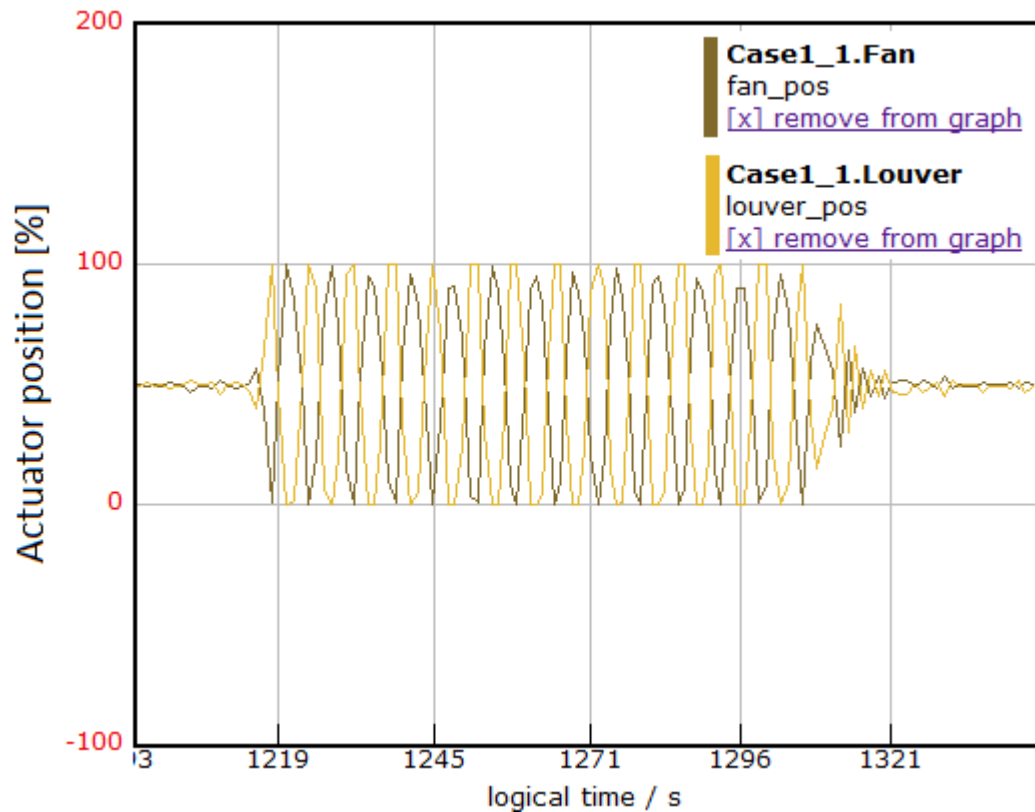


Figure 8.6: A well tuned control system using the same numerical proportional gains as figure 8.5 above. (Note that a dead zone filter near equilibrium point was not implemented at this time)

8.5 Alternative set point for fan control

The alternative fan control procedure shows better results than what explained in the previous section. The method is described in section 7.4.4 - Controller Design page 63.

All results except section 8.6 is based on fan control from the previous case. One can observe the damping improvement using the alternative approach compared to previous plots.

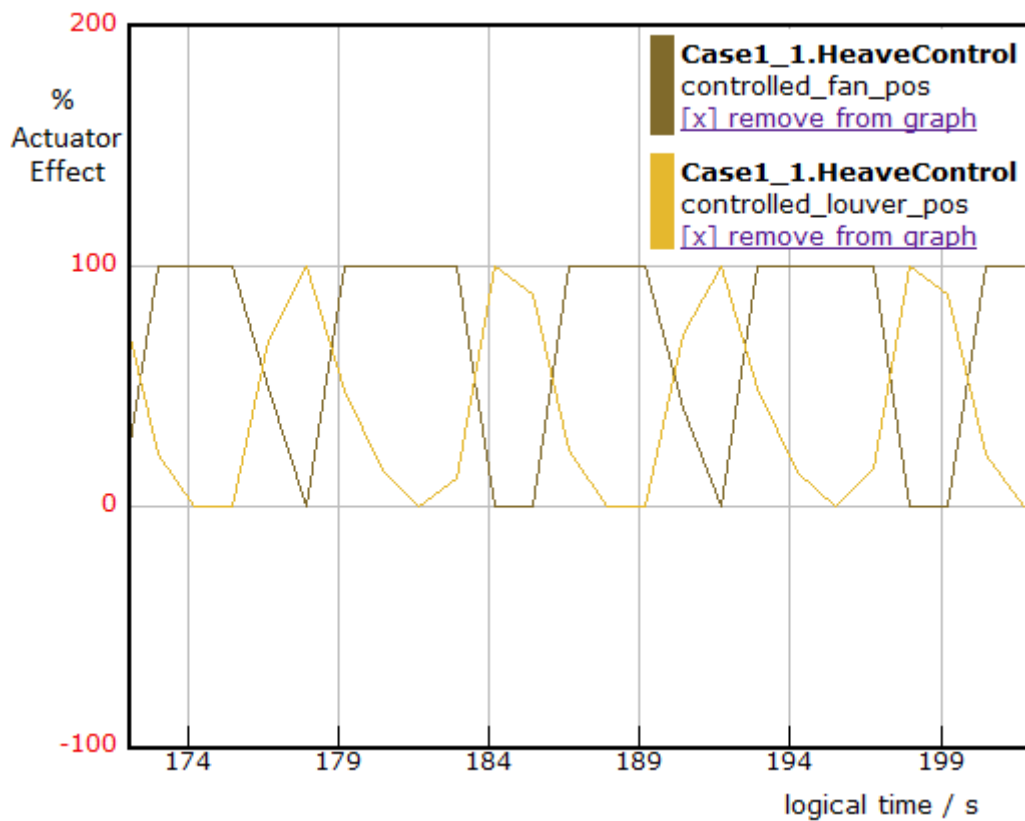


Figure 8.7: The control equilibrium point is $\text{fan_pos} = 100$ and not $\text{fan_pos} = 50$ as previously. This shows better heave control results since the fan air flow rate ($Q_{in}[\frac{m^3}{s}]$) is most effective at small cushion pressure which corresponds to the control point is positioned at the top of a wave. This effect is due to the fan characteristic figure (7.5).

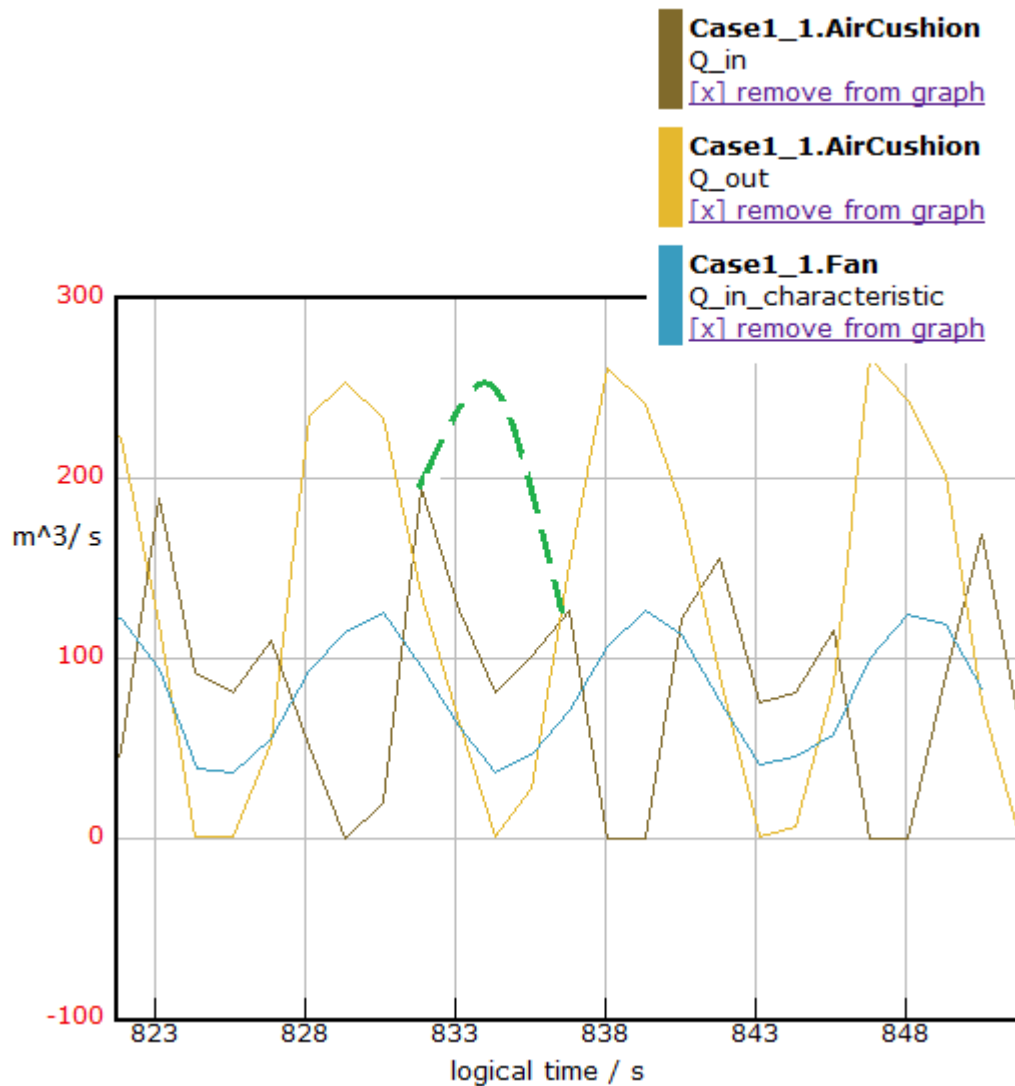


Figure 8.8: Using two lift fans: Q_{in} and Q_{out} is controlled in and out cushion air flow. Q_{inChar} shows maximum possible inflow (for a single fan). Although the dotted green line would ensure better fan control, this is according to figure 7.5 not possible.

The figure and figure caption above states that the fan control has its biggest damping effect with the control point the top of a wave where the louvers are closed and cushion pressure is small (due to a small cushion volume). This effect led to the alternative way of controlling the fan.

8.6 Heave Control

This section contains a system with properly tuned parameters.

Both louver and fan control are applied. Fan control is performed as specified in section 8.5. Note that the tests operate with the following leakage ratio around equilibrium state Q_0 and p_0 :

$$\frac{PassiveLeak}{PassiveLeak + LowerLeak} = \frac{A_{L_Passive_0}}{A_{L_Passive_0} + A_{L_Lower_Mean}} = \frac{0.33}{2.33} = 14.3\% \quad (8.6.1)$$

Using the mentioned condition, passive leakage ranges from 0.19 - 0.38 m^2 , using $passive_gain = 2.5$. $passive_gain$ is a parameter meant to include a realistic passive leakage contribution.

Note that there are really small dynamic passive leakage contributions, so by turning off the HCS, the lift ratio and pressure will be close to constant!

Involving the derivative effect of the controller will not increase damping itself, but it helps keeping the actuator input signal smooth. It slows the rate of actuator change (the output). The effect is therefore included in the following section (but not earlier results).

8.6.1 Simplified SES Hull (Case1_1)

Vital factors for the simplified SES simulation using regular waves :

Explanation	Symbol (in code)	Value
Maximum leakage area (per louver)	$A_{L_Louver_Max}$	$1m^2$
Total number of louvers	<i>number_of_louvers</i>	4
Number of Fans	<i>number_of_fans</i>	1
Wave Elevation Height	–	$2m$
Wave Direction	–	<i>HeadSea</i>
Wave Period	–	$9s$
Standard process deviation	<i>stdv_x</i>	0.06
Standard measurement deviation	<i>stdv_x</i>	0.01
Control point is vessel bow	<i>point_of_control</i>	1
Vessel speed	-	$0 \frac{m}{s}$
Static air flow rate	Q_0	$126.073 \frac{m^3}{s}$
Design pressure	P_0	$3500Pascal$
Contraction of air flow (see section 7.2.2)	c_n	0.8356
Proportional Gain	K_p	1.5
Derivative Gain	K_p	0.35
HCS ON	<i>time</i> \in	$< 0, 2140 > s$
HCS Off	<i>time</i> \in	$< 2140, inf > s$

The following figures indicates the behaviour of the simplified squared SES with properties specified in the table above. The heave controller starts on, but is then turned off. All figures are from the same run:

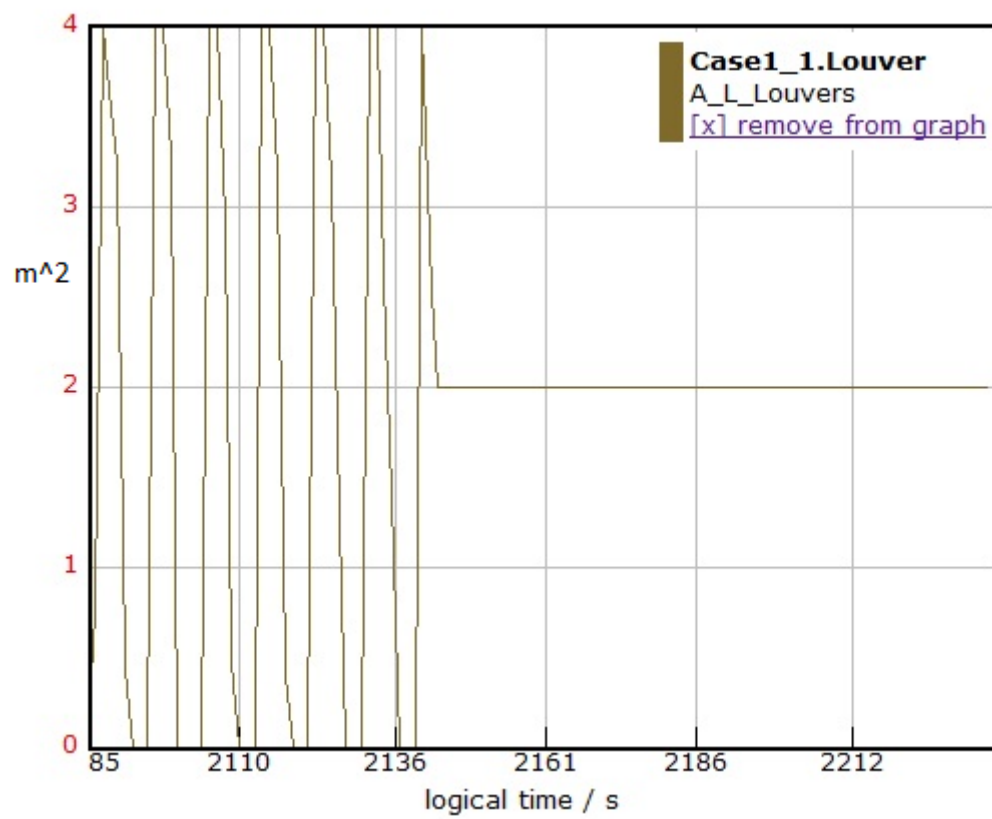


Figure 8.9:

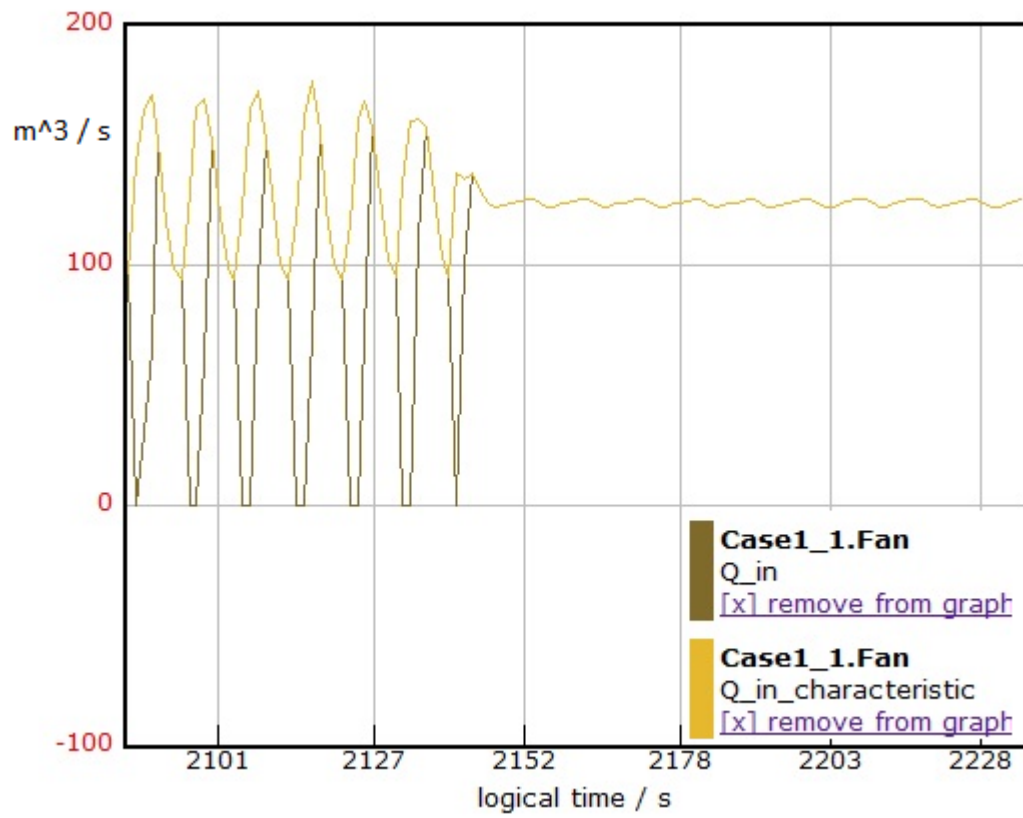


Figure 8.10:

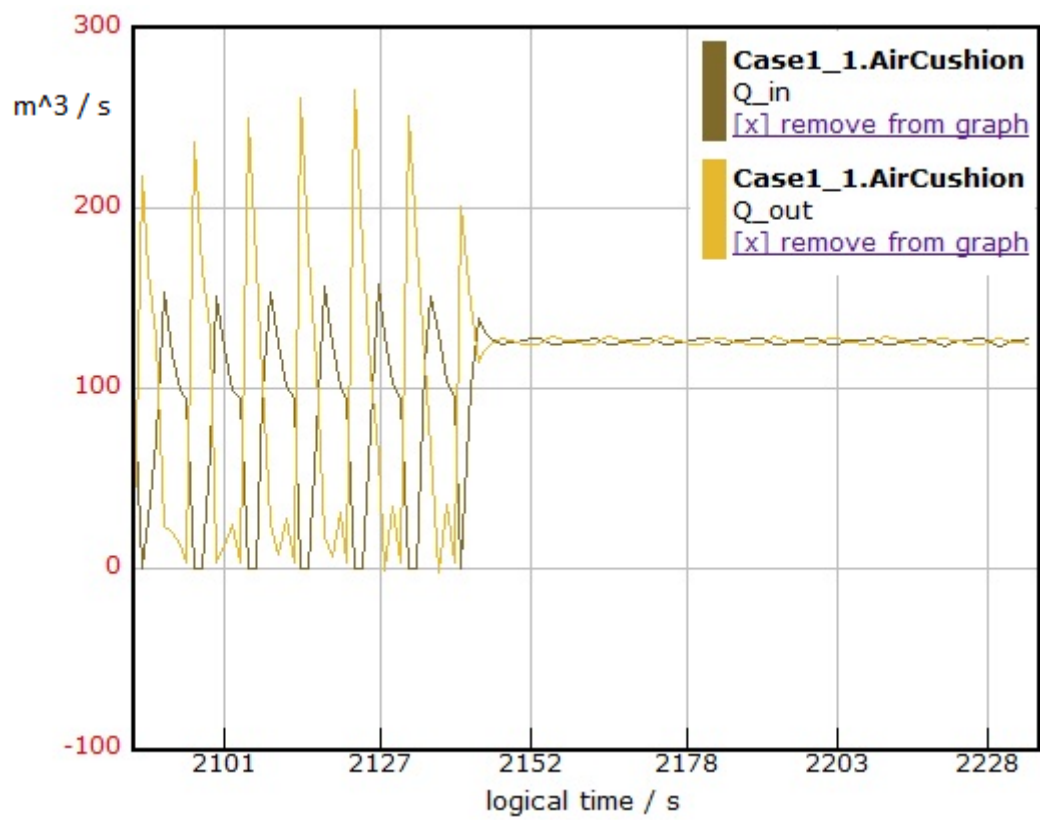


Figure 8.11:

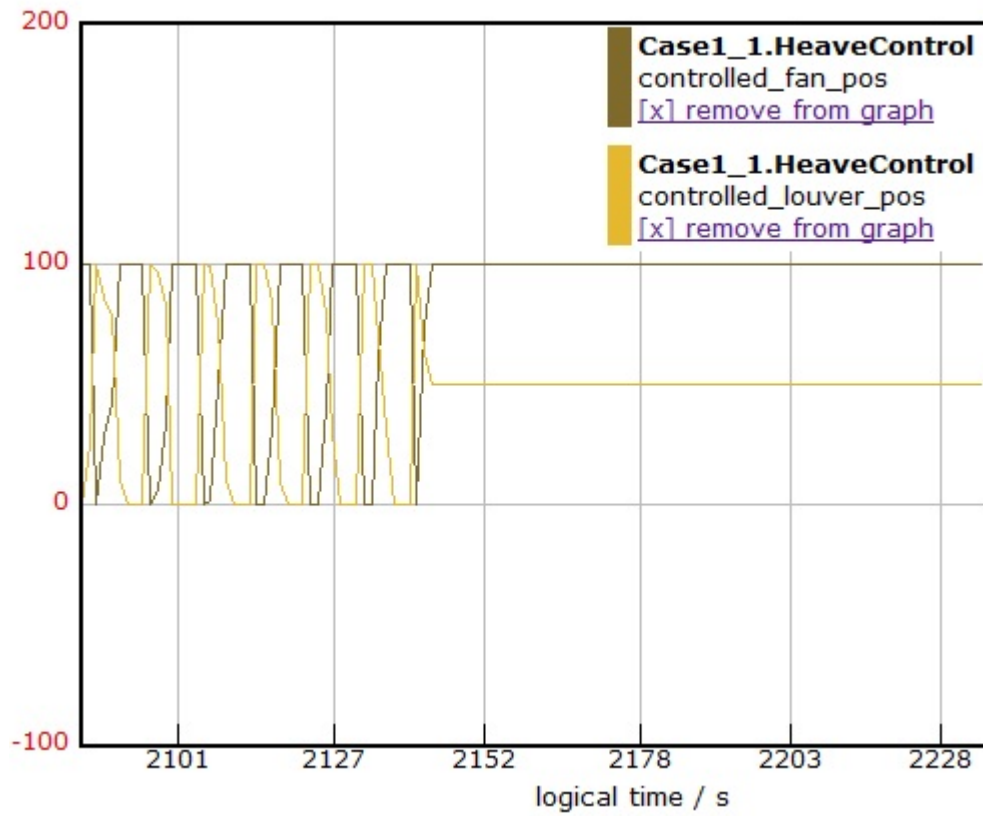


Figure 8.12:

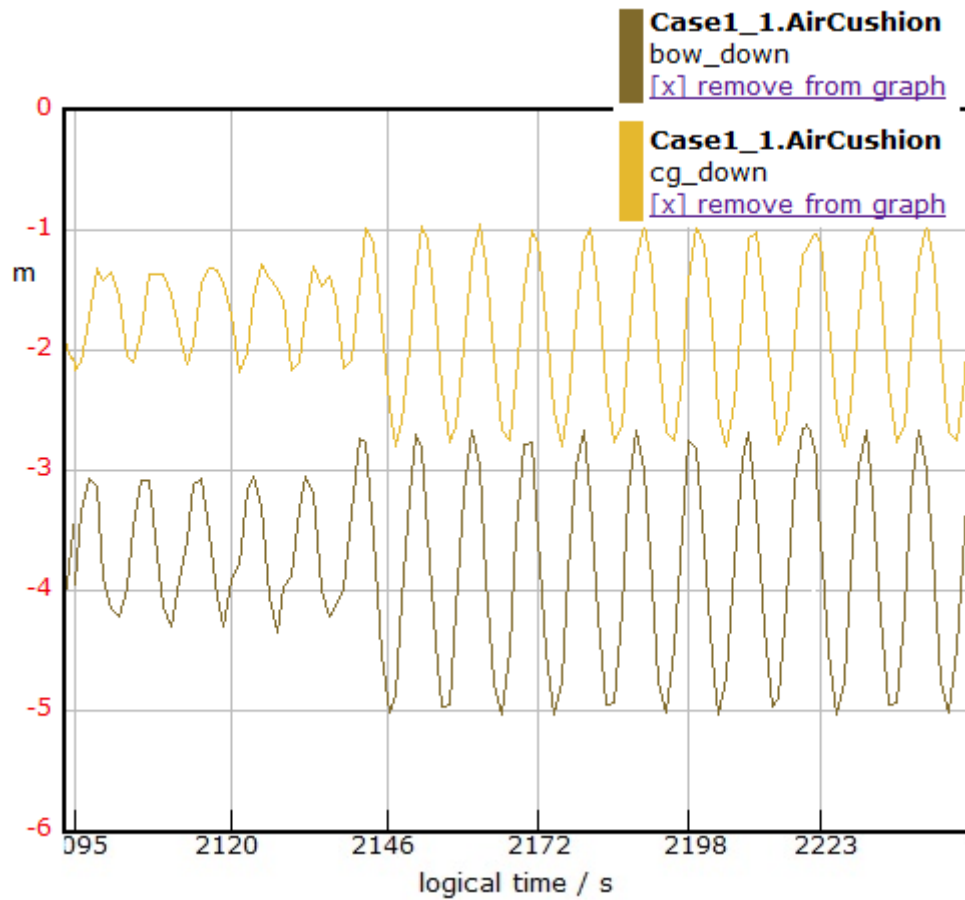


Figure 8.13:

8.6.2 The Wave Craft

Parameters that are not confidential, used for the Wave Craft results:

Explanation	Symbol (in code)	Value
Wave Elevation Height	–	2m
Wave Direction	–	<i>FollowingSea</i>
Wave Period	–	9s
Standard process deviation	<i>stdv_x</i>	0.06
Standard measurement deviation	<i>stdv_x</i>	0.01
Vessel speed	-	0 $\frac{m}{s}$
HCS ON	<i>time</i> ∈	< 0, 2400 >
HCS Off	<i>time</i> ∈	< 2400, inf >

HCS starts on, and is then turned off. Control point is Vessel Bow. All figures are from the same run:

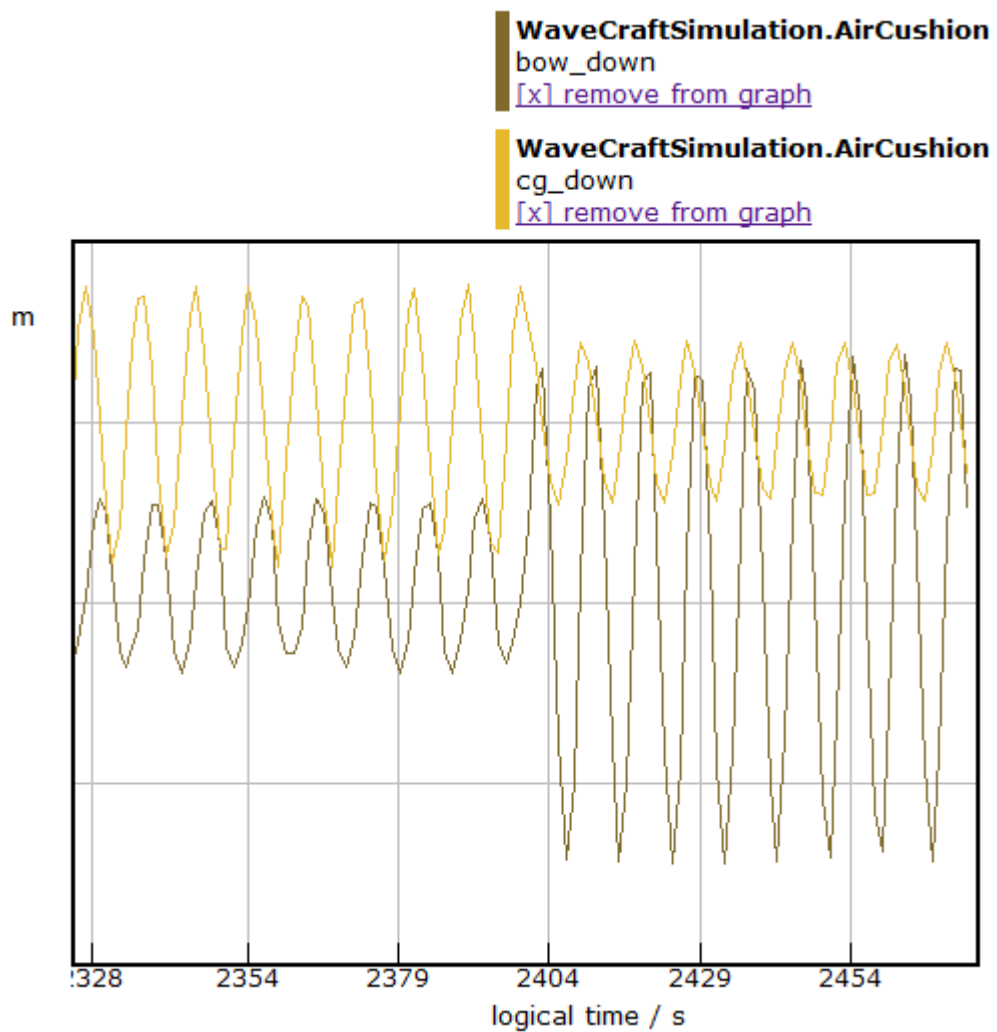


Figure 8.14: Vessel bow experience a motion reduction of 67.20%

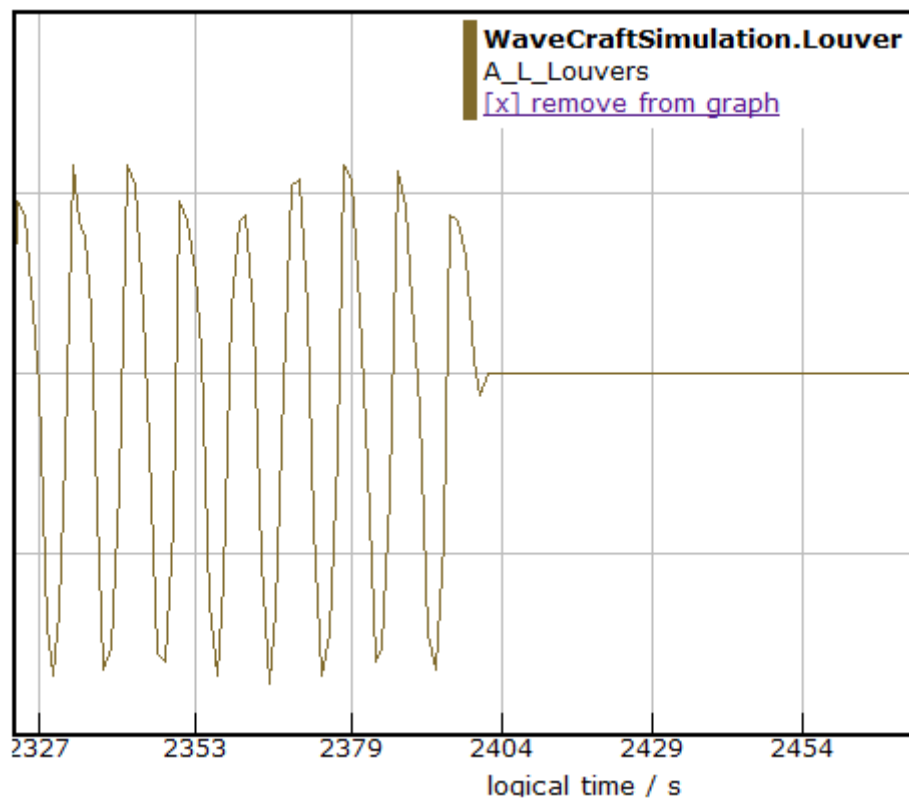


Figure 8.15: Controlled louver area

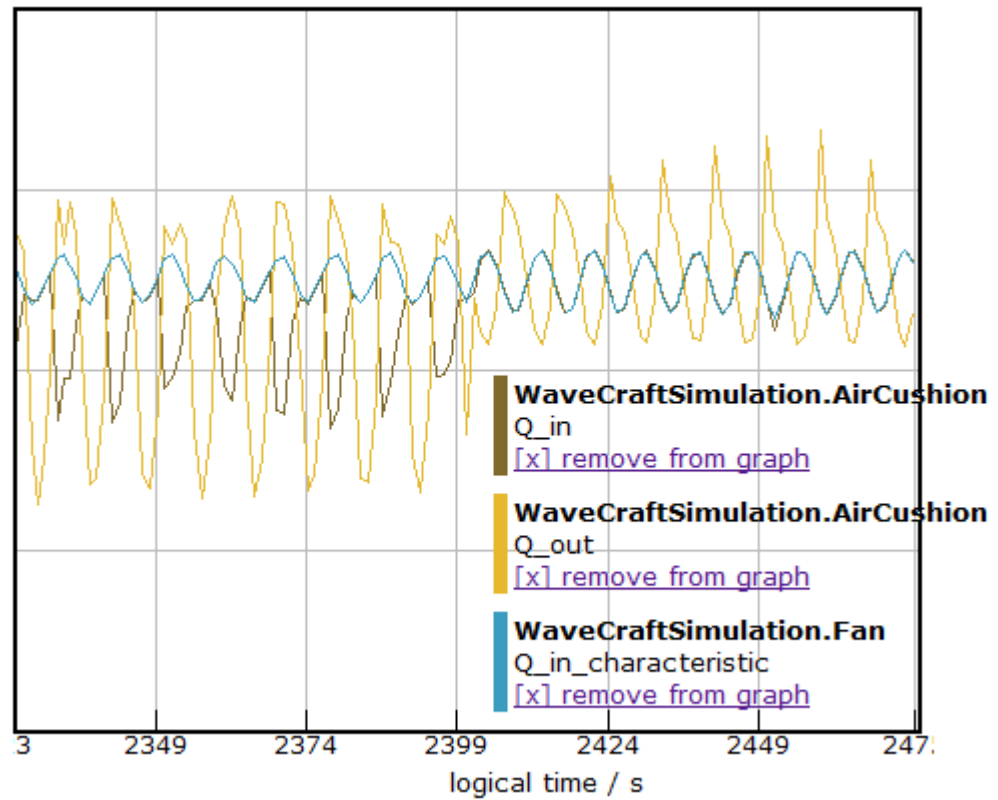


Figure 8.16: The controlled air flow in and out. Also the maximum available flow as a function of cushion pressure.

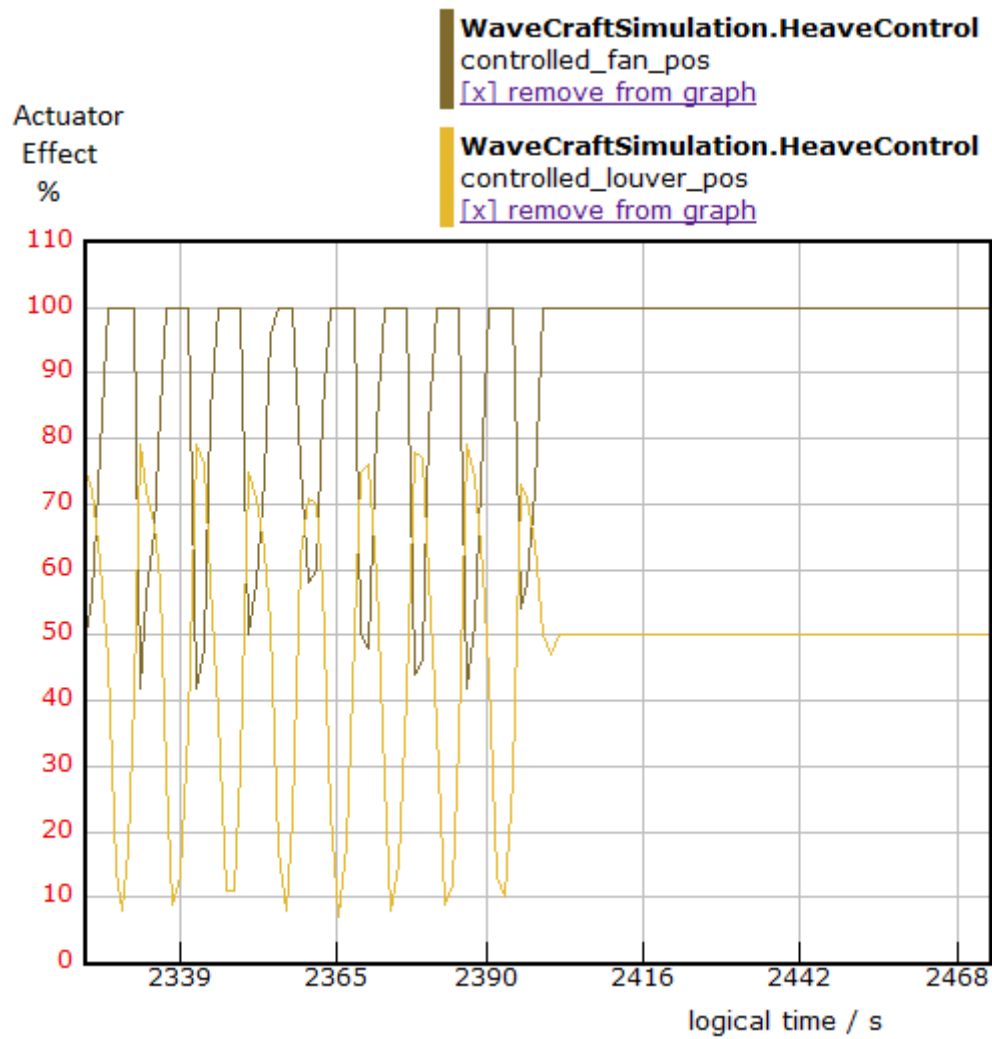


Figure 8.17: Actuator position. Closed louver: $\text{controlled_louver_pos} = 0$. Completely choked lift fan: $\text{controlled_fan_pos} = 0$

8.6.2.1 Control point changes from Center Of Gravity to Vessel Bow

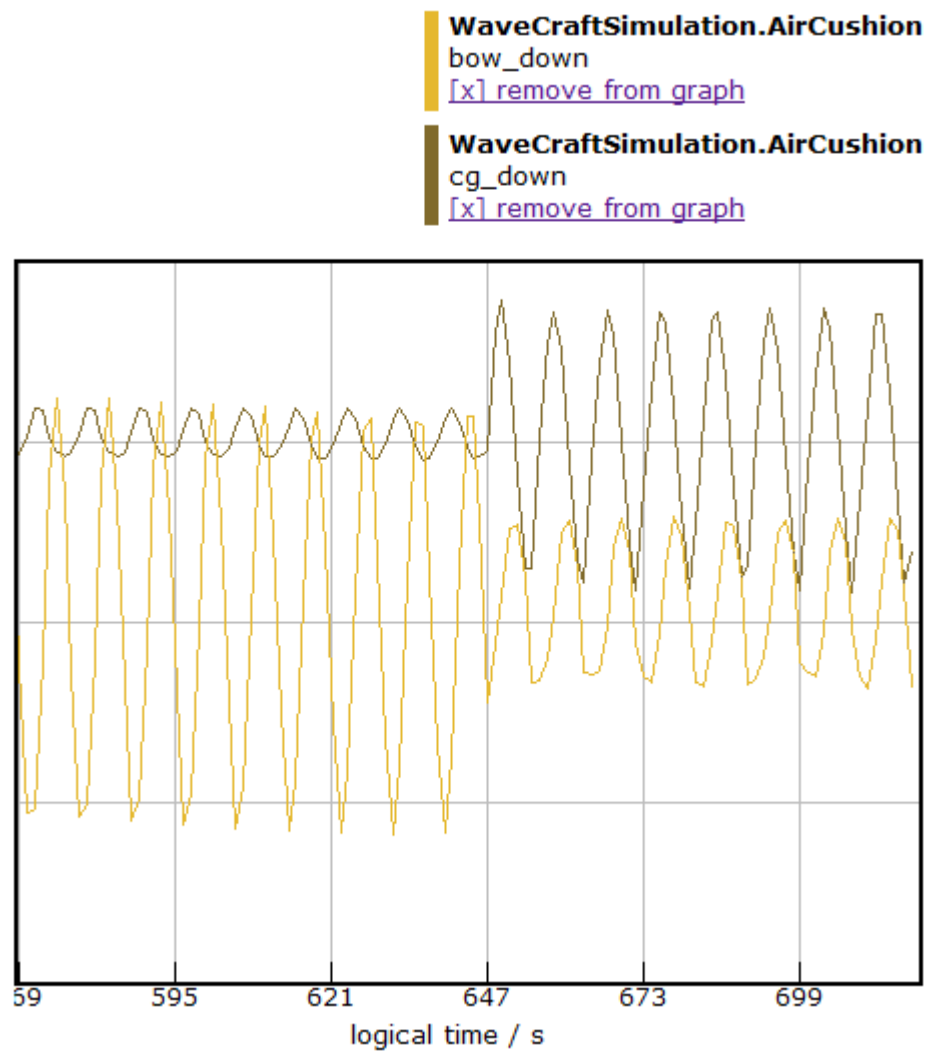


Figure 8.18: Changing control point online from vessel bow to CG. Shows heave position

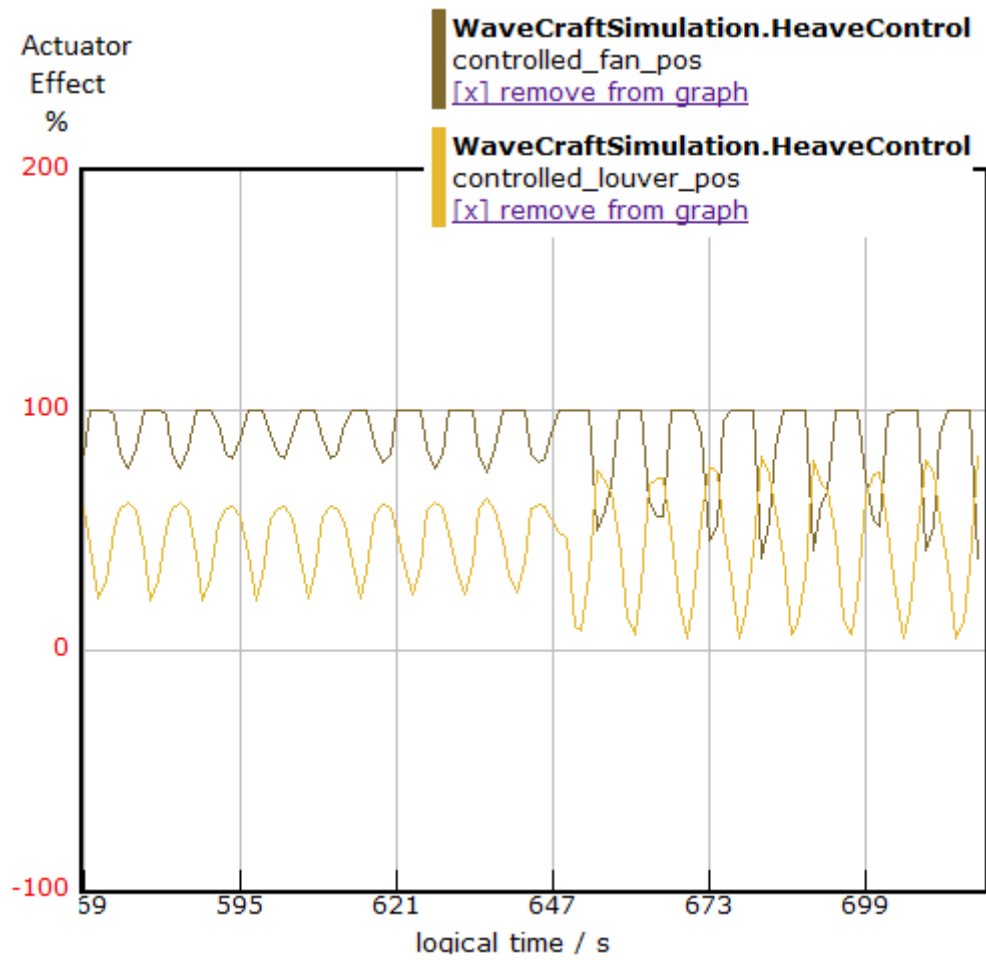


Figure 8.19: Changing control point online from vessel bow to CG. Shows actuator position

Chapter 9

Conclusion

A heave control system for damping of wave motions is presented. Two different SES are tested. Result section 8.6.2 covers the results from the Wave Craft while all other results are from the simplified hull squared SES.

The results covered by the simplified SES (section 8.6.1, figure 8.13) shows that the control system approximately removes 53 % of total vertical bow motion.

The second test is performed using the actual hull and actuator specifications for the current design of The Wave Craft. This test is documented in section 8.6.2. Figure 8.14 shows that the control system approximately removes 67.2 % of total vertical bow motions.

These results are obtained when the control point is set to the vessel bow. Figure 8.14 illustrates the heave behaviour if the control point is changed from center of gravity (CG) to vessel bow. When the control point is set to CG, the motions at this point is damped by 79.5 %.

The center of gravity has a larger potential of damping its motions since both the stern and bow functions as a "motion relief" in two directions. Only one direction of "motion relief" is presence when controlling the vessel bow.

It is expected in forehand that the real Wave Craft hull with corresponding actuators would perform better than the simplified squared SES. The Wave Craft is designed with an unusual narrow hull. The aft width is considerable wider than the bow width. On a regular catamaran, such a hull would give poor sea keeping properties. However, the air cushion lift forces enables this design. This gives the vessel bow a natural good damping environment.

The result stated above are very satisfactory. The results proves benefits one can achieve using a Ride/Heave Control System on a Surface Effect Ship. The results are better than expected beforehand.

Figure 8.2 and 8.3 proves that the Kalman filter with chosen mathematical model performs well. The latter figure proves that the heave position and velocity follows the true state even though the measurement contains much noise. If yet unclear:

- I The heave velocity is not measured only estimated
- II The estimated heave position highly rejects the heave measurement noise

Section (8.2) illustrates the problem that occur if the actuator lag exceeds a particular limit. This will results in a control system that increase heave motion instead of decreasing it. The actuator open/close lag (described in section 7.5.2) must be less than half the wave period in order to achieve motion damping.

The alternative approach for fan control (section 7.4.4 - Controller Design) shows better damping results than the first described method. The alternative approach finds the control heave reference position by setting the fan to perform at 100% effect instead of setting it to 50%. When utilizing a large range of cushion pressure one will experience a very low air inflow at high cushion pressure. Therefore one will benefit by obtaining maximum fan air flow around high cushion pressures.

Further explained, while the control point travels from the equilibrium set point and down to the wave bottom (minimum heave position) the fan does not have a very effective inflow due to the high pressure in the air cushion. Therefore, in this region the motion damping is increased by setting the fan to perform at full effect (instead of half of the effect).

9.1 Further work

Further work should involve implementation of air cushion spatially varying pressure in the air cushion. Sørensen presents the necessary equations for this in[12]. Spatially varying pressure will affect heave and pitch motions and in the certain vessel speed and sea state. One can provoce the vertical accelerations (as discussed in section 4.1 - Cobblestone Effects). Damping of these cobblestone effects could be done with the dissipative proportional controller Sørensen presented in the very same publication.

Along with the developed controller for this project, one could form a hybrid controller that could change operation between three states:

1. Using the HCS presented in this thesis: Damp wave induced motion at the bow in zero speed at wind turbine docking mode. Experiment with motion damping of the center of gravity in large sea states and slow/moderate vessel speed. Simulation has shown that the system gives an overall better transit experience for the crew.
2. In low and moderate sea state at relative high vessel speed one should damp the cobblestone effects using the dissipative proportional controller.

To validate the control system it is recommended to perform a model test.

Chapter 10

Summary

This thesis shows how one can achieve vertical motion control of a Surface Effect Ship (SES) by actively controlling the air inflow and out flow out from the air cushion. The air cushion is enclosed by two twin catamaran hulls and rubber seals in both ends. The air flow is actuated through lift fan(s) that fills the cushion with air and louver(s) which emits air out of the cushion.

A heave controller for damping of wave induced vertical motion at zero speed is presented and tested in simulation. A Kalman filter with a suitable mathematical model / process for estimating non-measurable states and neglect of measurement noise is applied. A proportional controller is presented and stability analysis of the system has been done. The final result shows a robust system that considerably damps vertical motions induced by wave propagations. See section 7 and figure 8.2, 8.3 and 8.14.

The report includes a literature review of the SES concept, the planned offshore service vessel - Wave Craft and the existing control literature concerning design of vertical motion damping of a SES (section 2 to 4).

The software tools and system setup are explained in section 5.

The already developed SES model at project takeover has been summarized in section 6.

Parallel with the work made by the writer of this thesis, MingKang Wu from Marintek has developed seal air leakage and forces acting on the seals. These leakages and forces are respectively added together with the louver & hull leakage and hydrodynamic, viscous & air cushion forces.

A louver system has been designed and implemented. Along with the fan system (which has been improved and is now controlled). Figure 8.16 shows how a typical fan operates at different cushion pressure. The louver and fan system contains air flow rate and air quantity saturation. The transition between the desired actuator position and the actual actuator position contains a lag that can be specified manually. If the lag exceeds the numerical value defined in section 8.2 the controller will increase vertical motions at the control point as seen in figure 8.4.

It is possible to vary the number of fans and louvers, along with the physical area size of the louver.

Figure 8.5 shows that the control point can be altered online between the center of gravity and vessel bow. Damping of the CG can show interesting results for the over-all passenger comfort while traveling in high sea states. While positioned close to the wind turbine, one can easily switch to bow control which enable personnel to safely enter the turbine due to motion control.

Bibliography

- [1] D. Fathi, “Vesim.” <http://www.sintef.no/home/MARINTEK/Software-developed-at-MARINTEK/VeSim/>, 2011.
- [2] C. person MARINTEK: Dariusz Fathi, “Shipx - vessel response.” <http://www.sintef.no/home/MARINTEK/Software-developed-at-MARINTEK/VERES/>, 2011.
- [3] T. E. Halvorsen, “Simulation of motion of ses in waves.” Master Thesis, Department of Marine Technology, NTNU, 2008.
- [4] T. E. Halvorsen, “Discussions and information from halvorsen via email, phone or meetings,” 2011.
- [5] STEEN, “Air cushion catamarans, surface effect ships (ses).” Lecture in TMR 4220, 2007.
- [6] O. Faltinsen, *Hydrodynamics of High-Speed Marine Vehicles chapter 5 Surface Effect Ships*. Cambridge University Press.
- [7] O. Faltinsen, *Figures respectively used are [5.3 , 5.4 , 5.10] from Hydrodynamics of High-Speed Marine Vehicles chapter 5 Surface Effect Ships p 141 ..* Cambridge University Press.
- [8] O. Faltinsen, *Hydrodynamics of High-Speed Marine Vehicles chapter 5.4*. Cambridge University Press.
- [9] T. E. Halvorsen, “Photos from simulation of motion of ses in waves. a): Figure 21, b) figure 22, c) figure 44.” Master Thesis, NTNU, 2008.
- [10] N. A. Forces, “Coastal corvette - skjold-class.” <http://mil.no/organisation/equipmentfacts/sea/Pages/default.aspx>, 2011.
- [11] P. taken by Tormod Salvesen. All rights reserved from Umoe Mandal, “Louver pictures.” ., 2011.

- [12] A. J. Sørensen and O. Egeland, *Design of Ride Control System for Surface Effect Ships using Dissipative Control*. From Automatica Vol 31, no 2 pp. 183 - 199. Elsevier Science LTD, 1995.
- [13] C. Trust, “Offshore wind accelerator access competition.” <http://www.carbontrust.co.uk/emerging-technologies/current-focus-areas/offshore-wind/Pages/offshore-wind-access-shortlisted.aspx>, September - 2011.
- [14] Øyvind Adrian Skogmo, “Stor tro på rask vedlikeholdsbat.” <http://www.1-a.no/Nyheter/tabid/296/Default.aspx?ModuleId=60281&articleView=true>, Oktober - 2011.
- [15] U. Mandal, “Wave craft flyer sent out in meeting november.” A4format, 2011.
- [16] Kaplan and Davies, *A simplified Representation of the Vertical Plane Dynamics of SES Craft*. AIAA/SNAME Advanced Marine Vehicle Conference, 1974.
- [17] B. P. B Kaplan and S. Davis, *Dynamics and Hydrodynamics of Surface Effect Ships*. Trans. SNAME VOL 89 1981 page 211 - 247, 1981.
- [18] F. Sørensen, Steen, *SES Dynamics in the Vertical Plane, pp 71-84*. Schiffstechnik, 1993.
- [19] P. B. Kaplan and S. Davis, *System analysis techniques for designing ride control system for SES craft in waves*. AIAA Paper No. 74-314, AIAA/SNAME Adv. Marine Vehicles Conf., 1974.
- [20] M. K. Basturk, Doblack, “Air cushion adaptive disturbance cancellation for the reduction of wave induced motion of ramp-connected ships.” 11th international Conference on Fast Sea Transportation, Honolulu Hawaii, USA September, 2011.
- [21] T. Ulstein and N. Odd M. Faltinsen Department of Marine Hydrodynamics, “Cobblestone effect on ses.” [ftp://ftp.rta.nato.int/PubFullText/RTO/MP/RTO-MP-015/\\$MP-015-13.PDF](ftp://ftp.rta.nato.int/PubFullText/RTO/MP/RTO-MP-015/$MP-015-13.PDF), 1998.
- [22] A. L. R. Company, *Lift System for the U.S Navy - the 2000 Ton Surface Effect Ship Program*. U.S. Navy, 1974.
- [23] S. Steen, *Cobblestone Effects on SES*. Dept. Marine Hydrodynamics, NTNU, 1993.
- [24] A. e. a. Nikiforov.

- [25] M. . S. . MARINTEK, “Simvis - visualisation of simulated marine operation.” http://www.sintef.no/upload/MARINTEK/Software/SIMVIS_Handout.pdf, 2011.
- [26] “Shipx.” <http://www.sintef.no/home/MARINTEK/Software-developed-at-MARINTEK/ShipX/>.
- [27] “Marintek.” <http://www.sintef.no/home/MARINTEK>.
- [28] M. T. H. O. M. Christian Wines, Sverre Steen, *Influence of Increased Weight on SES-performance in a Seaway*. Proceedings FAST2007, Shanghai, China, 2007.
- [29] M. Wu, “Working with leakage and forces acting on the seals of the exact same model as this thesis considers..” Concise Description of SES Seakeeping Model, 2011.

Appendix A

Contents on enclosed DVD

1. A video of a visualisation of how heave control is to be performed. Video made by Samir Mourad and Umoe Mandal
2. A vessel simulation(VeSim) video (using the ShipX plugin SimVis) that evidently shows that the vessel bow is being damped at zero vessel speed
3. Implemented java code and default VeSim libraries
4. Hull design for the simplified square SES. (The Wave Craft hull is classified)
5. Lift fan characteristic for the simplified SES
6. Pictures of the WaveCraft

Appendix B

The Kalman Filter

Note that the discrete Kalman filter is usually implemented using matrix notation such as Φ , Γ , Λ , \mathbf{H} . The code implementation uses $(\mathbf{A}, \mathbf{B}, \mathbf{E}, \mathbf{C})$. Thus, to avoid confusion the latter notation will be used in describing the Kalman filter.

Given the discrete linear system equation:

$$\mathbf{x}_{k+1} = \mathbf{A}\mathbf{x}_k + \mathbf{B}\mathbf{u}_k + \mathbf{E}\mathbf{w}_k \quad (\text{B.0.1})$$

And the measurement equation:

$$\tilde{\mathbf{y}}_k = \mathbf{C}\mathbf{x}_k + \nu_k \quad (\text{B.0.2})$$

Where

x	System state vector
A	State transition matrix
P	State error covariance matrix
u	Control input vector
B	Control input matrix
w	Process noise vector
E	Process noise input matrix
Q	Process noise covariance matrix
y	Output vector
C	Output matrix
v	Measurement noise vector
R	Measurement noise covariance matrix
K	Kalman gain, feedback matrix

The Kalman filter can be written as:

State initialization	$\hat{\mathbf{x}}_0 = E[\mathbf{x}_0]$
State error initialization	$\mathbf{P}_0 = E[(\hat{\mathbf{x}}_0 - \mathbf{x}_0)^2]$
State propagation	$\mathbf{x}_k^- = \mathbf{A}\hat{\mathbf{x}}_{k-1} + \mathbf{B}\mathbf{u}_{k-1}$
State error propagation	$\mathbf{P}_k^- = \mathbf{A}\mathbf{P}_{k-1}\mathbf{A}^T + \mathbf{E}\mathbf{Q}_{k-1}$
Kalman gain update	$\mathbf{K}_k = \mathbf{P}_k^- \mathbf{C}^T (\mathbf{C}\mathbf{P}_k^- \mathbf{C}^T + \mathbf{R}_k)^{-1}$
Measurement update	$\hat{\mathbf{x}}_k = \mathbf{x}_k^- + \mathbf{K}_k(\tilde{\mathbf{y}}_k - \mathbf{C}\mathbf{x}_k^-)$
State error update	$\mathbf{P}_k = ((\mathbf{P}_k^-)^{-1} + \mathbf{C}^T \mathbf{R}_k^{-1} \mathbf{C})^{-1}$

The following must be given: system model described as equation (B.0.1) and (B.0.2), an initial state for the system and a flow of (noisy) measurement. The Kalman filter described above will produce a flow or sequence of optimal state estimates. The estimates are based on a minimization of the expected least square error between the true system states and the estimate:

$$J = \min \sum_{k=0}^n (x_{est} - x)^2 \quad (\text{B.0.3})$$

Therefore one can say that the Kalman filter is optimal.

For this project, the steady state numerical values for the state error covariance matrix (P) and Kalman gain (K) has been found and implemented so that an optimal solution can be found at filter start up.

For further information regarding the Kalman filter, see Fossen 2011.

Appendix C

VERES hydrostatics for the Square-SES (Case 1_1) Model

HYDROSTATICS	ENCL.	1)
	REPORT	
	DATE	2011-12-18
	REF	

SHIP: **Case1.1**
Loading condition: Design WL
Draught AP/FP: 1.200 / 1.200 [m]

	Symbol	Unit	
Length overall	L _{OA}	[m]	30.000
Length betw. perp.	L _{PP}	[m]	30.000
Breadth moulded	B	[m]	10.000
Depth to 1 st deck	D	[m]	5.000
Draught at L _{PP} /2	T	[m]	1.200
Draught at FP	T _{FP}	[m]	1.200
Draught at AP	T _{AP}	[m]	1.200
Trim (pos. aft)	t	[m]	0.000
Rake of keel		[m]	0.000
Rise of floor		[m]	0.000
Bilge radius		[m]	0.000
Sea water density	ρ _s	[kg/m ³]	1025.00
Shell plating thickness		[mm]	2
Shell plating in % of displ.		[%]	0.40
Length on waterline	L _{WL}	[m]	30.020
Breadth waterline	B _{WL}	[m]	10.000
Volume displacement	∇	[m ³]	42.4
Displacement	Δ	[t]	43.6
Prismatic coefficient*	C _P	[-]	1.0003
Block coefficient*	C _B	[-]	0.1176
Midship section coefficient	C _M	[-]	0.1176
Longitudinal C.B. from L _{PP} /2	LCB	[m]	-0.000
Longitudinal C.B. from L _{PP} /2*	LCB	[% L _{PP}]	-0.000
Longitudinal C.B. from AP	LCB	[m]	15.000
Vertical C.B.	VCB	[m]	0.789
Wetted surface	S	[m ²]	171.07
Wetted surface of transom stern	A _T	[m ²]	1.36
Waterplane area	A _W	[m ²]	60.26
Waterplane area coefficient	C _W (L _{WL})	[-]	0.201
Longitudinal C.F. from L _{PP} /2	LCF	[m]	0.000
Longitudinal C.F. from AP	LCF	[m]	15.000
Immersion	DP ₁	[t/cm]	0.618
Trim moment	MT ₁	[t·m/cm]	1.545
Transverse metacenter above keel	KM _T	[m]	29.717
Longitudinal metacenter above keel	KM _L	[m]	106.783

Remarks: *Refers to L_{PP}
Hydrostatic corrections not included

Appendix D

Derivation Of Transfer Function $H(s)$ for stability analysis

$H(s)$ is defined as:

$$y = H(s)r = H(s)x_1^{ref} \quad (D.0.1)$$

Where

$$\mathbf{x} = \begin{bmatrix} x_1 \\ x_2 \end{bmatrix} = \begin{bmatrix} \eta^3 \\ \dot{\eta}^3 \end{bmatrix} \quad (D.0.2)$$

Using the equation of motion from eq. 7.4.1 and re-writing this using the proportional controller: $u = K(x_1^{REF} - x_1)$. Also, the superscript for η^3 denotes the third degree of freedom (heave) and not the power to three. This yields:

$$\dot{x}_1 = x_2 \quad (D.0.3)$$

$$\dot{x}_2 = \frac{1}{1 - dt} \left[x_1 + \frac{1}{2} dt^2 K(x_1^{REF} - x_1) \right] \quad (D.0.4)$$

using Laplace:

$$sx_1 = x_2 \quad (D.0.5)$$

$$sx_2 = \frac{1}{1 - dt} \left[x_1 + \frac{1}{2} dt^2 K(x_1^{REF} - x_1) \right] \quad (D.0.6)$$

Merging these equations yields:

$$x_1 = \frac{1}{s} x_2 \quad (D.0.7)$$

$$= \frac{1}{s^2} \frac{1}{1 - dt} \left[x_1 + \frac{1}{2} dt^2 K(x_1^{REF} - x_1) \right] \quad (D.0.8)$$

$$= \frac{1}{s^2(1 - dt)} \left[x_1 + \frac{1}{2} dt^2 K(x_1^{REF} - x_1) \right] \quad (D.0.9)$$

$$x_1 \left(1 - \frac{1}{s^2(1-dt)} + \frac{\frac{1}{2}dt^2K}{s^2(1-dt)} \right) = \frac{\frac{1}{2}dt^2K}{s^2(1-dt)} x_1^{ref} \quad (\text{D.0.10})$$

$$x_1 \left(\frac{s^2(1-dt) - 1 + \frac{1}{2}dt^2K}{s^2(1-dt)} \right) = \frac{\frac{1}{2}dt^2K}{s^2(1-dt)} x_1^{ref} \quad (\text{D.0.11})$$

$$x_1 = \frac{\frac{1}{2}dt^2K}{s^2(1-dt) - 1 + \frac{1}{2}dt^2K} x_1^{ref} = H(s)x_1^{ref} \quad (\text{D.0.12})$$

Closed loop input/output:

$$y = Cx = [1 \ 0] \begin{bmatrix} x_1 \\ x_2 \end{bmatrix} = x_1 = H(s)x_1^{ref} \quad (\text{D.0.13})$$